Investigating the role of eukaryotic translation initiation factor 4E in BRAF and cKit mutant human melanomas

by

Yao Zhan

Division of Experimental Medicine

Faculty of Medicine

McGill University

Montréal, Québec, Canada

April 2016

A thesis

Presented to the Faculty of Graduate Studies and Research

in partial fulfillment of the requirements for the degree of

Doctor of Philosophy (Ph.D.)

Table of Contents

Abstract

Protein synthesis is indispensible for cells to execute various functions such as proliferation, survival and development. The majority of mRNAs in eukaryotic cells are translated in a cap-dependent manner, which is dependent on the activity of the rate-limiting component known as the eukaryotic translation initiation factor eIF4E. eIF4E is overexpressed in a variety of human malignancies including breast, prostate, and lymphomas, but the role of eIF4E in the biology of melanoma remains elusive. The overarching hypothesis for this thesis work is that eIF4E promotes cell survival and facilitates acquired resistance to therapeutic inhibitors in human melanoma.

We assessed eIF4E expression in BRAF mutant melanomas and its activity in a model of acquired resistance to the BRAF inhibitor, vemurafenib. We demonstrated that melanoma cell lines overexpress eIF4E, compared to immortalized melanocytes. Moreover, we identified cell lines with differential sensitivity to the effects of eIF4E silencing. Specifically, the proliferation of only those melanoma cell lines, in our cohort, that expressed hyper-phosphorylated 4E-BP1 was inhibited in response to eIF4E depletion. More importantly, in a model of acquired resistance to vemurafenib, we showed that eIF4E activity is elevated compared to their parental counterparts. Elevation of eIF4E availability by stably knocking down its repressor proteins 4E-BP1, 4E-BP2 increased the resistance to the BRAF inhibitor vemurafenib in A375 melanoma cells.

Our next goal was to (1) broaden our understanding of the role of eIF4E in the biology of other subtypes of human melanoma, and (2) determine whether blocking mRNA translation is also promising in melanomas with aberrations other than BRAF. Mnk1/2 kinases are Mitogen-activated protein kinase (MAPK)-interacting kinases. One of the best-studied substrates of Mnk kinases is eIF4E. Recently Carter and colleagues have shown the phosphorylation of eIF4E is associated with melanoma aggressiveness. cKit aberrant melanomas have a worse prognosis, high metastatic capacity, and lack effective therapeutic options. Mnk1/2 have the potential to be activated downstream of oncogenic cKit signalling. We subsequently chose to interrogate the activity of the Mnk/eIF4E axis in cKit melanomas. We illustrated that melanoma cells harbouring mutant or amplified cKit express high levels of phospho-Mnk and phospho-eIF4E. Genetic or pharmacological inhibition of cKit suppressed cell proliferation, concomitant with ablation of phospho-Mnk and phospho-eIF4E expression. Depletion of Mnk1/2 in cKit mutant HBL cells significantly decreased its clonogenicity *in vitro* and blocked melanoma outgrowth *in vivo*. Moreover, the novel Mnk1/2 inhibitor SEL201 drastically reduced the migration and invasion of cKit mutant melanoma cells.

In conclusion, these data suggest that therapeutically targeting regulators of mRNA translation is a viable means of inhibiting BRAF mutant as well as acral, mucosal and triple wild type melanomas wherein cKit is frequently mutated or amplified. We also suggest that inhibiting the Mnk/eIF4E axis may also overcome some resistance mechanisms to targeted therapies in melanoma.

Résumé

La synthèse protéique est indispensable aux cellules pour exécuter différentes fonctions telles que la prolifération, la survie et le dévelopment. La majorité des RNAs messagers dans les cellules eucaryotes est transcrit d'une façon dépendente de l'activité du facteur d'initiation de la traduction eukaryote connu sous le nom d'eIF4E. La protéine eIF4E est surexprimée dans une variété de maladies humaines, incluant le cancer du sein, de la prostate et lymphomes, mais son rôle dans le dévelopment du mélanome n'est pas entièrement connu. L'hypothèse globale de ce travail de thèse est que la protéine eIF4E permet la survie des cellules et facilite leur acquisition de résistance aux inhibiteurs thérapeutiques dans les mélanomes humains.

Nous avons évalué l'expression de la protéine eIF4E dans les mélanomes présentant une mutation du gène BRAF et évalué son activité dans un modèle où la résistance au vemurafenib, qui est un inhibiteur de la protéine BRAF, a été acquise. Nous avons démontré que les lignées cellulaires de mélanome surexprimaient la protéine eIF4E par rapport à des mélanocytes immortalisés. Nous avons de plus identifié des lignées cellulaires présentant différents degrés de sensibilité à l'extinction de la protéine eIF4E. Nous avons montré spécifiquement que seule la prolifération des lignées cellulaires de mélanomes qui surexprimaient la protéine super-phosphorylée 4E-BP1, était inhibée en réponse à l'absence de la protéine eIF4E. De façon plus intéressante, nous avons montré que dans le contexte d'un modèle où la résistance au vemurafenib a été acquise, l'activité de la protéine eIF4E est plus importante que dans le modèle originel sans resistance. L'augmentation de la disponibilité de la protéine

eIF4E, par la diminution de façon permanente de l'activité de ses protéines represseurs 4E-BP1 et 4E-BP2, augmente la resistance au vemurafenib, protéine inhibitrice de BRAF, dans les cellules de mélanome A375.

Un autre objectif était (1) d'élargir notre compréhension du rôle de la protéine eIF4E dans la biologie d'autres sous-types de mélanomes humains et (2) de déterminer si l'arrêt de la traduction de eIF4E pouvait être aussi appliqué dans les mélanomes qui présentent des mutations autres que celles de BRAF. eIF4E est un des substrats des kinases Mnk1/2. Récemment Carter et ses collègues ont montré que la phosphorylation de la protéine eIF4E était associée avec l'agressivité des mélanomes. Les mélanomes présentant des aberrations de la protéine c-Kit ont un mauvais prognostique, sont métastatiques et n'ont pas d'options thérapeutiques efficaces. Les protéines Mnk1/2 ont le potentiel d'être activées en aval de la voie de signalisation de la protéine oncogénique c-Kit. Nous avons donc choisi d'étudier l'activité de l'axe Mnk/eIF4E dans les mélanomes présentant des aberrations de la protéine c-Kit. Nous avons montré que les mélanomes ayant des mutations ou une surexpression de la protéine c-Kit présentaient aussi une expression élevée des protéines phosphorylées Mnk et eIF4E. Les inhibitions génétiques ou pharmacologiques de la protéine c-Kit arrêtent la proliferation cellulaire avec en parallele une perte d'expression des protéines phosphorylées Mnk et eIF4E. La réduction des protéines Mnk1/2 dans les cellules HBL, mutantes pour c-Kit, diminue de façon accrue leur clonogénicité in vitro et bloque la croissance des mélanomes in vivo. De plus, le nouvel inhibiteur SEL201 des protéines

Mnk1/2 diminue de façon drastique la migration et l'invasion des cellules de mélanomes ayant une protéine c-Kit mutée.

En conclusion, nos données suggèrent que les inhibiteurs thérapeutiques, ciblant les régulateurs de la transcription des RNA messagers, sont un moyen viable d'inhiber les mélanomes présentant une mutation de BRAF ainsi que les mélanomes acraux, muqueux ou mélanomes de type sauvage ou la protéine c-kit est fréquemment mutée ou surexprimée. Nous suggerons aussi que l'inhibition de l'axe Mnk/eIF4E peut être aussi un moyen de surmonter les méchanismes de resistance lors de thérapie ciblée de mélanomes.

List of Figures

Figure 2S3 The role of eIF4E in developing acquired resistance to vemurafenib.

Figure 3.1. cKit mutant melanoma patients overexpress high phospho-Mnk and phospho-eIF4E.

Figure 3.2. cKit inhibitor dasaatinib suppresses cell proliferation and the activation of Mnk/eIF4E axis in cKit melanomas.

Figure 3.3. Stable knockdown or inhibition of Mnk1/2 in HBL cells suppresses clonogenicity and tumor growth.

Figure 3.4. Mnk inhibition reduces cell migration and invasion capacities in cKit mutant HBL melanoma cells.

Figure 3.5 cKit and Mnk1/2 inhibition impairs cyclin E1 mRNA translation in cKit mutant melanoma cells.

Supplementary Table 1 Clinical information, including age, sex, thickness (Breslow), ulceration (The scores of phospho-eIF4E, phospho-Mnk1 and Mnk1 IHC staining were provided.)

Figure 3S1. Mnk1 expression detected by IHC in cKit wild type and mutant patient samples.

Figure 3S2. Imatinib only inhibits the Mnk/eIF4E axis in cKit L576 aberrant M230 melanoma cells. Overexpressing Mnk partially increases the resistance to Dasatinib in cKit mutant HBL cells.

Figure 4.1 Schematic workflow of isolating polysomes fractions and performing RNAseq

Figure 4.2 Schematic workflow of shRNA library based synthetic lethality screen

List of Abbreviations

α-MSH	Alpha-melanocyte–stimulating hormone
AREs	AU-rich elements
AUF1	ARE RNA-binding protein 1
Akt	V-akt murine thymoma viral oncogene homolog 1
Bcl-xl	B-cell lymphoma-extra large, also known as Bcl2-like 1
β-catenin	Beta-catenin
BRAF	V-Raf murine sarcoma viral oncogene homolog B
cAMP	Cyclin adenosine monophosphate
CDKN2A	Cyclin-dependent kinase Inhibitor 2A
CDK4 kinase	Cyclin-dependent kinase 4
cKit	V-kit Hardy-Zuckerman 4 feline sarcoma viral oncogene homolog
c-MYC	V-myc avian myelocytomatosis viral oncogene homolog
COT	Mitogen-activated protein kinase kinase kinase 8, MAP3K8
CREB	Cyclic AMP response element-binding protein
CSD	Chronic sun damaged (melanoma)
CTLA-4	Cytotoxic T lymphocyte antigen-4
E-box	Enhancer box
eEFs	Eukaryotic elongation factors
EGFR	Epidermal growth factor receptor
eIF4E	Eukaryotic translation initiation factor 4E
eRFs	Eukaryotic releasing factor 1
ERK	Extracellular signal-regulated kinase
GAP	GTPase activating protein
GAPDH	Glyceraldehyde-3-phosphate dehydrogenase

GDP	Guanosine diphosphate
GEF	Guanosine exchange factor
GIST	Gastrointestinal stromal tumors
GNAQ	Guanine nucleotide-binding protein G(q) subunit alpha
GNA11	Guanine nucleotide-binding protein subunit alpha-11
GTP	Guanosine triphosphate
HGF	Hepatocyte growth factor
HRAS	Harvey rat sarcoma viral oncogene homolog
HuR	Human antigen R
IGF-1R	Insulin-like growth factor I receptor
IL-2	Interleukin 2
IRES	Internal ribosome entry site
JAK	Janus kinase
KRAS	Kirsten rat sarcoma viral oncogene homolog
MAPK	Mitogen-activated protein kinases
MC1R	Melanocortin 1 receptor
Mcl-1	Myeloid cell leukemia 1
MDM2	Mouse double minute 2 protein
MEK	Mitogen-activated protein/extracellular signal-regulated kinase kinase
Met	Hepatocyte growth factor receptor
Met- tRNAi	Methionyl initiator tRNA
MHC	Histocompatibility complex
MITF	Microphthalmia-associated transcription factor
MMPs	Matrix metalloproteinases
MNKs	Mitogen-activated protein kinase (MAPK)-interacting kinases
mRNA	Messenger Ribonucleic Acid

mTOR	Mammalian target of rapamycin
NF-1	Neurofibromin 1
NGS	Next generation sequencing
NRAS	Neuroblastoma RAS viral (v-ras) oncogene homolog
Non CSD	Non chronic sun damaged (melanoma)
ORFs	Open reading frames
p38 MAPK	Mitogen-activated protein kinase 14, MAPK14
PAX3	Paired box 3
PD-1	Programmed death l
PDGFR β	Platelet derived growth factor receptor beta
PDK1	3-phospho-inositide-dependent protein kinase 1
PFS	Progress free survival
PI3K	Phosphoinositide 3-kinase
PIP2	Phosphatidylinositols
PIP3	Phosphatidylinositol phosphate
PKB	Protein kinase B, also known as Akt
PTC	Peptidyl transferase center
PTEN	Phosphatase and tensin homologue
Rb	Retinoblastoma
RGP	Radial-growth phase
RTKs	Receptor tyrosine kinases
SCF	Stem cell factor
SOX10	Sex determining region Y)-box 10
STAT	Signal transducer and activator of transcription
TP53	Tumor protein p53
tRNA	Transfer Ribo Nucleic Acid

TYR	Tyrosinase
TYRP1	Tyrosinase-related protein 1
UTRs	Untranslated regions
UV radiation	Ultraviolet radiation
VEGF	Vascular endothelial growth factor
VGP	Vertical-growth phase
43S PIC	43S pre-initiation complex
4E-BPs	Eukaryotic translation initiation factor 4E binding proteins

Acknowledgements

The experience of obtaining a Ph.D degree from McGill is like a dream come true, and it would not be happening without all the support from the people around me. The whole process of my Ph.D training in Dr. Wilson Miller's lab not only equipped me with a great deal of science research skills, both technically and perceptively, but also taught me the value of being patient, dedicated, motivated and persistent in doing scientific research or any work in my life.

First, I want to express my sincere gratitude to my supervisor Dr. Wilson Miller for his continuous support, guidance, and encouragement throughout my graduate studies. The most invaluable thing that I have learned from Dr. Wilson Miller is his critical thinking. He is always aware of tiny details from pieces of data, and from that, arising questions, making scientific presumptions and finally linking figures by inner logical flows. His perspective of tackling questions and his keenness and motivation to his job demonstrated to me the perfect example of what outstanding scientists do and how to succeed. Moreover, as my supervisor, Dr. Miller never hesitated to help broaden my options for post-graduate opportunities, and facilitated finding potential collaborations for my projects. I am certain, with bearing these methodologies in mind, it will benefit me during my whole life.

I would also like to thank my mentor Dr. Sonia Del Rincon, the work presented in this dissertation would not have been possible without her invaluable effort, generous help and countless support. Her strict training and high expectations for me

promote me to move forward and grow as a strong scientist and a critical thinker. Dr. Del Rincon always gave me the freedom to develop my own projects and ideas but at the same time made sure that my projects headed in the right direction. Meanwhile, she is also a respectful friend. She is always considerate to her students and taking care of other people in the lab, making the work environment in the lab orderly and productive. I remember she kindly provided me the opportunity of reading scientific papers and presenting to her, in an effort to help me prepare for my comprehensive exam. Also, she is always showing up for me in each of my committee meetings to protect me and help me out from every embarrassing moment. I have no doubt that her training will nourish my scientific career and her optimistic attitudes towards everything will influence me to be a better person.

I also would like to thank my committee member Dr. Leon van Kempen. He is fully supporting me for collaborating with melanoma projects. Every time I consulted him with melanoma related questions, he was always willing to explain in detail to me with patience, not merely like a professional expert but also like an old friend. Moreover, he tries his best to provide me all the materials that I need, sometimes, even with the extremely precious human samples, which are usually too limited to obtain. He is also a humorous and generous teacher to share his knowledge to his students. I still remember the time when I was preparing for my comprehensive exam, Leon lent me his textbook, which contains the comprehensive introduction of human melanoma, and this helped me a lot for increasing my understanding of melanoma and preparing answers for questions in the exam. I appreciate all the support Leon has given to me, and feel

lucky that melanoma research links us together and to have him as one of my committee members.

I would also like to thank my other committee members: Dr Lorraine Chalifour, Dr. David Dankort and Dr. Kathy Borden. Dr. Lorraine Chalifour is my Acdemic Advisor and she is always having an open door policy to a graduate student needing an understanding ear. Dr. David Dankort and Dr. Kathy Borden always provided helpful advice and guidance for my successful training at McGill University. Their encouragement and guidance taught me there is always room for improvement and expanded my knowledge of thinking.

I would also like to thank all the members of the Miller/Mann lab that I have had the pleasure to work with over the years.

Finally, my deepest gratitude goes to my parents for raising me up, and the endless love, support, patience and encouragement. I have no perfect word that can fully describe my gratitude of being their child and my acknowledgement to the substantial support of helping me fulfill my dreams. I give my deepest thanks for everyone's support and love in the completion of this dissertation.

Contribution of authors:

The candidate performed the majority of the research described in this thesis with the supervision of Dr. Wilson H. Miller and mentorship of Dr. Sonia del Rincon. The contribution of other authors to this work is as follows:

In Chapter 2, the candidate and Sonia Del Rincon designed the research. The candidate performed the research except Figure 2.2.B, Michael S. Dahabieh performed Figure 2.2.B. Marie-Noe¨l M'Boutchou, Lucy Shiru L. and Leon van Kempen provided critical reagents. Filippa Pettersson, Monica C. Dobocan, Leon van Kempen, Sonia Del Rincon, and Wilson H. Miller Jr. provided critical advice. Christophe Goncalves provided technical support, Arjuna Rajakumar provided technical support of Figure 2.D. Yao Zhan, Michael S. Dahabieh, and Sonia Del Rincon wrote the article. Filippa Pettersson, Leon van Kempen, Ivan Topisirovic Sonia Del Rincon, and Wilson H. Miller Jr. provided critical reading and editing recommendations for the paper presented in Chapter 2.

In Chapter 3, the candidate and Sonia Del Rincon designed the research. The candidate performed all the experiments. William Yang helped with tumor measuring after 19 days of initial tumor cell injection. Sonia Del Rincon helped protein validations for potential Mnk/eIF4E sensitive targets. Bonnie Huor helped establish the pBABE/ca-MNK HBL stable cells. Qianyu Guo helped remove primary tumors from pBABE/ca-MNK (3+3) mice. Ghanem Ghanem, Fabrice Journe and Leon van Kempen provided cKit mutant melanoma cell lines and critical information. Ghanem Ghanem, Fabrice Journe, Leon van Kempen, Sonia Del Rincon, and Wilson H. Miller Jr. provided critical

advice. Fan Huang, Christophe Goncalves provided general technical support. Marie Cargnello, Yutian Cai provided technical consulting for polysome profile. Yao Zhan wrote and Sonia Del Rincon edited the article.

In the General Discussion, Hongbo Chen, Sidong Huang helped perform the shRNA library synthetic lethality screen in HBL cells with Mnk inhibitor SEL201. Meng Ma, Yan Kong, Jun Guo provided all melanoma patient samples. Christophe Goncalves and Naciba Benlimame provided general technical support for IHC staining in melanoma human samples.

Chapter 1

Introduction and literature review

1.1 Melanoma

1.1.1 Melanoma incidence and mortality in the world

The skin, one of the largest organs in the human body, protects us from injury, bacteria infection(1), ultraviolet radiation from the sun(2) as well as regulates body temperature(3, 4). The skin comprises the epidermis, dermis and subcutaneous tissues layers (Figure1.1). The epidermis is the outermost layer of the skin that is in direct contact with the environment, and is the place where skin cancer (i.e. melanoma) usually arises(5). Squamous cells, basal cells and melanocytes are three major cell types within the epidermis. Skin cancers that arise from transformed squamous cells or basal cells do exist and account for around 98% of skin cancer cases. Squamous cell and basal cell carcinomas have a low metastatic capacity and are easily removed(6-9). Melanoma, on the other hand, originates from melanocytes that proliferate abnormally, and is one of the most devastating cancers.

Although only accounting for about 2% of all skin cancer patients, melanoma is the deadliest form of skin cancer and is responsible for as high as 80% of skin cancer associated deaths, whereas in nonmelanoma skin cancers such as squamous cell carcinoma, 4% of the patients develop nodular metastasis and only 1.5% dies from this disease (10-12). The incidence and mortality of melanoma has rapidly increased

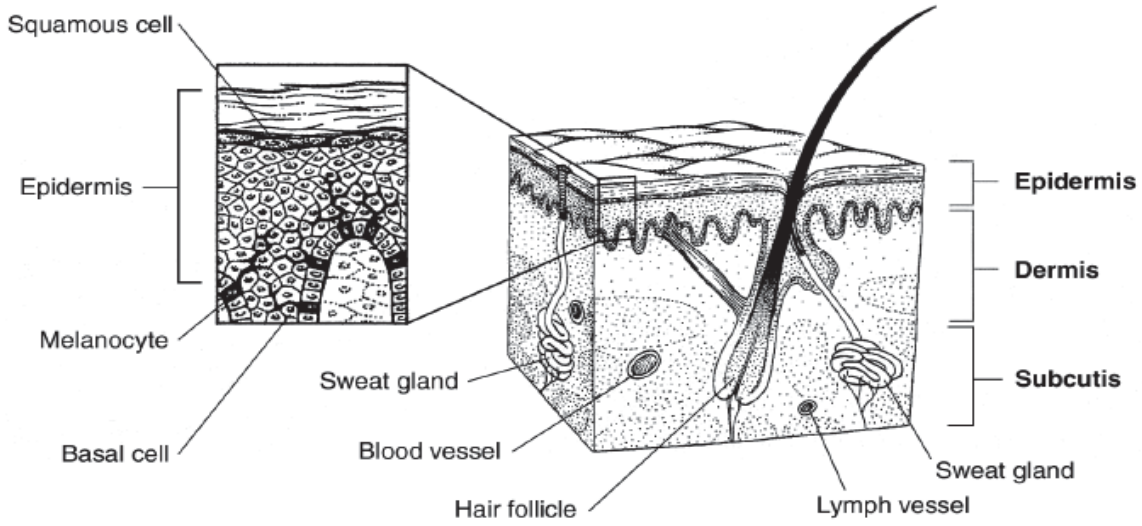

Figure1.1

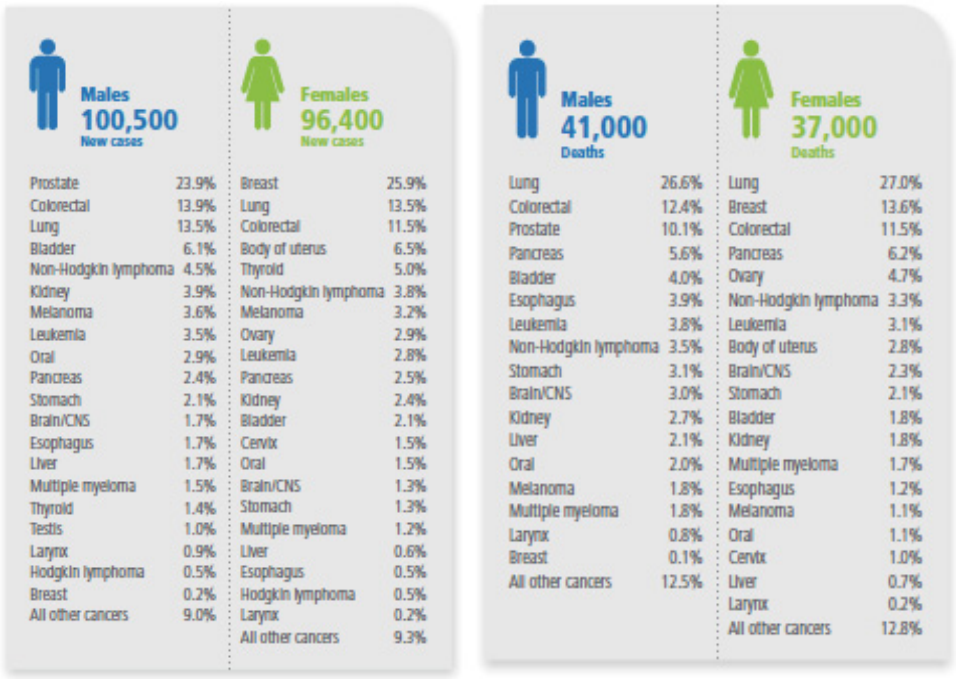

Figure1.2

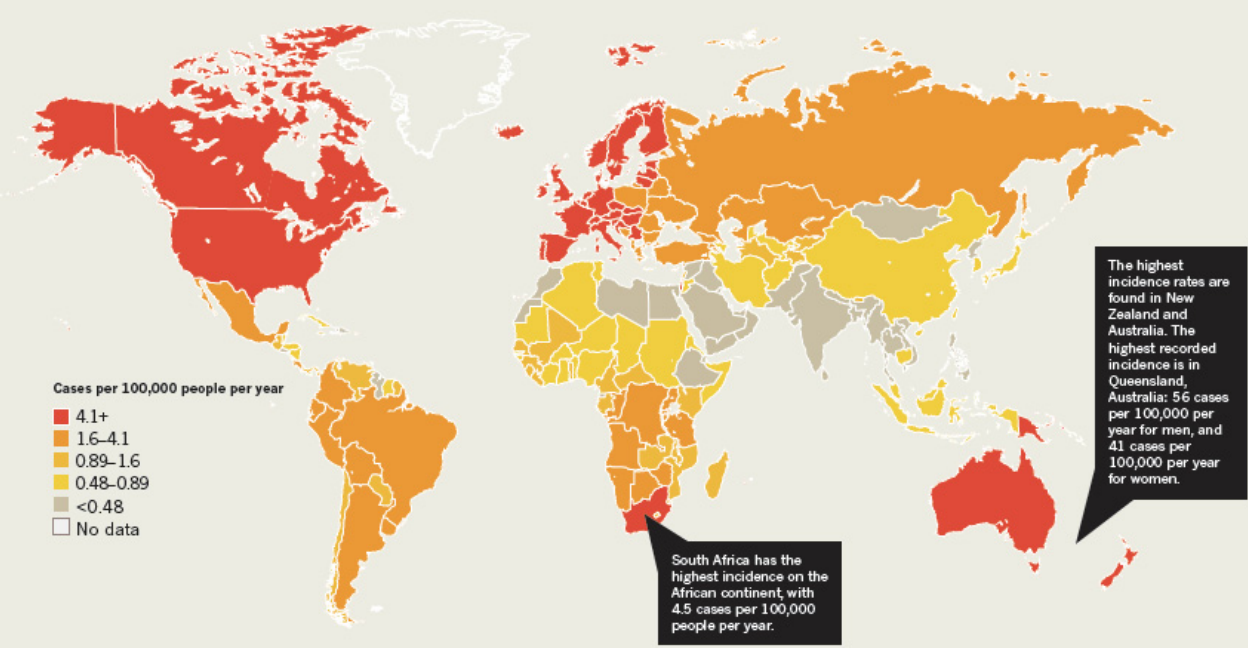

Figure 1.3

Figure 1.1 Anatomy of the skin, showing epidermis, dermis and subcutaneous structures. Adapted from the American Cancer Society website (http://www.cancer.org/cancer/skincancer-melanoma/detailedguide/melanoma-skin-cancer-what-is-melanoma)

Figure 1.2 Estimated new cases diagnosed (left) and deaths (right) in various human cancers. Adapted from Canadian Cancer Society, 2015 cancer statistics. (http://www.cancer.ca/statistics)

Figure 1.3 Global incidence of melanoma in 2012 (13).

over the past decades, according to the World Heath Organization published cancer statistics in 2012, the newly diagnosed melanoma cases were 232,000. Compared to other parts of the world, North America is one of the places with the highest incidence of melanoma(13). In 2015, it is estimated that 73,870 new cases of melanoma will be diagnosed and 9,940 of these will die in the U.S(14). Similarly, in Canada between 2001 and 2010, the incidence of melanoma has increases of 2.3% and 2.9% per year in men and women, respectively. In Canada, there will be 6,500 newly diagnosed melanoma patients and around 1,150 deaths in 2015.

Worldwide, light skinned populations are more likely to develop melanoma than tanned or black skinned populations. Northern Europe, North America, Australia and New Zealand, where light skinned inhabitants predominantly live, have the highest rates of melanoma compared to other regions in the world(13). It is believed that the susceptibility of melanoma in these people is attributed to differences in the amount and types of melanin produced by melanocytes. Different skin and hair color between races results from the different type and distribution of melanin secreted by melanocytes. There are two types of melanin, eumelanin and pheomelanin. Eumelanin, the insoluble black to brown coloured melanin, is commonly present in black and tan skinned people. Eumelanins are transferred from melanocytes to keratinocytes to form large, condensed melanosomes to serve as an “umbrella” to protect the skin from the UV radiation of the sun(15). Pheomelanins, on the other hand, are more commonly found in light skinned populations, and are a type of soluble and yellow to reddish-brown colored melanin. Unlike eumelanin, pheomelanin always displays a small and poorly aggregated pattern

of melanosome in the epidermis, thus failing to effectively protect the skin from the sun's UV radiation (16, 17).

Melanoma originates from dysfunctional melanocytes, so melanoma can be potentially found in any place where a melanocyte exists. Cutaneous melanoma, commonly found in skin, is the most predominant form of melanoma in western countries. Unlike cutaneous melanoma, certain melanoma subtypes such as those arised from acral sites and mucosal membranes are generally less prevalent. But what is interesting is that the incidence of these two types of melanoma is specifically increased in certain area of the world. It has been reported that some regions such as China and other East Asian countries, there is a substantial population of mucosal and acral melanoma(18-20). However, the reasons of this phenomenon that mucosal and acral melanoma are specifically enriched in these eastern countries are yet still elusive. Although the prevalence and death rate of different melanoma subtypes are substantially distinct from one to another; however, generally speaking, both the incident and the mortality of melanoma are keeping growing rapidly these years worldwide. Therefore, there is an urgent need to define new therapies for human melanoma.

1.1.2 Melanoma development and progression

When normal cells become cancer cells, this is a multistep process involving the acquisition of several hallmarks of cancer(21). Melanoma is one of the best models to clearly exemplify the notion that with the accumulation of multiple gene mutations, the

disease gradually completes the evolution from non-malignant, low tendency of migrated melanocytes to highly malignant and highly invasive melanomas. We currently have an understanding of the mutated genes contributing to each step of melanoma progression(10). Based on Clark's model, the development of the benign nevus is the first step of melanoma evolution(22). In this phase, a proliferation of melanocytes, due to the NRAS or BRAF gene mutations, usually occurs. Although NRAS and BRAF, known oncogenes are mutated in about 20% or over 50% melanoma patients, respectively(23), single NRAS or BRAF mutation is only capable of inducing benign nevus. This is attributed to the NRAS- or BRAF-induced senescence in melanocytes, and may explain the reason that benign nevus rarely progress to melanoma(24, 25).

The next stage toward melanoma, from benign nevus, is dysplastic nevi, which occur from either a pre-existing benign nevus or in a new location. Dysplastic nevi exhibit irregular borders and uneven colors with enlarged sizes(22) and usually require additional genetic alterations beyond BRAF or NRAS mutation. The CDKN2A gene is often mutated in dysplastic nevi (26). CDKN2A encodes 2 different products $p16^{INK4A}$ and $p19^{ARF}$, both of which function in cell cycle progression, serving as tumour suppressors in normal cells(27). $p16^{INK4A}$, the inhibitor of CDK4 and CDK6 kinase, regulates the G1/S phase cell cycle checkpoint. CDK4 is the kinase of D-type cyclins, the binding between which leads to the hyper-phosphorylation and inactivation of the tumour suppressor protein Rb. Subsequently, E2F protein is released from Rb, and then activates the transcription of genes needed for the transition from G1 to S phase (28, 29). However, excessive CDK4 activity leads to unlimited DNA synthesis and

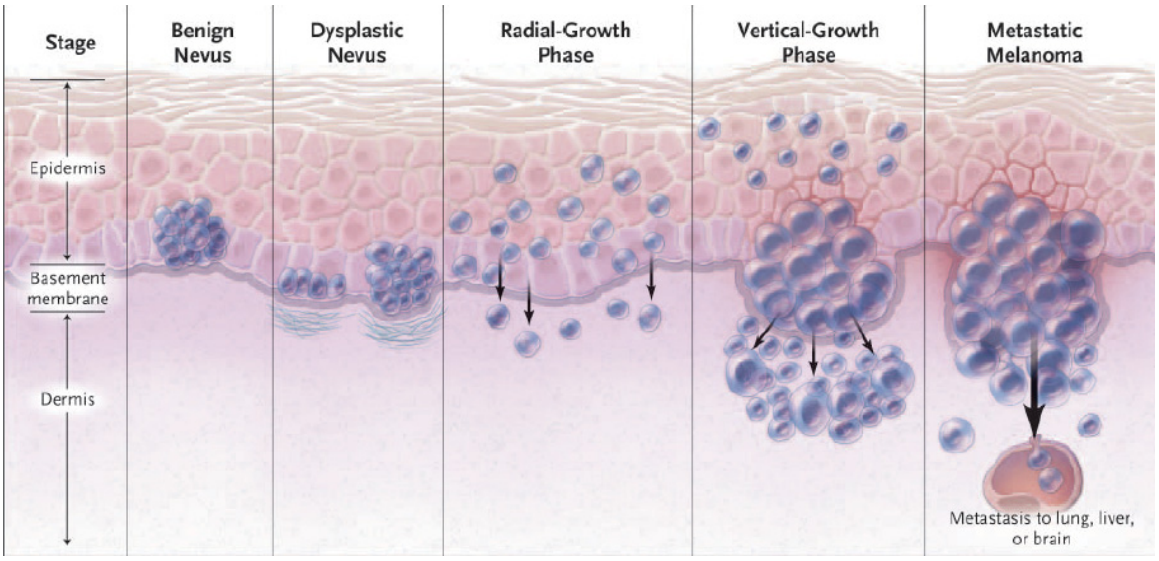

Figure 1.4

Figure 1.4 Melanoma development and progression(10).

uncontrolled cell proliferation, which can be often found in human melanomas(30, 31). So, the function of CDK4 needs to be strictly constrained, which in normal cells is regulated by $p16^{INK4A}$(32). The other protein encoded by the CDKN2A gene is $p19^{ARF}$, transcribed via an alternative reading frame. $p19^{ARF}$ is a regulator of the G2/M cell cycle checkpoint, and regulates the P53 pathway. $p19^{ARF}$ binds the mouse double minute 2(MDM2) protein, which has the ability to sequester and ubiquitinate P53(33). $p19^{ARF}$ therefore ensures that P53 is not ubiqutinated and that cells with damaged DNA arrest or apoptose if having unfixable genetic defects. This guarantees that only successfully replicated cells can go through the G2/M cell cycle checkpoint and be ready for subsequent cell mitosis(34).

The radial-growth phase (RGP) is the next stage of melanoma development after desplastic nevus. Phosphatase and tensin homologue (PTEN) loss and Akt overexpression are found in the radial-growth phase of melanoma(35, 36). PTEN dephosphorylates phosphatidylinositol phosphate (PIP3), an intracellular second messenger molecule activated by the association of upstream growth factor receptors and its corresponding ligand. Dephosphorylated PIP3 can not cause subsequent phosphorylation and activation of Akt(37). Akt (also called protein kinase B, PKB) is one of the master regulators of cell proliferation, survival and apoptosis. AKT hyperactivation, which may result from the absence of PTEN function, often leads to uncontrolled cell proliferation and resistance to apoptosis, and is thus an important pathway promoting tumorigenesis(38).

The transition from radial-growth phase to vertical-growth phase (VGP) and finally to metastatic melanoma is very important for its malignancy, because melanocytes acquire the ability to invade from the epidermis to the deeper dermis through the interfacing basal membrane. In order to fulfill these tasks, melanocytes have adapted themselves to regulate proteins that are responsible for modulating cell-cell junctions, cell survival as well as cell migration and invasion. For example, E-cadherin, a protein mostly expressed in epithelial cells and responsible for cell-cell contact, is decreased in the process of transitioning from radial-growth phase to vertical-growth phase melanoma lesions. In contrast, N-cadherin, which facilitates melanoma cells to interact with other N-cadherin expressing cells, such as dermal fibroblasts and vascular endothelial cells, increases during this transition (39, 40). Matrix metalloproteinases (MMP) are also critical regulators in the development of vertical-growth phase and metastatic melanomas. In normal skin, melanocytes, basal cells and squamous cells are compartmentalized and confined by a basement membrane to maintain the integrity and function of the skin. However, in vertical-growth phase and metastatic melanoma lesions, cancer cells degrade components of the basement membrane such as collagens and gelatins, via the activity of MMPs(41, 42). Cancer cells then migrate through the compromised basement membrane to colonize the dermis or a secondary region, via blood vessels or lymph nodes, to form metastases. Thus, melanoma initiation and progression is the collaborative result of the accumulation of various genetic aberrations in melanocytes.

1.1.3 Melanoma categorization and leading genetic alterations

According to different originating sites, melanoma can be categorized into distinct subgroups including cutaneous, acral, mucosal and uveal melanomas. More importantly, each subgroup of the melanoma posses characteristic genetic alterations(43).

Cutaneous melanoma usually arises from skin sites that cover our body such as the face, trunk, arms and legs, and this type of melanoma is the most common form of human melanoma(44). Chronic sun damaged and non-chronic sun damaged regions are included in this category, both of which have significantly different genetic aberrations. In non-chronic sun damaged melanomas, BRAF V600 mutations have been identified in more than 50% of melanomas(45). 70% of BRAF mutant patients harbour a Valine (V) to Glutamic acid (E) substitution(46). Other less common mutations in BRAF V600 include V600K and V600R, with the mutation frequency of 20% and 5%, respectively(47, 48). All these activating BRAF V600 mutations dramatically elevate the kinase activity of BRAF and cause constitutive activation of MAP Kinase signalling(49).

On the other hand, unlike the non-chronic sun damaged melanoma cases, about 15-25% of melanomas occurring in chronic sun damaged sites often contain NRAS mutations. These NRAS mutations are prevalent in codon 61, predominantly Q61K/R (34% and 35%, respectively). NRAS is also mutated at Q61L (8%) and G12D (4%) (50-52), albeit less frequently. The RAS family (N-,K-,H-RAS) encode small GTPases, that function in the activation of the RAF-MEK-ERK MAP Kinase and the PI3K-Akt-mTOR

signalling pathways. Thus, activating mutations in NRAS lead to constitutive activation of both MAP Kinase and PI3K-Akt-mTOR signalling pathways(53, 54).

Unlike the high prevalence of cutaneous melanoma, melanomas occurring on acral and mucosal sites are less common, only accounting for 5-10% of all melanoma cases(20, 55, 56). However, acral and mucosal melanoma has a poor prognosis and significant worse patient overall survival compared to cutaneous melanoma (55, 57). In a multi-center analysis of 295 patients with melanoma, the frequency of cKit aberrations in acral, mucosal, and CSD melanomas was found to be 23.8%, 24.7%, and 9.2%, respectively (58).

cKit belongs to the type III tyrosine kinase receptor family which comprises five extracellular immunoglobulin like domains, a trans-membrane domain, a self-inhibitory juxtamembrane domain and two kinase domains in the cytoplasmic compartment (59). By binding its ligand stem cell factor (SCF), it triggers the dimerization and autophosphorylation of cKit receptors. Activated cKit then recruits adaptor proteins to activate various downstream signalling pathways including the MAPK, PI3K-Akt-mTOR and JAK (Janus kinase)-STAT (signal transducer and activator of transcription) signalling pathways (60, 61). It is known these pathways are involved in cell growth, survival, migration and differentiation, thus the function of cKit is crucial for melanocyte development and maturation (62). The most common cKit alteration in melanoma is the L576P mutation located in exon 11 within the juxtamembrane domain. The L576P cKit mutation has also been found in over 80% of gastrointestinal stromal tumors (GIST)

patients and other cancers (63). Other cKit point mutations occur in exons 9, 13, 15 and 17, and cKit amplifications have also been identified (64). These activating somatic cKit alterations lead to ligand-independent, thus constitutive activation of the cKit receptor and downstream signalling pathways, producing both proliferation and survival advantages (65).

Uveal melanomas are extremely rare, accounting for less than 5% of all melanoma patients (66). More than half of uveal melanoma patients harbour mutually exclusive GNAQ or GNA11 activating mutations in their lesions. Guanine nucleotide-binding protein G(q) subunit alpha (GNAQ) and guanine nucleotide-binding protein subunit alpha-11 (GNA11) form a G-protein complex. This G-protein complex couples transmembrane domain receptors to intracellular signalling pathways such as MAP Kinase and PI3K pathways (67). 40-50% of human uveal melanomas possess a GNAQ mutation in codon 209 (Gln209Leu, denoted as $GNAQ^{Q209L}$) (68), which prevents hydrolysis of GTP and locks GNAQ in its active GTP- bound state and subsequent constitutive activation of the MAP kinase signalling pathway. $GNAQ^{Q209L}$ mutations lead to melanocyte proliferation in mice and can cooperate with other oncogenes to transform 3T3 cells and melanocytes (68, 69). Moreover, somatic activating mutations in GNA11 have been reported in 32% of GNAQ wild type uveal melanomas (70). The mutual exclusivity between GNAQ and GNA11 mutations in uveal melanomas suggests that both mutations share common downstream signalling pathways.

1.1.4 The mutation landscape in human melanoma

1. The RAS-RAF-MEK-ERK MAP Kinase signalling pathway

The RAS-RAF-MEK-ERK MAP Kinase pathway has been identified as the most aberrantly mutated signalling pathway in almost 90% of human melanoma patients(71). With the increased use of next generation sequencing (NGS), major components involved in this signalling pathway are mutated with a higher frequency in melanoma than in other human malignancies(45). BRAF and NRAS are two of the most frequently mutated genes in cutaneous melanoma, which account for over 50% and 25% of melanoma cases, respectively. In comparison, mutations in MAP2K1 (MEK1) and MAP2K2 (MEK2) genes, two kinases immediately downstream of RAS and RAF, are less commonly mutated than RAS and RAF, only occurring in about 8% of melanoma patients (72), but MEK1 and MEK2 have been identified involved in resistance to BRAF inhibitors (see detailed discussion in resistance mechanism section). Mutations in the small G proteins GNAQ and GNA11 are mutually exclusive, and prevalent in about 90% of human uveal melanoma. GNAQ and GNA11 mutations affect the subunit alpha q and alpha 11 of the G protein respectively, which renders the G protein and downstream MAP Kinase signalling pathway constitutively active (68).

2. NF-1

Neurofibromin 1 (NF-1) is another negative regulator associated with the RAS-RAF-MEK-ERK signalling pathway. The *NF-1* tumour suppressor gene encodes a GTPase activating protein, which facilities the hydrolysis of RAS-GTP to RAS-GDP(73). RAS is a small G protein requiring the binding with GTP for its full activation.

Accordingly, the maintenance of NF-1 expression is crucial for modulating the activity of RAS in normal cells. NF-1 inactivating mutation or deletion have been reported in familial cancer syndrome neurofibromatosis type I, lung cancer and glioblastoma(74, 75). In human melanoma, NF-1 ablation overcomes BRAF induced senescence and in a mouse model it promotes melanocyte proliferation and desensitizes to BRAF inhibitors(76). Recently, two independent large-scale, comprehensive analyses of melanoma patient samples showed that NF-1 is mutated and mutations in this gene are the third most frequent in cutaneous melanoma, accounting for about 14% within the melanoma patient cohort(77, 78). Loss of NF-1 function leads to hyper-activation of RAS and thus contributes to constitutive activation of the MAP Kinase and PI3K-AKT-mTOR signalling pathways in melanoma. Melanomas mutated in NF1 are mutually exclusive with BRAF and RAS mutations (78).

3. Receptor tyrosine kinases (RTKs)

Receptor tyrosine kinases are transmembrane cellular surface proteins that transduce signals from extracellular stimuli, by activating signalling cascades that ultimately trigger an intracellular response. The phosphorylation of tyrosine residues on receptor tyrosine kinases is crucial for their auto-activation and subsequent activation of downstream effectors, thus, the activation of RTKs has to be strictly controlled(79). Activating mutations in receptor tyrosine kinases can facilitate tumorigenesis in various cancers, including melanoma. cKit is frequently mutated in mucosoal, acral and chronic sun damaged melanomas. Activating mutations have been identified in cKit exons 11,

13, and 17, which result in the constitutive activation of cKit and constitutive downstream MAP Kinase and PI3K-AKT-mTOR signalling(65).

Mutations and amplifications in the epidermal growth factor receptor (EGFR) have been documented in melanoma. In a study of 25 melanoma patients with lung metastases, 17.5% of the cases with polysomy on chromosome 7 was found EGFR overexpressed(80); in another study of 110 nodular melanoma, EGFR amplification was detected in 4% of the samples(81). On the other hand, 238 genetic mutations on 19 oncogenes were analyzed in 58 acral and mucosual melanoma samples, in which EGFR mutation was only detected in 2 (3.5%) cases(82). Several *in vitro* based studies using melanoma cell lines have revealed the importance of EGFR to melanoma biology. For instance, EGFR overexpression facilitates melanoma cell proliferation, while inhibition of EGFR blocks proliferation (83, 84). In an inducible $HRAS^{V12G}$ mutant mouse model, the EGF family of ligands were overexpressed and autocrine EGFR activation ensued. Furthermore, inhibition of EGFR activity by introducing a dominant negative EGFR into the $HRAS^{V12G}$ mouse model dramatically ablated tumor formation, compared to the wild type counterparts (85). Similar to cKit, the activation of EGFR also triggers the activation of dual MAP Kinase and PI3K-AKT-mTOR signalling pathways.

The Met receptor tyrosine kinase binds to its ligand hepatocyte growth factor (HGF) and activates downstream MAP Kinase and PI3K-AKT-mTOR signalling pathways. Depletion of Met activity has also been reported in melanoma cell lines to be associated with RAS mediated tumor growth and metastasis. Introducing a functionally

inactivated, dominant negative mutant version of Met in melanoma cell lines abrogated RAS induced cell transformation *in vitro*. Furthermore, inhibition the HGF/Met signalling

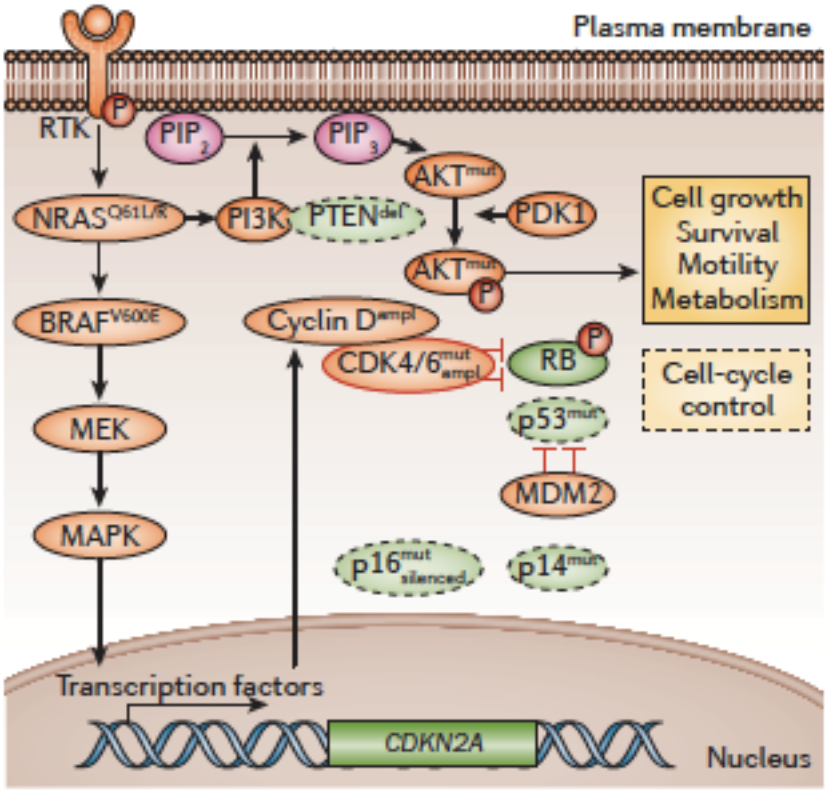

Figure 1.5

Figure 1.5 Genetic aberrations in signalling pathways in human melanoma (Schadendorf D, *et al.*(2015) Melanoma. *Nature Reviews Disease Primers,* 10.1038/nrdp.2015.3)

pathway causes decreased tumor growth as well as a reduction of lung metastasis in a mouse model(86).

4. The PI3K-AKT-mTOR signalling pathway

Next-generation sequencing of large-scale human melanoma samples revealed that the PI3K-AKT-mTOR was commonly mutated in melanoma patients(44, 87). PI3K is activated by RTKs and RAS proteins. Activated PI3K then adds a phosphate group on phosphatidylinositols (PIP2) to generate the intracellular secondary messenger molecule-phosphatidylinositol phosphate (PIP3). PIP3 is attached on the cytoplasmic membrane surface to recruit and activate the 3-phospho-inositide-dependent protein kinase 1 (PDK1), which will eventually function with mTORC2 kinase to contribute to the full activation of the serine/threonine kinase AKTs (AKT1, AKT2, AKT3). The activation of the PI3K-AKT-mTOR signalling cascade is crucial for cell proliferation, protein synthesis, motility and metabolism. PTEN reduces the production of PIP3, by dephosphorylating it into PIP2, thereby limiting the activity of the PI3K-AKT-mTOR pathway. PTEN mutations or deletions have been reported in about 40% of human melanomas(44). PTEN aberrations have been proposed to be associated with the intrinsic resistance to BRAF inhibitors (88). Mutations in PTEN can co-exist with BRAF mutations to collaborate in melanomagensis. On the contrary, PTEN is rarely found to be mutated in tumors with NRAS mutations, which makes sense when one considers that NRAS and PTEN aberrations share the activation of common downstream signalling pathways(89). Other components that are mutated in this signalling pathway

include PI3KCA (encoding the catalytic subunit of PI3K, mutant in 2-6% of melanoma), AKT1 (1-2%) and AKT3 (1-2%) (90).

5. The cell cycle regulation pathways

As mentioned in section 1.2, a major regulator of cell cycle progression that is mutated in over 10% of all melanoma patients is CDKN2A. In familial melanoma cases, CDKN2A alterations have been identified in over 40% of patients' genome (91, 92). CDKN2A encodes two tumor suppressors $P16^{INK4A}$ and $P14^{ARF}$ and these are responsible for the transitions from the G1 to S phase and S phase to G2 phase of cell cycle, respectively.

Beyond CDKN2A gene mutations, other genes involved in the $p16^{INK4A}$/CDK/RB and $P14^{ARF}$/MDM2/P53 pathways are mutated in human melanoma. According to a recent article of genetic mutation analysis of 331 cutaneous melanoma patients, P53 and RB1 mutations were reported in 15% and 3.8% of the samples respectively (78). In another report, based on exome sequencing of 121 melanoma patient samples, CDK4 amplification was found in 3% of the samples and cyclin D1, the activator of CDK4, was amplified in 11% of patients in this cohort (44).

6. The pigmentation regulation pathway

Melanoma arises from the specialized pigment-producing melanocytes. Melanocytes are derived from neural crest progenitors and then localize to the skin, mucosal epithelia, and eye. The development of melanocytes depends on the regulation

of cKit and the master regulator of pigmentation gene microphthalmia-associated transcription factor (MITF) (93). Pigment production in melanocytes is associated with the activation of the melanocortin 1 receptor (MC1R). MC1R is a G protein coupled receptor that transduces signals from the extracellular membrane alpha-melanocyte–stimulating hormone (α-MSH). Binding with α-MSH triggers MC1R activation and subsequent phosphorylation of cyclin adenosine monophosphate (cAMP). cAMP production activates cAMP response element-binding protein (CREB) mediated transcriptional activation of MITF. MITF in turn transcribes various pigmentation synthesis genes such as TYRP1 (tyrosinase-related protein 1) and TYR (tyrosinase) (94). MC1R mutations are associated with fair skin and susceptibility to melanoma in light skinned populations. Furthermore, MITF amplifications have also been found in 4-21% of melanomas (44, 95). Genes that are involved in pigmentation regulation such as PAX3 (paired box 3), SOX10, beta-catenin (β-catenin), have also been reported mutant in melanoma (89, 94).

7. The crosstalk between the MAPK and PI3K-AKT-mTOR signalling pathways

Both MAPK and PI3K-AKT-mTOR signalling pathways are highly activated in various human cancers, including melanoma, and are responsible for cell proliferation and survival. Although the MAPK and PI3K pathways can facilitate distinct cellular functions, it has been shown that there is crosstalk between these two important signalling cascades.

First of all, extracellular signal-regulated kinase (Erk) in the MAPK signalling pathway is able to phosphorylate and inactivate the inhibitory TSC complex, thus activating the PI3K-AKT-mTOR pathway. TSC complex is a Rheb (Ras homolog enriched in brain)-GTPase activated protein, which is located downstream of AKT. Usually, the TSC complex hydrolyzes Rheb-GTP into Rheb-GDP, therefore blocking downstream mTOR signalling (96). ERK-dependent phosphorylation dissociates the TSC complex and markedly impairs its ability to inhibit mTOR signalling, cell survival and oncogenic transformation (97). On the other hand, It has also been found that the P90 ribosomal S6 kinase (RSK) 1, the mitogen-activated protein kinase (MAPK)-activated kinase, interacts with and phosphorylates the TSC complex at a regulatory serine-1798, to negatively regulate the tumor suppressor function of the TSC complex, resulting in increased mTOR signalling (98). Together, these data show that the MAPK and PI3K pathways converge on the tumor suppressor TSC to inhibit its function.

Other than indirectly activating mTOR signalling, by stimulating Rheb GTP-loading through the inactivation of TSC complex, RSK can also directly phosphorylate and thus promote mTOR activity. RSK phosphorylates three evolutionarily conserved serine residues on Raptor (ser719, ser721, ser722), which is one of the components of the mTOR complex. RSK stimulated phosphorylation of Raptor leads to a conformational change in Raptor that allows the activation of mTOR (99). More recently, it is been found that ERK kinases phosphorylate Raptor on three proline-directed residues (ser8, ser696, ser863) to activate mTOR. Together, these findings support that the members of the MAPK pathway, ERK or RSK, activate mTORC1 signalling via a

two-fold mechanism, the phosphorylation of both the TSC complex and Raptor (Figure 1.6).

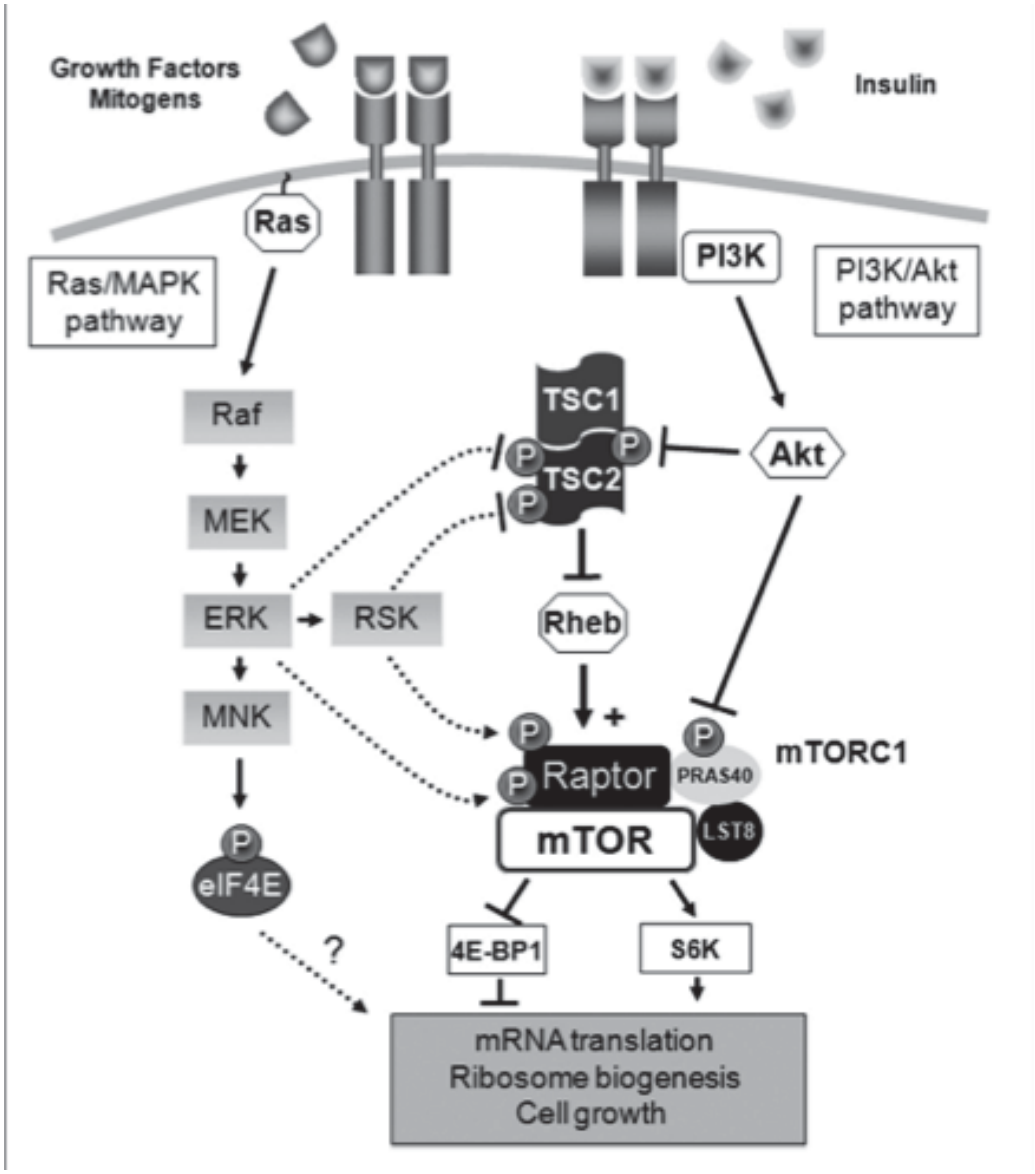

Figure 1.6 Potential for crosstalk between the MAPK and the PI3K signalling pathways.

1.1.5 Current therapies in human melanoma

Surgical excision, the gold standard for treating the majority of early stage human malignancies, is used to treat melanoma patients showing no regional metastases to lymph nodes. However, once these patients get distant metastases, surgical intervention is no longer suitable. Over the past 35 years, there were only two chemotherapeutic drugs, dacarbazine and high-dose interleukin 2 (IL-2), approved to treat unresectable or metastatic melanoma. Nevertheless, both drugs neither improved the median overall survival (100), nor did they lead to significant response rates in metastatic melanoma patients. The response rate of dacarbazine is 15-20%, and that of high dose IL-2 is lower than 16% (101, 102). Both drugs exhibited severe toxicities in melanoma patients; therefore, developing novel therapies with higher efficacy and specificity were urgently needed.

In the past five years, the melanoma research field has witnessed the unprecedented success of translating basic science discoveries from the bench to the clinic. The successive approval of six therapeutic drugs (ipilimumab, vemurafenib, dabrafenib, trametinib, pembrolizumab, nivolumab) for treating metastatic melanomas by the US FDA has elicited public attention toward targeted therapies and immunotherapies for this deadly disease.

1. The RAS-RAF-MEK-ERK MAP Kinase pathway targeted therapies

In 2002, Davies and colleagues published their seminal work (45), identifying BRAF alterations in about 50% of human melanomas. Since then, a lot of work has

been done in analyzing the mutation landscape in human melanomas. Multiple components of the RAS-RAF-MEK-ERK MAP Kinase pathway are mutated and lead to hyper-activation of MAPK signalling in human melanomas (NRAS, BRAF, NF-1, MEK1/2 mutations have been identified, see section 1.4 for details). Given this, several therapeutic drugs with high specificity and efficacy for targeting the RAS-RAF-MEK-ERK MAP Kinase signalling pathway were designed.

Vemurafenib (Zelboraf, Hoffmann-La Roche Inc., Basel, Switzerland), is a BRAF selective inhibitor, and the first US FDA approved targeted therapeutic drug for metastatic melanoma patients harbouring the BRAF V600E mutation. Vemurafenib exhibited dramatic response rates and overall survival benefits for patients with metastatic melanoma (103). The phase I clinical trial identified that 960mg twice daily was an appropriate dose of vemurafenib for use in patients(104). The phase II clinical trial of vemurafenib (BRIM-2 study), demonstrated a 53% response rate in the 132 BRAF V600E mutant melanoma patients enrolled. Furthermore, the median duration of response was 6.7 months and the median progression free survival (PFS) was 6.8 months (105). The results of the BRIM-2 study encouraged the opening of a phase III clinic trial of vemurafenib (BRIM-3 study). The primary endpoint of this trial was to determine the superiority of vemurafenib over dacarbazine in improving patient overall survival. 675 BRAF V600E/K mutant melanoma patients without previous treatment were randomly separated into the vemurafenib group (n=337, 960mg/kg, twice daily) or dacarbazine group (n=338, 1000mg/m^2, every 3 weeks) (103, 106). Promisingly, Vemurafenib treated patients showed improved median overall (13.6 months versus 9.7

months) survival and PFS (6.9 months versus 1.6 months) over the dacarbazine treated group. Therefore, based on the outstanding effect of vemurafenib in this phase III study, the US FDA approved the usage of vemurafenib in BRAF V600E mutant metastatic melanomas on August 17, 2011.

Another BRAF selective inhibitor, dabrafenib (Tafinlar, GlaxoSmithKline, London, UK), showed similar efficacy in BRAF V600 mutant melanoma patients. The phase I and II trials of dabrafenib in BRAF V600E/K mutant melanoma patients achieved 69% and 59% of response rate, respectively (107, 108). The phase II trial of dabrafenib also identified the median PFS was 6.3 months, and a median overall survival of 13.1 months (108). In the phase III clinical trial, the survival benefit of dabrafenib over dacarbazine was compared in 250 patients. In this study, BRAF V600 mutant metastatic melanoma patients received either dabrafenib (150 mg twice daily, orally) or dacarbazine (1000mg/m^2 intravenously every 3 weeks) in a 3:1 ratio. A 53% over 6% response rate was observed in patients treated with dabrafenib compared to those with dacarbazine. Furthermore, an improved PFS was reported in patients with dabrafenib compared to the dacarbazine group (5.1 months compared to 2.7 months) (109). Based on the superior effect of dabrafenib over dacarbazine reported in this phase III clinical trial, in May 29, 2013, the US FDA approved dabrafenib for use in BRAF V600E mutant metastatic melanoma patients.

Trametinib (Mekinist, GlaxoSmithKline), a targeted inhibitor for MEK1/2 kinases, has also shown dramatic effects in clinical trials of patients with BRAF V600

mutant metastatic melanomas. In a phase I clinical trial of Trametinib, BRAF V600E/K mutant melanoma patients with no previous BRAF inhibitor treatment showed a 33% response rate (110, 111). In a phase II clinical trial, 97 patients were divided into two groups based on prior use of BRAF inhibitor. In group A, 40 patients had received prior BRAF inhibitor, while the remaining 57 patients had prior treatment with immunotherapy or chemotherapy (group B). Trametinib had no effect on patients with previous BRAF inhibitor treatment (group A) but led to a 25% response rate in BRAF inhibitor naïve patients (group B) (112). This observation implies that patients refractory to BRAF inhibitor treatment are not suitable for subsequent of MEK inhibitor treatment. In the phase III clinical trial of 322 BRAF V600E/K mutant metastatic and treatment naïve melanoma patients, trametinib showed superior progression free survival and response rate over standard chemotherapeutics. Patients were randomly assigned to receive trametinib (2 mg once daily, orally) or chemotherapy (dacarbazine 1000 mg/m2 intravenously or paclitaxel 175 mg/ m2, every 3 weeks) in a 2:1 ratio. Trametinib showed increased median PFS (4.8 months) and overall survival (81%) at six months compared to chemotherapy group (1.5 months PFS and 67% overall survival). In addition, trametinib treatment demonstrated 22% response rates in enrolled patients (113). The US FDA subsequently approved the use of trametinib for BRAF V600E/K mutant metastatic melanoma patients in May 29, 2013.

Although BRAF inhibitors successfully repress melanomas and improve overall survival in patients with BRAF V600 mutations; these effects are not sustainable. Almost all patients will develop acquired drug resistance about 6 months after their

initial response to BRAF inhibitor treatment. Investigation of preclinical models with acquired resistance to BRAF inhibitors revealed that reactivation of the MAP Kinase signalling pathway substantially contributes to the process of developing BRAFi resistance. Therefore, these studies prompted the evaluation of combining BRAF and MEK inhibitors in BRAF V600 mutant metastatic melanoma patients. The first phase I/II clinical trial with combined BRAF plus MEK inhibitor therapy demonstrated the superior progression free survival over monotherapy. In this clinical trial, 162 patients were randomly divided into either group I or group II to receive dabrafenib (150 mg, twice daily) and trametinib (1mg, once daily in group I; 2mg, once daily in group II). Patients in group II showed improved median PFS compared to dabrafenib monotherapy (9.4 months versus 5.8 months). This group also showed increased response rates compared to dabrafenib monotherapy (76% versus 54%). Although the BRAF and MEK inhibitor combination group showed decreased frequency of developing secondary cutaneous squamous cell carcinomas over dabrafenib monotherapy (7% versus 19%), the patients on this trial had more frequent adverse effects such as fever, nausea and vomiting (114). In the phase III clinical trial, 423 patients were randomized to receive dabrafenib plus placebo (D+P) or dabrafenib plus trametinib (D+T). Both median progression free survival (9.3 months versus 8.8 months) and response rate (67% versus 51%) were significantly improved in the D+T group compared to the dabrafenib monotherapy group (115). Considering these facts, the US FDA granted accelerated approval for the combination of dabrafenib plus trametinib in patients with BRAF V600 mutant metastatic melanoma in January 14, 2014. Two additional phase III clinical trials of BRAF plus MEK inhibitors have been reported. One was comparing the superiority of

vemurafenib plus cobimetinib (MEK inhibitor) versus vemurafenib, and the other was comparing the superiority of dabrafenib plus trametinib over BRAF inhibitor vemurafenib. These two clinical trials demonstrated improved median progression free survival and increased response rates in the BRAF plus MEK inhibitor treated group over the single BRAF inhibitor treated group (116, 117). Together, these trials have culminated in the standard clinical use of BRAF and MEK inhibitor combination therapy for the treatment of BRAF V600 mutant metastatic melanoma.

2. Immunotherapy

There are two major types of immunity in the human body: innate and adaptive. Innate immunity is associated with nonspecific defense mechanisms against unrecognized antigens that appear in the body. This type of immunity usually engages the secretion of cytolytic enzymes or inflammatory factors by macrophages, granulocytes and antigen presenting cells to kill exogenous infections. Unlike innate immunity, adaptive immunity involves antigen-antibody recognition and the effect of this type of immunity usually lasts long, attributed to the presence of memory immune cells generated in this process. The adaptive immunity triggers the activation of two types of lymphocytes: antibody producing B lymphocytes and cytotoxic T lymphocytes. T lymphocyte activation is regulated by the co-stimulatory and co-inhibitory receptors located on the surface of the cells to fine tune the homeostasis of self-protection and autoimmunity. The full activation of T cells requires two steps: Initially, the T cell receptor binds to the tumor antigen presented with major histocompatibility complex (MHC) proteins and secondly, the co-stimulatory receptor CD28 on T cells binds to ligand B7.1 and B7.2 on antigen presenting cells. The inhibitory T cell receptor cytotoxic

T lymphocyte antigen-4 (CTLA-4) can compete with CD28 for binding to B7.1 and B7.2, therefore dampening the function of T lymphocytes. Another inhibitory receptor on T lymphocytes is programmed death I (PD-1) receptor. PD-1 eliminates the activation of cytotoxic T cells by binding with its ligands PD-L1 and PD-L2 on tumor cells to evade immune surveillance. Cancer cells use the CTLA-4 and PD-1 immune checkpoints as a means of evading immune assaults. Several monoclonal antibodies that target these immune checkpoints have been invented to counteract the action of CTLA-4 and PD-1.

Ipilimumab (Yervoy, Bristol-Myers Squibb) is the first humanized IgG1 monoclonal antibody that blocks the CTLA-4 receptor to restore T cell activation in metastatic melanomas. In phase I/II clinical trials, ipilimumab showed prolonged median survival and sustained benefit in melanoma patients (118, 119). In a phase III clinical trial, 676 metastatic melanoma patients were randomly assigned to receive ipilimumab (3mg/kg intravenously every 3 weeks) plus vaccine gp100, ipilimumab alone, or gp100 alone. Ipilimumab significantly increased median overall survival (10.1 months compared to 6.4 months in the vaccine group)(120). Another phase III clinical trial randomly assigned 502 patients to receive ipilimumab (10mg/kg) plus dacarbazine or dacarbazine plus placebo. Similarly, patients receiving ipilimumab treatment had a dramatically improved overall survival (11.2 months versus 9.1 months) over the dacarbazine group (121). Given this result, the US FDA approved ipilimumab for treating metastatic melanomas in March 25, 2011.

Pembrolizumab (Keytruda, Merck & Co) is a humanized IgG4 monoclonal antibody against PD-1. A phase I clinical trial in 173 metastatic melanoma patients that

had progressed after ipilimumab or BRAF/MEK inhibitors showed that patients receiving pembrolizumab (either 2 mg/kg or 10 mg/kg every 3 weeks) had a overall response rate of 26%. Furthermore, 88% of the responders continued to respond after 8 months of treatment. (122). Based on these results, in September 2014, the US FDA, granted accelerated approval of pembrolizumab for the treatment of advanced melanomas that are resistant to other therapies (ipilimumab or BRAF/MEK inhibitors). Nivolumab (Opdivo1, Bristol-Myers Squibb) is the second FDA-approved anti-PD1 monoclonal antibody. Similar to pembrolizumab, nivolumab also showed superiority in improving median duration of response, overall survival (1 year 72.9% versus 42.1% in the chemotherapy group) and objective response rates of 32% versus 11% in the chemotherapy arm (123, 124). Therefore, the US FDA granted accelerated approval for nivolumab on December 22, 2014 for metastatic melanomas with disease progression following ipilimumab or BRAF inhibitor treatment.

Combinatorial therapies targeting both CTLA-4 and PD-1 are currently under investigation. Results from the phase I clinical trial combining nivolumab with ipilimumab appear encouraging. Dual administration of immune checkpoint inhibitors of CTLA-4 and PD-1 show greater response rates compared to targeting either receptor alone. In this trial, 53 patients were assigned to receive ipilimumab plus nivolumab concurrently and 33 patients with previous ipilimumab treatment were assigned to receive nivolumab. This trial showed the responses are durable, with a 2-year survival rate of 79%. In a recent phase III study, nivolumab plus ipilimumab therapy was compared with ipilimumab or nivolumab alone in patients with metastatic melanoma. Once again, the

phase III trial showed superiority of combinatorial anti-CTLA-4 and anti-PD-1 therapy over single immune checkpoint inhibitor therapies. The results showed median progression-free survival was improved to 11.5 months with nivolumab plus ipilimumab from 2.9 months with ipilimumab alone or from 6.9 with nivolumab alone (125). Actually there are several clinical trials of combining targeted and immune therapies going on nowadays such as Dabrafenib ± trametinib + ipilimumab (NCT01767454), Vemurafenib + Anti PDL1 (MPDL3280) (NCT01656642), Dabrafenib + trametinib + anti PD1(MK-3475) (NCT02130466) and Trametinib ± dabrafenib + anti PDL1(MEDI4736) (NCT02027961), it will be of great interest to see in the future if the combination therapy in afore-mentioned trials is superior than single therapy alone.

3. cKit targeting therapies

cKit is a member of the tyrosine kinase receptor family, and can be activated by its ligand stem cell factor (SCF). Kit aberrations have been found in acral, mucosal and chronic sun-damaged melanomas (126). In melanoma, approximately 70% of KIT mutations occur in the juxtamembrane or kinase domains, leading to constitutive activation of downstream cKit signalling. Various tyrosine kinase inhibitors (TKIs), such as imatinib, sunitinib, nilotinib and dasatinib, have been tested to treat melanomas with cKit aberrations.

Imatinib is a multi- kinase inhibitor, which can suppress the activity of BCR-ABL, cKit, and platelet-derived growth factor receptor (PDGFR). Imatinib showed remarkable efficacy in gastrointestinal stromal tumors (GIST) patients with *KIT* alterations, however it showed very limited effect in cKit melanoma patients (127, 128).

In addition, melanoma patients also exhibited poor responses to the cKit inhibitor dasatinib (129). In a phase II clinical trial, the cKit inhibitor sunitinib showed no significant difference in response or overall survival in patients with or without *KIT* mutation (130). However, more recent clinical trials demonstrated that cKit inhibitors benefited only those patients with selective Kit mutations. For instance, although a phase II clinical trial of imatinib showed moderate response rates, 90% of those who showed partial responses harboured mutations in cKit exon 11 or 13 (131). Similar results were obtained in another imatinib clinical trial, demonstrating durable responses in patients harbouring cKit mutations, but not amplification (58). These reports clearly suggested that Kit inhibitors should be used in selected patients who have cKit mutations, but not in those having wild type or amplified cKit (132).

1.1.6 Mechanisms of acquired resistance to BRAF inhibitors

While BRAF inhibitors achieve dramatic response rates in BRAF V600 mutant human melanomas, these are not durable. About 10% of BRAF V600 mutant melanoma patients have progressive disease as their best response, implying that a portion of BRAF V600 mutant melanoma are intrinsically resistant to BRAF inhibitor targeted therapies. Moreover, even in patients who do respond to BRAFi treatment, complete response rates are low and variable (about 5%). The reported median progression free survival was only 7 months, and patients receiving BRAF inhibitor treatment inevitably develop acquired resistance to BRAF targeted therapeutic agents.

Multiple mechanisms have been identified in melanomas with acquired resistance to BRAF inhibitors, and two core pathways involved in this process are reactivation of MAP Kinase signalling and PI3K-AKT-mTOR signalling activation. In a comprehensive analysis of 100 melanoma specimens including baseline tumors and progressing tumors, MAP Kinase signalling reactivation was found in 52% of cases, whereas, the activation of PI3K-AKT-mTOR signalling accounts for 18% of the samples. In this same cohort, 4% of tumors had only PI3K-AKT-mTOR signalling activation (133). These data demonstrate that the reactivation of MAP Kinase signalling is still the predominant mechanism for developing acquired resistance to BRAF inhibitors in BRAF mutant melanomas.

Although concurrent RAS and BRAF mutation are mutually exclusive in baseline melanoma tumors, the activation of N-or K-RAS are found in approximately 37% of tumors with acquired resistance to BRAF inhibitors (133). In a model of *in vitro* acquired resistance to vemurafenib, the NRAS Q61K mutation upregulated RAS kinase activity and the reactivation of MAP Kinase signalling conferred drug resistance to vemurafenib (134). In the same paper, the authors identified another cohort of vemurafenib resistant cells that were overexpressing the tyrosine kinase receptor PDGFR β. Other tyrosine kinase receptors, such as IGF-1R and EGFR, have also been reported to be upregulated in other models of acquired resistance to vemurafenib (135, 136). Of note, NRAS or RTK upregulation activate not only MAP Kinase signalling, but also the PI3K-AKT-mTOR pathway in tumors with acquired resistance to BRAF inhibitors. Tumor micro-environment can also induce resistance to the BRAF inhibitor

vemurafenib. As reported in an co-culture *in vitro* model, the secretion of hepatocyte growth factor (HGF) by stromal cells in the tumor micro-environment bound to MET receptor on cancer cells and triggered the MAP Kinase and PI3K-AKT-mTOR signalling activation, thus promoting resistance to BRAF inhibitor vemurafenib. In addition, the author also found that in 34 patients with melanoma, those who expressed high HGF had poor response to BRAFi treatment than the HGF low counterparts (137).

The modulation of BRAF kinase has also been identified as a mechanism of acquired resistance to BRAF inhibitors. While secondary BRAF mutations are rarely found, a 61-kDa splice variant form of BRAF V600E was identified in an *in vitro* model of acquired vemurafenib resistance. This splice variant form of BRAF (p61BRAF V600E) lacks exons 4 to 8, which are responsible for RAS-binding activity, thus, it has a low affinity for RAS GTPase. However, the p61BRAF V600E displays enhanced dimerization activity compared to the BRAF V600E to activate downstream signalling in a RAS independent manner (138). BRAF amplification is yet another mode of developing resistance to vemurafenib (139).

In order to identify potential targets that lead to the development of acquired resistance to vemurafenib, Johannessen and colleagues expressed 600 kinase and kinase-related open reading frames (ORFs) in parallel, and compared the effect of this on sensitivity to vemurafenib. They identified that MAP3K8 (COT kinase) promoted the activation of MAP Kinase pathway and drove resistance to vemurafenib. Further experiments showed that COT phosphorylated MEK1/2 kinases to activate downstream

ERK in a RAF independent manner (140). Other than COT kinase, MEK mutations were also found associated with acquired resistance to vemurafenib in a phase II clinical trial. Interestingly, 92 patients with mutations in MEK1 P124 coexisting with BRAFV600 were still sensitive to vemurafenib. Whereas, the presence of secondary mutations in MEK1 Q56P or MEK1 E203K were identified in patients with acquired resistance to vemurafenib, and these MEK1 mutations were associated with elevated ERK1/2 levels and reactivation of MAP Kinase signalling pathway (141). Similarly, the MEK1 C121S mutation was reported in a patient who developed resistance to vemurafenib and it was associated with increased MEK1 kinase activity and conferred robust resistance to both RAF and MEK inhibition (142). Recently, another mechanism involved increased activity of translation initiation factor eIF4E has been reported in melanoma with acquired resistance to BRAF inhibitor vemurafenib both in cell line models and in patients, which arised a novel perspective of targeting protein translation initiation in melanoma therapies(143, 144). Considering the inevitable resistance to current BRAF or MEK inhibitors, new therapeutic targets are urgently needed.

1.1.7 Mechanisms of resistance to cKit inhibitors

Although cKit inhibitors have shown dramatic clinical effects in gastrointestinal stromal tumors (GIST) patients, with almost 80% response rates (145), unfortunately these inhibitors have diminished efficacy in cKit aberrant melanoma patients. The mechanisms of resistance to these targeted therapies in melanoma are still largely unknown. This may be due, at least in part, to the limited number of patients on different kinase inhibitors. Some evidence, from both clinical and pre-clinical studies, may

provide some clues to explain the underwhelming responses to cKit inhibitors in melanoma.

In a given cancer type, there is a predominant or leading genetic alteration, and usually within this alteration 1 or 2 mutation hotspots, for example BRAF mutations in cutaneous melanoma, or cKit mutations in GIST. In contrast, the mutation spectrum in cKit mutant melanoma is much wider. It has been reported that cKit mutant melanomas harbour 30 somatic mutations per Mb of the genome, and such a high mutation burden results in an increased frequency of genetic mutations other than in cKit. For instance, pre-existing H-RAS activating mutations, as well as loss-of-function of tumor suppressor $p16^{INK4a}$, results in patients being refractory to cKit targeted therapies (146). In addition, several clinical trials have reported that patients with cKit amplifications respond poorly to cKit inhibitors, whereas cKit mutant patients (cKit L576P) are sensitive to these inhibitors (131, 147). The complexity of the mutation landscape of cKit melanoma patients emphasizes the importance of stratifying patients based on their mutational profile, before providing cKit targeted therapies.

Activation of cKit causes subsequent stimulation of the PI3K and MAPK signalling pathways, which are both essential for cell proliferation, survival, metastasis and development (148-150). Besides the essential role that these two pathways play in cKit melanomas, the re-activation of PI3K and MAPK signalling has also been employed by cKit melanomas as a mechanism of developing acquired resistance to cKit inhibitors. For instance, Rizos group reported that secondary mutations in cKit (A829P or T670I)

resulted in the development of acquired resistance of the cKit L576P mutant M230 melanoma cell line, after prolonged exposure to imatinib (151). Point mutations associated with imatinib resistance are frequently located in the drug and ATP binding pocket of cKit (encoded by exons 13 and 14, such as the T670I mutation) or in the activation loop (encoded by exons 17 or 18, such as the A829P mutation). Interestingly, these secondary mutations exhibit differential sensitivity to various cKit inhibitors: the cKit A829P mutant cells are resistant to imatinib and sunitinib, but these cells remain sensitive to nilotinib and dasatinib (151). In contrast, sublines with the second-site cKit T670I mutation displayed resistance to imatinib, nilotinib and dasatinib, but responded to sunitinib. Despite the variety of secondary cKit mutations that present in cells with acquired resistance to the cKit inhibitor imatinib, the authors demonstrated that all cKit inhibitor resistant M230 sublines had reactivated MAPK and PI3K signalling and remained sensitive to the concurrent inhibition of these two pathways. In conclusion, these data highlight the central role of the PI3K and MAPK cascades in c-Kit mutant melanoma, and the clinical potential of concurrently inhibiting these pathways to circumvent acquired drug resistance to cKit inhibitors. In addition, these data indicate that selecting an effective second-line therapy requires a comprehensive analysis of resistance mechanisms and their role in activating oncogenic survival pathways in cKit melanoma.

1.2 Eukaryotic translation and the role of translation initiation factor eIF4E in cancer

1.2.1 Eukaryotic translation elongation and termination

Protein synthesis, in general, can be defined in three steps: initiation, elongation and termination. The initiation step will be discussed in next section in detail.

Once translation initiation is completed, the translation process moves to the elongation step. At this stage, an 80S ribosome is associated with an mRNA, in which, the anticodon Met- tRNAi matches with the start codon AUG and occupies the P site of the 80S ribosome. The second codon in the open reading frame of the mRNA is now present at the A (acceptor) site of the 80S ribosome and awaiting for matching with the cognate aminoacyl-tRNA. In eukaryotic cells, eEF1A is responsible for escorting the cognate aminoacyl-tRNA to the A site in a GTP dependent manner. Cognate aminoacyl-tRNA and corresponding codon recognition triggers the hydrolysis of the GTP on eEF1A, which in turn, accommodates the tRNA into the A site. At this stage, both P and A sites in the 80S ribosome are occupied by iniator tRNA (Met-tRNAi) and cognate aminoacyl-tRNA, respectively, and the subsequent peptide bond forms between the P and A site peptidyl-tRNA. After peptide bond formation, the conformational change of the ribosomal subunits leads to the movement of the stem domain of the first tRNA from the P to E (exit) site and the second tRNA from the A to P site.

To translocate the remaining anticodon domains of tRNAs to E and P sites, another GTPase elongation factor eEF2 is required. The incorporation of eEF2 stabilizes the above-mentioned tRNA P to E and A to P site transitions. The addition of eEF2 at this step also facilitates the hydrolysis of GTP by the eEF2 factor. This hydrolysis is critical because it induces a conformational change that contributes to

unlocking the ribosome, allowing for movement of the tRNA and mRNA. In this post translocation state, a deacylated tRNA presents in the E site and the peptidyl-tRNA is in the P site, leaving the A site vacant for the entry of the next cognate aminoacyl-tRNA escorted by eEF1A. By repeating these steps, codons on an mRNA will be translated with high fidelity and a growing immature peptide will be produced for post-translational modifications. The regulation of translation elongation primarily focuses on eEF1 recycling. As discussed, the elongation factor eEF1A accommodates aminoacyl-tRNA into the A site by hydrolysis the GTP and the remaining eEF1A-GDP is released from the ribosome. Meanwhile, the guanosine exchange factor (GEF) eEF1B is responsible for catalyzing guanine nucleotide exchange on eEF1A, ensuring the elongation process proceeds.

Translation termination occurs when the ribosomes scan a stop codon (UAA, UGA, UAG) on the mRNA entering the A site. There are two factors involved in the termination process: eukaryotic releasing factor 1 (eRF1) and eukaryotic releasing factor 3 (eRF3) (152). In this process, eRF1 is primarily required for the recognition of the stop codons and the peptidyl-tRNA hydrolysis, whereas the eRF3 is a translational GTPase to facilitate the termination of translation. eRF1 is a protein with similar structure to tRNAs. eRF1 mainly comprises three functional domains: the amino terminal domain used for stop codon recognition, a M domain mimicking the acceptor stem of the tRNA and a carboxyl terminus for contacting with eRF3 GTPase (153). The distal loop located in the amino terminus of eRF1 contains a highly conserved NIKS motif capable of forming codon-anticodon-like interactions, and in this way, eRF1

recognizes the stop codon on an mRNA. Then, the M domain of eRF1 extends to the peptidyl transferase center (PTC) to facilitate the release of the produced peptide on the tRNA presented on P site. The universally conserved Gly-Gly-Gln (GGQ) motif appears to be critical in modulating peptide hydrolysis (154). Finally, the carboxyl terminus domain of eRF1 is involved in binding with eRF3 to modulate translation termination efficiency. The addition of the eRF1-eRF3-GTP ternary complex into the ribosome triggers the hydrolysis of GTP and leads to the M domain of eRF1 to enter PTC. In this stage, eRF3 serves similarly as the elongation factor eEF2 to deliver a tRNA into the PTC, then the M domain catalyzes the cleavage and the release of the peptide from the tRNA, in P site of the ribosome, thereby completing one cycle of mRNA translation. Afterward, the mRNA is dissociated with the 40S and 60S ribosome subunits for the recycling or reinitiating of the new rounds of mRNA translation.

1.2.2 The regulation of the eukaryotic translation initiation

Compared to the magnitude of regulation on translation elongation and termination, translation initiation is more extensive and complicated. Firstly, the number of regulatory factors that function during initiation are far more than the sum of those involved in elongation and termination. Secondly, the highly structured 5’ untranslated region on some mRNAs require initiation factor eIF4A to unwind it. Furthermore, intracellular signalling pathways, such as the MAP kinase and PI3K-AKT-mTOR pathways, directly modulate several translation initiation factors. Therefore, it is not surprising that translation initiation is the rate-limiting step of protein synthesis and the most highly regulated process in eukaryotes (155, 156). There are several well-studied

translation initiation factors- eIF4F, eIF1, eIF1A, eIF2, eIF3 and eIF5. Each of these factors have distinct functions,and by cooperating with one another, they facilitate mRNA translation initiation in eukaryotic cells.

All eukaryotic mRNAs are capped at the 5' terminus(157). The 7'-methyl-guanosine cap modification on the mRNA is believed to have two functions: on the one hand, 5' capping prevents the mRNA from being degraded(158); and on the other hand, this structure promotes mRNA translation initiation, which is associated with the function of initiation complex eIF4F (159). Three components make up the eIF4F complex: the helicase eIF4A, the scaffolding protein eIF4G, and the least abundant cap binding protein eIF4E (160, 161). The purpose of the eIF4F complex is to bring the mRNA to the 40S ribosome to facilitate its further assembly into 80S ribosomes. eIF4E specifically recognizes the 5' cap on mRNAs by using two conserved tryptophans within the cap binding domain (162). In the meantime, eIF4A unwinds any secondary structure within the mRNA, in an ATP-dependent manner. By bridging the cap structure and the 40S ribosome, the scaffolding protein eIF4G brings the mRNA to 40S ribosomes and modulates the addition of subsequent initiation factors.

The 40S ribosome binds initiation factors eIF1, eIF1A, eIF2-Met-tRNAi-GTP, eIF3 and eIF5 to form the 43S pre-initiation complex (PIC). The purpose of these initiation factors is to prepare a correct mRNA entry channel and decoding sites (A, P and E sties as discussed in last section) on 40S and facilitate subsequent formation of the 43S-mRNA initiation complex and scanning for the start codon. eIF1 and eIF1A bind

with decoding sites to alter the confirmation for the entry of mRNA(163). eIF2 selectively binds with Met-tRNAi to accelerate the binding of Met-tRNAi with 40S ribosomes. There are three subunits in eIF2 factor: α, β and γ, in which the γ subunit directly contacts the tRNA, GTP and 40S ribosomes and the other two subunits are believed to facilitate this binding process(164-166). eIF3, a 13 subunit complex that has 800KDa molecular weight, serves as a scaffold to bridge eIF4G and 43S ribosomes(167). eIF3 binds with eIF1/1A and eIF2 to prevent premature binding with 60S ribosomes(168). Once the mRNA is loaded on the 43S ribosome, the ribosome will migrate in the 5' to 3' direction on the mRNA to scan for the start codon. eIF4A is needed to unwind the mRNA into a linear strand to enable mRNA entry into the channel on 40S ribosome(169). It is worth noting that although the eIF4F complex is required for the majority of mRNAs that have highly structured 5' UTRs, other mechanisms of mRNA translation exist. Internal ribosome entry site (IRES) driven initiation is cap-independent, therefore, instead of using the association between the eIF4F complex and cap structure on the mRNA, the 43S ribosome directly binds with IRES sequences to scan for the start codon and initiate protein synthesis. IRES-mediated translation is found in the translation of some viral and a few mammalian mRNAs(170).

Start codon selection is completed by base pairing between codons within the mRNA and anti-codon domain on the initiator tRNA. eIF1 and eIF1A are critical for the fidelity of this recognition. eIF1 binds with the P site on the decoding domain of 43S ribosome and partially blocks the full entry of the initiator tRNAi-eIF2-GTP ternary complex into this spot. The loose association between the mRNA and tRNA facilitates

the 43S ribosome to smoothly scan the mRNA. Once the 43S finds the correct start codon on the mRNA, eIF1 is displaced by the Met-tRNAi-eIF2-GTP complex(171). This event changes the confirmation of 43S and locks the mRNA on the decoding sites. In the meantime, the confirmation change on 43S also alters the position of eIF5. eIF5, the GTPase activating protein (GAP), triggers the hydrolysis of the GTP bound to eIF2, leading to GDP-eIF2 leaving the initiator tRNA. At this step, the 43S and mRNA complex stops further scanning, and eventually the correct start codon is selected(172). After the recognition of the start codon, eIF1/1A, eIF2-GPD, eIF3 and eIF5 are dissociated from the 40S ribosome, and a 60S ribosome subunit is added to form a complete 80S ribosome and translation initiation is finished. By repeating the process of translation elongation, termination (introduced in last section), ribosome recycling and reinitiation, new proteins are synthesized.

1.2.3 Eukaryotic translation initiation factor eIF4E and its regulation

Among all the translation initiation steps mentioned in previous sections, the cap binding protein eIF4E is one of the members that are the most critical for protein synthesis. First of all, eIF4E is indispensible for the eIF4F complex assembly, on which the majority of mRNAs rely to be recruited to the ribosomes for translation. Moreover, eIF4E can stimulate the unwinding of secondary mRNA structure by facilitating eIF4A's activity (173). Most importantly, eIF4E has tumorigenic properties(174). The Ruggero group recently reported that a 50% reduction in eIF4E expression in mouse embryos did not affect their normal development. Global protein synthesis and either cap-dependent or IRES-dependent (cap-independent) mRNA translation was also unchanged in eIF4E

haploinsufficient mice. Strikingly, a 50% decrease of eIF4E expression in MEFs led to its resistance to RAS and Myc induced cellular transformation, By comparing both the transformed and untransformed wild type and eIF4E haploinsufficient MEF cells, the authors identified mRNA candidates that are eIF4E-dependent, which included regulators of oxidative phosphorylation, mitochondria ribosome, proteasome, cell recognition, immune response, cell cycle control, and cell adhesion (174). Although modulating eIF4E expression has little effect on overall protein synthesis (174, 175), mRNAs that are regulated by eIF4E manipulation has revealed that these possess complex 5' UTR mRNAs such as c-MYC, cyclin D, VEGF, Bcl-xl, Mcl-1 and metalloproteinases (MMPs) are all sensitive to eIF4E modulation (176-179). In comparison, mRNAs that have simple 5' UTRs, such as house keeping genes GAPDH and actin, are not sensitive to manipulating eIF4E levels. Therefore, eIF4E is critical for cell proliferation, ribosome biosynthesis, resistance to apoptosis and cell migration and invasion processes.

Two ways of regulating eIF4E activity have been well studied: eIF4E availability and eIF4E phosphorylation. There are two types of eIF4E binding proteins that regulate the availability of eIF4E for mRNA translation initiation; namely the eIF4Gs and 4E-BPs. By binding with the motif that contains a YXXXXLφ (where X is any amino acid and φ is a hydrophobic) sequence on the dorsal face of eIF4E, eIF4G binds eIF4E and increases its affinity for the mRNA cap, thus stabilizing the eIF4F complex and facilitates translation initiation(180). On the other hand, the eIF4E inhibitory 4E-BPs can bind the same motif on eIF4E as eIF4G, and thus prevent eIF4E from binding eIF4G and

blocking assembly of the eIF4F complex and subsequent translation initiation. 4E-BPs can serve as tumor suppressors (181). There are four phosphorylation sites on 4E-BPs, Thr 37/Thr 46 and Thr 70 and Ser 65, that can be phosphorylated and inactivated by mTOR(182). Hyperphosphorylated 4E-BPs are found in human cancers and associated with poor prognosis in melanoma, prostate and breast cancer (183-185). eIF4E activity can also be modified by phosphorylation on serine 209, by the mitogen-activated protein kinase (MAPK)-interacting kinases (MNK) 1 and 2, which are activated in response to the activated MAPK kinase (MEK)/extracellular signal-regulated kinase (ERK), and p38 MAPK pathways(186). Although whether phosphorylation of eIF4E facilitates its cap-binding ability remains controversial, it is evident that eIF4E phosphorylation is required for full tumorigenesis, lymphomagenesis and tumor metastasis, but has little effect on normal development in mouse models (187-189).

In addition, eIF4E can also be regulated on the level of transcription and posttranscription. The conserved enhancer box (E-box) domains in the promoter of eIF4E mRNA could be bound by transcription factor c-MYC to facilitate the expression of eIF4E (190). Interestingly, c-MYC mRNA itself is a translational target of eIF4E, therefore, a regulatory feed-forward loop, where c-MYC facilitates eIF4E transcription and, in turn, transcribed eIF4E promotes c-MYC translation, can occur in transformed cells. At the posttranscriptional level, the stability of eIF4E mRNA can be modulated by AU-rich elements (AREs) binding proteins: Human antigen R (HuR) and ARE RNA-binding protein 1 (AUF1). By binding with AU-rich elements of eIF4E, HuR facilitates its mRNA stability; by contrast, AUF1 counteracts with HuR to destabilize eIF4E mRNA

(191). Additionally, eIF4E protein turnover could be regulated by ubiquitination on lysine 159 amino acid(192).

1.2.4 eIF4E in human melanoma and current therapies targeting eIF4E

Different groups have investigated the expression of eIF4E in melanoma in recent years. By performing IHC using large-scale tissue microarray cores, Yang and colleagues initially examined eIF4E level in various human cancers including in tumors of the breast, colon, lymphoma, non-small cell lung cancer, ovary, prostate and human melanoma. In this study, the authors reported eIF4E was overexpressed in about 60% of the cases; moreover, they also found some eIF4E downstream targets such as VEGF and cyclin D1 were also significantly overexpressed in eIF4E positive samples (193). In a more recent study, Khosravi and colleagues also performed IHC screen for eIF4E in a tissue microarray of 448 melanocytic lesions. Interestingly, they demonstrated compared to desmoplastic nevi, the primary melanoma tissues expressed elevated eIF4E protein and further increased in metastatic melanomas. More importantly, the authors correlated the higher eIF4E expression with poorer prognosis in patients (194).

Beside the overexpression of total eIF4E, the regulation of eIF4E activity has also been studied in human melanomas. Recently, Carter and colleagues reported that both eIF4E and its phosphorylation are associated with the metastatic progression of melanoma. Importantly, the authors showed that phospho-eIF4E is strongly associated with worse survival in melanoma patients (195). Konicek and colleagues demonstrated that the inhibitor of Mnk1/2, cercosporamide, suppressed the phosphorylation of eIF4E

and expression of its downstream anti-apoptotic target Mcl-1 in the B16 melanoma cell line. Cercosporamide treatment for 6 days led to dampened cell proliferation, anchorage-independent growth and increased apoptosis in B16 cells. More importantly, Cercosporamide curtailed tumor growth and lung metastasis in B16 xenograft model by reducing eIF4E serine 209 phosphorylation (196). Another signalling pathway that modulates eIF4E's activity is the PI3K-AKT-mTOR pathway, because 4E-BPs, the suppressor of eIF4E, are phosphorylated by activation of this signalling pathway and it has been reported that in human melanoma, high p-4E-BP1 levels were associated with poor overall and post-recurrence survival (184). Other genes either positively or negatively regulating the PI3K-AKT-mTOR pathway such as PTEN, NF1, NRAS, CKIT, EGFR, MET, AKT, PIK3CA have all been identified aberrant in some melanoma cases, thus, the deregulation of eIF4E activity, via modulating 4E-BPs, is common in human melanoma (36, 78, 197).

Nowadays, researchers are paying attention to investigating how to block mRNA translation initiation steps in human cancers. One option is to decrease eIF4E availability by using inhibitors of the PI3K-AKT-mTOR signalling to de-phosphorylate 4E-BPs, which then bind tightly to eIF4E. Inhibitors such as rapamycin, everolimus and temsirolimus can allosterically inhibit the mTORC1 complex. However, there are some shortcomings to use of these inhibitors. For instance, in a phase II clinical trial of temsirolimus, 33 metastatic melanoma patients were registered, however, only one patient achieved a partial response (198). In 2 clinical trials of combining sorafenib with temsirolimus, 0 out of 25, and 3 out of 63 melanoma patients achieved partial response,

respectively (199, 200). Similar disappointing effects have also been observed in clinical trials of everolimus (201, 202). One reason for the modest effects of these inhibitors and quick acquired resistance is due to the negative mTOR/S6K/IRS-1 feedback loop, leading to an unwanted activation of the insulin receptor (203-205). In an attempt to circumvent this issue, dual PI3K-mTOR inhibitors have been tested for the treatment of metastatic melanomas. Marone and colleagues demonstrated that dual PI3K-mTOR inhibitor BEZ235 significantly repressed cell cycle progression, compared to PI3K or mTOR inhibitor treatment alone. In a B16 mouse syngeneic melanoma model, BEZ235 strongly inhibited tumor growth and facilitated tumor necrosis (206). In 2011, a phase I clinical trial to determine the maximum tolerated dose of the orally administered PI3K/mTOR inhibitor BEZ235 in combination with the MEK1/2 inhibitor MEK162 in patients with malignant melanoma, and other advanced solid tumors with KRAS, NRAS, and/or BRAF mutations. Dose escalation and safety and preliminary anti-tumor activity of the combination of BEZ235 and MEK162 will be assessed (NCT01337765). The result of this clinical trial is important for the application of MEK and PI3K/mTOR combination therapy in clinical settings.

Targeting eIF4A helicase activity, a component of eIF4F complex, is another strategy to inhibit translation initiation. It has been reported that genetic inhibition of eIF4A by siRNA decreases the proliferation of human melanoma cells (207). Furthermore, transgenic mice that had overexpress PDCD4, the suppressor of eIF4A, in epidermis showed attenuated translation efficiency of 5’ UTR highly structured eIF4E sensitive mRNAs such as CDK4 and ornithine decarboxylase (ODC) in primary

keratinocytes. In a chemically induced murine skin tumor model, the authors demonstrated that PDCD4 overexpression decreases tumor development and malignant progression (208). More recently, Boussemart and colleagues showed not only did the eIF4A inhibitor flavagline inhibit eIF4F dependent mRNA translation in melanoma cells, but it also synergized with the BRAFi vemurafenib to significantly suppress tumor growth in a BRAF inhibitor resistant xenograft model (143).

Directly reducing expression of eIF4E using antisense oligonucleotides (ASO) showed dramatic antitumor activity. eIF4E silencing (80%) had marginal effect on global protein synthesis (only 20% decrease), whereas, strongly suppressed eIF4E responsive pro-survival genes, and tumor growth in breast and prostate xenograft models by eliciting apoptosis (209). The phase I dose escalation study of eIF4E ASO illustrated low toxicity in humans, moreover, two eIF4E downstream targets VEGF and cyclin D1 were drastically inhibited in patients (210). Unfortunately, no tumor responses were observed with eIF4E ASO treatment (210), which suggested that eIF4A ASO may need to be combined with other regimens in treating human advanced cancers. Ribavirin, the proposed eIF4E pharmacological inhibitor, has also been used as anti-cancer therapy by impeding eIF4E mediated oncogenic transformation. In a Phase II clinical trial, ribavirin treatment led to substantial clinical benefit in M4/M5 subtypes of acute myeloid leukemia (AML) patients (211). Our group has previously shown ribavirin suppresses proliferation of breast cancer cells in an eIF4E dependent manner. Moreover, although eIF4E seemed to be overexpressed in all types of breast tumors from a microarray analysis of 621 breast cancer cases, eIF4E's prognostic value was restricted to luminal

B cases (212). In addition, we found ribavirin suppresses breast tumor formation, and inhibits lung metastasis *in vivo*. Molecularly, we demonstrated that the effects of eIF4E inhibition were mediated, at least in part, by reducing the expression of epithelial-to-mesenchymal transition (EMT) makers such as matrix metalloproteinase (MMP)-3 and MMP-9 (213).

The interaction of eIF4E with the scaffolding protein eIF4G has also been employed as a potential anti-cancer target. As introduced in previous session, the YXXXXLφ motif (where X is any amino acid and φ is hydrophobic) located on the dorsal face of eIF4E is bound by either eIF4G or 4E-BP. 4EGI-1 mimics 4E-BPs function, by competitively binding eIF4E, leaving eIF4G unbound and therefore inhibiting eIF4E dependent mRNA translation and inducing apoptosis in multiple tumor cell lines (214). Chen and colleagues illustrated that 4EGI-1 strongly inhibit growth of human breast and melanoma cancer xenografts with low cytotoxicity (215). However, besides inhibiting eIF4E-dependent protein synthesis, 4EGI-1 has also been shown to induce an, eIF4E-independent, endoplasmic reticulum stress response and promote the expression of the proapoptotic protein NOXA (216). More recently, the effect of a novel eIF4E/eIF4G inhibitor SBI-0640756 (SBI-756) was tested in human melanoma. Feng and colleagues showed that SBI-756 impaired eIF4F complex formation and attenuated cell proliferation of BRAF-resistant and BRAF-independent melanoma cells. SBI-756 reduced tumor onset and the incidence of melanoma development. Furthermore, SBI-765 synergized with the BRAF inhibitor vemurafenib to delay the development of BRAFi resistant tumors (217).

eIF4E is phosphorylated by two kinases: Mnk1 and Mnk2 (218, 219). Although Mnk activity is dispensable for normal cell development (220), eIF4E phosphorylation is essential for full tumorigenesis, lymphomagenesis and tumor metastasis (187-189). The small molecule inhibitor CGP57380 blocks eIF4E phosphorylation, cell proliferation, and colony formation in glioblastoma multiforme. Moreover, Konicek and colleagues demonstrated that another Mnk inhibitor, cercosporamide, significantly suppressed lung metastasis of B16 melanoma and the tumor growth of HCT116 colon cancer xenograft *in vivo*, with little cytotoxicity (196).

In summary, considering all the promising results from targeting components of the eIF4F complex in various human cancers, the mRNA translation initiation step might be a novel therapeutic target in treating human malignancies.

1.3 Rationale and objectives

Melanoma is the deadliest skin cancer. According to distinct genetic mutation profiles, melanoma is classified into subgroups as shown in Figure 1.7. In the second chapter of this thesis, we focus on BRAF mutant melanoma, the most predominant form of melanoma in the world. As discussed in previous sections, multiple components, including positive and/or negative regulators of the MAPK signalling pathway such as RTKs, NF-1, BRAF, MEK have been identified extensively aberrant in BRAF mutant melanomas. Moreover, over 20% of BRAF mutant melanomas possess concurrent PTEN aberrations (43), causing concurrent activation of PI3K-AKT-mTOR signalling.

Activation of the PI3K-AKT-mTOR pathway has been reported as an evading mechanism for developing acquired resistance to BRAFi and MEKi therapies, but the efficacy of PI3K/AKT/mTOR inhibitors are largely limited by the subsequent activation of the mTOR/S6K/IRS-1 negative feedback loop, as discussed in the previous section, therefore novel targets are urgently needed. As shown in Figure 1.8, eIF4E is the convergence point of activated MAPK and PI3K-AKT-mTOR pathways, thus in chapter 2, we investigated the role of eIF4E in response and resistance to the BRAF inhibitor vemurafenib.

We were also interested in expanding our research spectrum, beyond BRAF mutant melanomas, to investigate other subtypes of human melanomas. Compared to other subtypes, cKit aberrant melanomas have a worse prognosis, high metastatic capacity, and lack of therapeutic options. As shown in Figure 1.9, cKit activates both the MAPK and PI3K-AKT-mTOR pathways, thus the activation of Mnk-eIF4E axis and formation of the eIF4F complex to facilitate mRNA translation. Therefore, in chapter 3, we interrogated the role of Mnk-eIF4E axis in cKit aberrant melanomas, to elucidate whether blocking eIF4E function is a viable option in melanomas beyond BRAF aberrations.

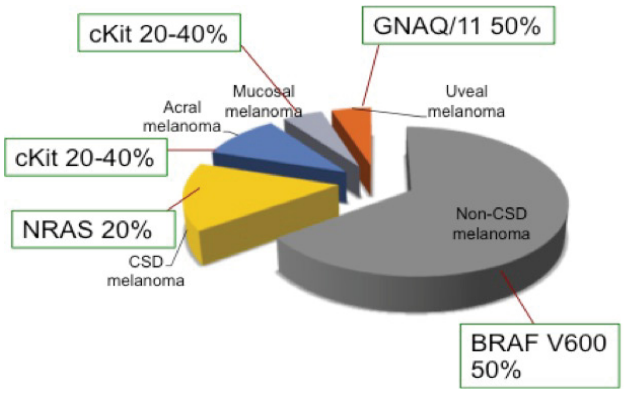

Figure 1.7 Melanoma subtypes and mutation frequencies.

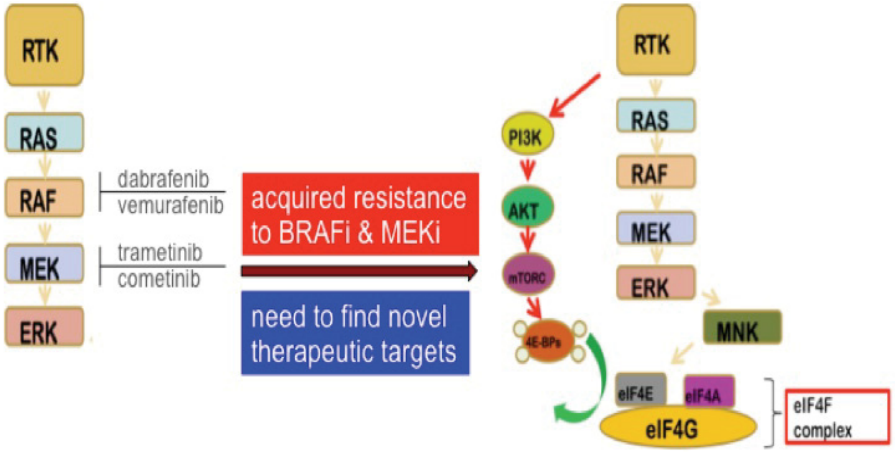

Figure 1.8 Signalling pathways activated in BRAF aberrant human melanoma.

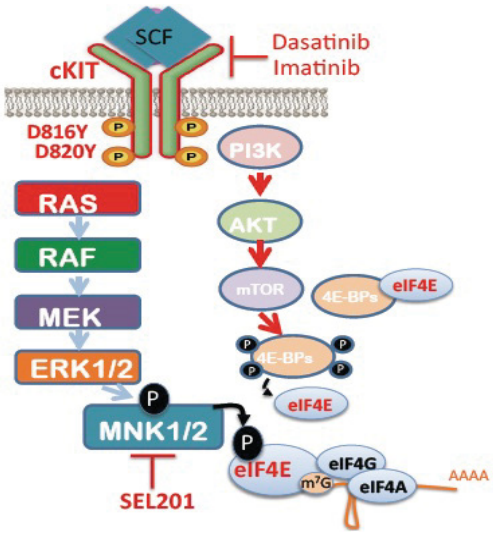

Figure 1.9 Signalling pathways activated in cKit aberrant human melanoma.

Chapter 2

The role of eIF4E in response and acquired resistance to vemurafenib in melanoma.

2.1 Abstract

In eukaryotic cells, the rate-limiting component for cap-dependent mRNA translation is the translation initiation factor, eIF4E. eIF4E is overexpressed in a variety of human malignancies, but whether it plays a role in melanoma remains obscure. We hypothesized that eIF4E promotes melanoma cell proliferation and facilitates the development of acquired resistance to the BRAF inhibitor, vemurafenib. We show that eIF4E is overexpressed in a panel of melanoma cell lines, compared to immortalized melanocytes. Knock-down of eIF4E significantly repressed the proliferation of a subset of melanoma cell lines. Moreover, in $BRAF^{V600E}$ melanoma cell lines, vemurafenib inhibits 4E-BP1 phosphorylation, thus promoting its binding to eIF4E. Cap-binding and polysome profiling analysis confirmed that vemurafenib stabilizes the eIF4E - 4E-BP1 association and blocks mRNA translation, respectively. Conversely, in cells with acquired resistance to vemurafenib, there is an increased dependence on eIF4E for survival, 4E-BP1 is highly phosphorylated and thus eIF4E - 4E-BP1 associations are impeded. Moreover, increasing eIF4E activity by silencing of 4E-BP1/2, renders vemurafenib responsive cells more resistant to BRAF inhibition. In conclusion, these data suggest that therapeutically targeting eIF4E may be a viable means of inhibiting melanoma cell proliferation and overcoming vemurafenib resistance.

2.2 Introduction

Cutaneous melanoma is the most predominant form of skin cancer, with approximately 50% of melanomas carrying activating BRAF mutations (221). The $BRAF^{V600E}$ mutation leads to a five hundred-fold activation of BRAF and constitutive activation of the MAPK signalling pathway (45, 222). In 2011, the US FDA approved vemurafenib, a BRAF V600E inhibitor, for clinical use in advanced melanoma (223). Although patients initially respond well, with pronounced tumor regressions (224), drug resistance almost inevitably develops, with a median response duration length of six months. Multiple mechanisms involved in vemurafenib resistance have been reported, including acquired EGFR upregulation (225), MAPK signalling pathway reactivation (141, 226), BRAF V600E and COT (MAP3K8) copy number gains (139, 140), BRAF V600E splice variants (138), as well as PI3K-AKT-mTOR activation (227)

One potential vemurafenib resistance mechanism that has not been well defined in melanoma involves the eIF4F complex, which consists of eIF4A, an RNA-dependent ATPase and helicase, eIF4G1, a scaffolding protein that mediates 40S ribosomal bridging with eIF4F, and eIF4E, a m^7GpppN (N is any nucleotide) cap-dependent RNA binding protein (159). eIF4E facilitates the translation of pro-oncogenic mRNAs, such as VEGF, cyclin D3 and Mcl-1 (159). *In vitro,* overexpression of eIF4E is sufficient to induce transformation (228, 229) while *in vivo* overexpression is associated with prostate cancer and lymphoma (183, 230), amongst other cancers. Moreover, in human breast cancer cells, blocking eIF4E decreases mRNA translation and anchorage-independent growth (231), and also inhibits cell proliferation (212). Although eIF4E has

been reported to be overexpressed in various haematological malignancies and solid tumors (232), its role in melanoma remains largely unknown.

The activity of eIF4E is regulated by its binding proteins and upstream signaling pathways. Several eIF4E-binding proteins have been documented in the literature, but the best characterized are eIF4E-binding protein (4E-BP) 1 and 2 (181, 233). When 4E-BP1 is hypophosphorylated, it binds to eIF4E, inhibiting cap-dependent translation (234). Conversely, when 4E-BP1 is hyperphosphorylated via activated mTOR, eIF4E is liberated, allowing cap-dependent translation to proceed (235). Thus, the PI3K/Akt/mTOR pathway activates eIF4E via hyperphosphorylation of 4E-BP1. When this pathway is constitutively activated, the eIF4E-mRNA complex forms and cap-dependent translation is active, which leads to continuous cell proliferation (236).

In this report, we characterize the role of eIF4E and its binding partners in a panel of melanoma cell lines. Importantly, we provide evidence that melanoma cells can escape the effects of vemurafenib by a mechanism involving increased phosphorylation of 4E-BP1 and bioavailability of eIF4E. Our findings provide the groundwork for novel combinatorial therapeutic approaches targeting BRAF V600E and eIF4E in melanoma.

2.3 Material and Methods

2.3.1Reagents

Vemurafenib was obtained from Plexxikon (California, US), PP242 was purchased at Sigma Aldrich. All drugs were dissolved in DMSO to 10mM, and aliquots

were stored at -80°C. Antibodies: eIF4G1, 4E-BP1, phospho-4E-BP1 (T37/46), phospho-eIF4E (Ser209), phospho-ERK (T202/Y204), 4E-BP2, c-Myc, phospho-AKT (Ser 473) AKT, cyclin D3, phospho-S6 (S240/244), S6, phospho-P70S6K (Thr 389), P70S6K and GAPDH were purchased from Cell Signalling Technology. eIF4E antibody was purchased from BD Bioscience. Immobilized r-Aminophenyl-m^7GTP agarose beads were purchased from Jena Science. Transfection reagents Lipofectamine 2000 or Lipofectamine RNAiMax were purchased from Invitrogen.

2.3.2 Cell Culture

All cell lines used in this paper, except A375 and vemurafenib resistant lines R1 and R2, were kindly provided by Dr. Ghanem Ghanem (Institut Jules Bordet, Bruxelles). The A375M cell line is a metastatic derivative of the A375 cell line originally reported by Dr. JM Kozlowski (237). A375M, BLM, SkMel28, A375 and MelST were maintained in monolayer culture in Dulbecco's modified Eagle medium with 10% fetal bovine serum (FBS) and 1% Penicillin/Streptomycin; MM117, MM111, MM102, WM164, MM57, 451Lu and MM94 were cultured in HAM's F10 with 10% FBS and 1% Penicillin/Streptomycin. Vemurafenib resistant cell lines AR1 and AR2 were maintained in 2.5μM vemurafenib in DMEM with 10% FBS and 1% Penicillin/Streptomycin. For vemurafenib wash-off cell lines termed AR1WO and AR2WO, AR1 and AR2 cells were maintained in DMEM with 10% FBS and 1% Penicillin/Streptomycin for one month in the absence of vemurafenib. All cell lines were maintained at 37°C in a humidified incubator in 5% CO_2.

2.3.3 Proliferation assay

Cell proliferation was tested by sulforhodamine B (SRB) assay. Cells were seeded on a 96-well plate the day before treatment. Cells were then treated with vemurafenib, for 24, 48, or 96 hours. For each time point, 96-well plates were harvested and fixed with 10% trichloroacetic acid (TCA) for 1 hour. Plates were then washed and sterilized with water three times and allowed to air-dry overnight. Once the fixation was completed, plates were stained with 0.4% (w/v) SRB 100 µl/well in 1% acetic acid for at least 30 minutes. After staining, plates were washed with 1% acetic acid three times and air-dried overnight. Bound SRB was solubilized by adding 100 µl/well of 10mM unbuffered Tris base, pH 10.5 for 10 minutes. Absorbance at 564 nm was read using FLUOstar OPTIMA plate reader.

2.3.4 Plasmids, Virus Production, Stable Cell Selection

Human sh4E-BP1, sh4E-BP2 vectors were purchased from Sigma (MISSION shRNAs), shRNAs were co-transfected with three Lentivirus packaging constructs: PLP1, VSVG, PLP2 into 293FT cells using Lipofectamine 2000 (Invitrogen). Viral supernatants were harvest 48 hours post-transfection and spun at 1000 rpm for five minutes. For establishing shBP1+BP2 stable knockdown cell lines, control or shBP1/2 viral supernatants were added to 10 cm dishes with adhered A375 cells, for overnight infection. After two rounds of infection, cells were treated with puromycin (1µg/ml) for 48 hours, and positive subclones were maintained.

2.3.5 Polysome profiling

Polysome profiling was performed as previously described by (238). For sucrose gradient fractionation and polysome isolation, A375 cells were seeded in 15 cm dishes with or without 2.5μM vemurafenib for 24 hours. Cells were treated with cycloheximide (100 microgram/ml) five minutes prior to harvesting, washed in cold PBS containing 100 microgram/ml cycloheximide, and then spun for 5 minutes at 1500 rpm. Cell pellets were lysed in hypotonic buffer (5 mM Tris-HCl (pH 7.5), 2.5 mM $MgCl_2$, 1.5 mM KCl and 1X protease inhibitor cocktail (EDTA-free), containing 1mM DTT and RNAse inhibitor (100 units). Samples were kept on ice for 12 minutes, then centrifuged at 13,000 rpm for 8 minutes. The supernatants were harvested and added on to 10–50% sucrose gradient. Gradients were centrifuged at 35,000 rpm for 2 hours at 4°C. Fractions were collected (24 fractions, 12 drops each) using a Foxy JR ISCO collector and data (absorbance, 254 nm) were collected.

2.3.6 Western blot analysis

Cells were treated with vemurafenib (2.5μM) or PP242 (1μM) with indicated times, and pellets were harvested to obtain protein extracts. Briefly, cell pellets were lysed in RIPA buffer (50 mM Tris-HCl, pH 8.0, with 150 mM sodium chloride, 1.0% Igepal CA-630 (NP-40), 0.5% sodium deoxycholate, and 0.1% sodium dodecyl sulphate). After sonication, cell lysates were centrifuged at 13,000 rpm for 15 minutes. The supernatants were collected and protein concentrations were quantified. Equal amounts of protein were loaded on a 10% SDS-PAGE. After transferring to a nitrocellulose membrane (BioRad), 5% milk/TBS was used to block for 1 hour, then

probed for target antibodies overnight at 4℃. After incubation with horseradish peroxidase (HRP) conjugated secondary antibodies for 1 hour at room temperature, the signals of targeted protein were developed with chemiluminescence substrate (Amersham).

2.3.7 RNA interference

Cells were seeded in 10 cm dishes at 80% confluency. eIF4E siRNA or control siRNA was added into dishes after 20 minutes incubation with transfection reagent Lipofectamine RNAiMAX following manufacturer's instructions. After 16 hours, cells were washed with 1X PBS and fresh medium was added. At day 4 of transfection, cell pellets were harvested for western blotting. The sequences of the previously validated eIF4E siRNA pair were as follows: 5′ -AGA GUG GAC UGC AUU UAA AUU UGdA dT-3′ and 5′ -AUC AAA UUU AAA UGC AGU CCA CUC UGC-3(212). AllStars Negative Control siRNA (Qiagen) was used as non-silencing control.

2.3.8 m^7GTP Pull-down assay

Cells were treated with vemurafenib (2.5μM) or PP242 (1μM) with indicated times, and whole cell lysate were harvested. For eIF4E pull down assay, 20μl m^7GTP agarose beads were added in each tube and washed with IP buffer (Tris-HCl pH 7.5 50mM, NaCl 150mM, EDTA 1mM, EGTA 1mM, TritonX-100 1%, NP-40 0.5%) three times. Quantified protein extracts were then added on top of the m^7GTP agarose beads at equal amounts in each tube, and were incubated with beads on the rotator overnight,

at 4 °C. Western blot was performed to determine the association between eIF4E and 4E-BP1 or eIF4G1.

2.3.9 RNA isolation

To isolate mRNAs in each polysome fractions, Trizol (Invitrogen) was added in each fraction tube. After 5 minutes incubation at room temperature, 200µl of chloroform was added in each tube and mixed well for 15 seconds. Following centrifugation at 12,000 x g for 15 minutes at 4°C, the clear phase was carefully obtained and placed into a clean tube. 500µl of isopropanol was added to the clear phase and this mixture was centrifuged for 30 minutes (12,000 x g, 4°C). The isopropanol was then removed and remaining pellets were washed with 1ml of 75% ethanol (in DEPC water), and centrifuged for 5 minutes (12,000 x g, 4°C). The liquid was then carefully removed and pellets were allowed to air-dry. 20µl of DEPC water was added to dissolve RNA pellets, which were then quantitated (Thermo scientific Nanodrop 1000).

2.3.10 Semiquantitative reverse transcription polymerase chain reaction (sqRT-PCR) and real-time qRT-PCR

Before performing the reverse transcription, 0.3µg of mRNA was visualized by ethidium bromide agarose gel (2%) to check the quality of mRNAs (integrity of 28S and 18S bands). For cDNA production, a one-step RT-PCR kit (Bio-Rad) was used following the manufacturer's instructions. The sequences of human cyclin D3, GAPDH and β-actin primers were as follows: cyclinD3 forward 5'-CTG GAT CGC TAC CTG TCT TG-3', cyclinD3 reverse 5'-TCC CAC TTG AGC TTC CCT AG-3', GAPDH forward 5'-AAT

CCC ATC ACC ATC TTC CA-3', GAPDH reverse 5'-TGA GTC CTT CCA CGA TAC CA -3'. β-actin forward 5'-ACC ACA CCT TCT ACA ATG AGC-3', β-actin reverse 5'- GAT AGC ACA GCC TGG ATA GC-3' To perform sqRT-PCR, Taq DNA polymerase kit (Invitrogen) was used. For each of the transcripts (cyclin D3, GAPDH, β-actin), two cycle numbers (25 and 35 cycles) were performed to make sure the PCR results were in the linear range. Furthermore, cDNA were amplified for cyclin D3, GAPDH and β-actin by real-time PCR analysis (ABI Prism7500; Applied Biosystems) using SYBR green technology according to the manufacturer's instructions.

2.3.11 Clonogenic assay

300 cells per well were seeded in 6-well plates the day before treatment. After overnight incubation, the attached cells were treated with DMSO or vemurafenib in indicated concentration, in triplicates. After 14 days, incubating medium was removed and cells were stained with 0.5% (W/V) crystal violet in 70% ethanol. After one hour of incubation at room temperature, staining dye was washed and the number of colonies was counted manually.

2.4 Results

2.4.1 Melanomas with elevated phospho-4E-BP1 and phospho-AKT protein levels are more sensitive to eIF4E knockdown

To determine the role of eIF4E in melanoma, we first analyzed the expression of eIF4E and eIF4G1, components of the eIF4F complex, within a panel of melanoma cell

lines, versus immortalized melanocytes, MelST (239). As shown in Figure 1a, various melanoma cell lines, expressing either wild-type or mutant BRAF, expressed high levels of eIF4E compared to immortalized MelST melanocytes. We also analyzed the eIF4F complex scaffolding protein, eIF4G1, and found that its expression varied across cell lines (Supplementary Figure S1a), as did the expression of 4E-BP1 (Figure 1a). Interestingly, profiling of the phosphorylation status of ERK and AKT in the panel of melanoma cells revealed a striking correlation between 4E-BP1 hyperphosphorylation, and phospho-AKT (Figure 1b). Increased phospho-4E-BP1 suggests that the bioavailabilty of eIF4E is increased in a subset of melanoma cell lines, since the phosphorylated form of 4E-BP1 fails to bind and repress eIF4E.

We then investigated whether eIF4E is a regulator of cell proliferation in a subset of melanoma cells. Following eIF4E knockdown via siRNA we found that four lines were highly sensitive to eIF4E silencing: A375M, MM117, MM102, and MM111 (Figure 1c, Supplementary Figure S1b, S1d). Although BLM and SKMel28 exhibited intermediate responsiveness, the remaining cell lines (WM164, MM57, 451Lu, and A375) continued to proliferate in comparison to control siRNA (siCTL), despite eIF4E knockdown (Figure 1c, Supplementary Figure S1b). Interestingly, the cell lines with the greatest cell proliferation inhibition upon eIF4E silencing expressed the highest levels of phospho-AKT and phospho-4E-BP1 (Figures 1b, 1c, 1d, Supplementary Figure S1c), suggesting that cells with increased eIF4E activity were more dependent on this pathway for survival. All ten cell lines examined had a similar efficiency of eIF4E depletion, thus the differences in proliferation following eIF4E knockdown were not simply due to

differential silencing of eIF4E in one cell line versus another (Figure 3a and Supplementary Figure S1d).

2.4.2 Vemurafenib reduces the phosphorylation of the eIF4E inhibitory protein, 4E-BP1, in BRAF^{V600E} mutant lines

Having demonstrated that silencing eIF4E can block the proliferation of some but not all melanoma cell lines examined, we next wanted to determine if vemurafenib had any effect on the eIF4F complex. We assessed the phosphorylation of 4E-BP1 after treatment with vemurafenib in three BRAF^{V600E} mutant melanoma cell lines: A375, SKMel28, and A375M. In all three cell lines, we observed a time dependent decrease in the phosphorylation of 4E-BP1 using a phospho-specific 4E-BP1 antibody and by detecting a reduction in the hyperphosphorylated, slower migrating forms of 4E-BP1 following vemurafenib treatment (Figure 2a). Furthermore, as shown in Figure 2a, there is a marked decrease in ERK activation (phospho-ERK) upon 4 hour vemurafinib treatment, demonstrating an early inhibitory role of vemurafenib on the MAPK pathway. We next assessed the levels of phospho-p70S6K, and phospho-S6, which lie downstream of mTOR. Consistent with previously published data, we found that the phosphorylation of S6 was decreased by vemurafenib treatment (Figure 2b) (240, 241). No consistent changes in AKT and P70S6K activation (phospho-AKT and phospho-P70S6K) were detected in these cell lines treated with vemurafenib (Figure 2b).

To further explore the effect of vemurafenib on the eIF4E/4E-BP1 association, we performed cap-binding assays using 7-methyl-GTP-bound agarose beads (Figure

2c). In this assay, eIF4E present in cell lysates binds to cap-mimicking beads, also enabling proteins bound to eIF4E to be assessed upon elution (242). In vemurafenib-treated cells, we observed increased binding between eIF4E and 4E-BP1, which occurs when 4E-BP1 is dephosphorylated, leading to decreased cap-dependent translation. Of note, PP242, an mTORC1/2 inhibitor, was used as a positive control, leading to 4E-BP1 hypophosphorylation and increased eIF4E:4E-BP1 association (Figure 2a, 2c).

Dephosphorylation of 4E-BP1 and subsequent eIF4E:4E-BP1 complex formation typically corresponds to an inhibition of translation initiation. To further investigate this, we assessed the effect of vemurafenib on the polysome distribution in $BRAF^{V600E}$ mutant melanoma cells. Treatment of A375 cells with vemurafenib for 4 hours did not result in an inhibition of translation (data not shown). However, after 24 hours, there was a decrease in the abundance of polysomes (Figure 2d), consistent with a block in eIF4F complex formation. Western blot analysis showed that the expression of the eIF4E translational targets VEGF, cyclin D3, c-Myc and Bcl-2 expression was drastically repressed by vemurafenib treatment (Figure 2d). Cyclin D3 is a well-characterized eIF4E-sensitive mRNA (243, 244). In keeping with our results that vemurafenib can block mRNA translation, we observed a shift in the polysome loading, from heavy to light polysomes, of cyclin D3 mRNAs in A375 cells treated with vemurafenib (Figure 2e, Supplementary Figure S2). Moreover, vemurafenib had no impact on the polysome loading of two eIF4E-insensitive mRNAs: glyceraldehyde 3-phosphate dehydrogenase (GAPDH) and β-actin (Figure 2e and Supplementary Figure S2). These data suggest

that vemurafenib-induced reduction in cell proliferation is associated with defects in eIF4E-mediated translation initiation.

2.4.3 eIF4E contributes to vemurafenib resistance in A375 BRAF^{V600E} melanomas

Having demonstrated that vemurafenib functions in part by repressing 4E-BP1 phosphorylation and increasing eIF4E:4E-BP complex formation, we next examined the status of the eIF4F complex in cells with acquired resistance to vemurafenib. Here, we obtained the parental BRAF^{V600E} mutant human melanoma cell line, A375, and corresponding vemurafenib-resistant cell lines, denoted A375(A)R1 and AR2 (245). To ensure that AR1 and AR2 cell lines were valid models of acquired resistance, and not merely chronically adapted to vemurafenib, we maintained the AR1 and AR2 cell lines in the absence of vemurafenib for one month and referred to these as AR1 and AR2 wash-off (WO) cell lines, AR1WO and AR2WO, respectively. We next challenged AR1WO and AR2WO cells with vemurafenib, and as shown in Supplementary Figure S3a, withdrawal of vemurafenib from the media for one month does not cause AR1 and AR2 cell lines to regain sensitivity to vemurafenib. Next, to determine whether eIF4E activity is associated with acquired resistance to vemurafenib, we performed eIF4E knockdown in both parental and resistant lines, with or without vemurafenib, and confirmed the efficiency of silencing by western blot (Figure 3a). The proliferation of AR1 and AR2 is significantly inhibited by eIF4E silencing, compared to their parental counterpart (Figure 3a). Furthermore, evidence supporting a role of vemurafenib working via suppression of eIF4E activity is demonstrated by data (e.g. AR1WO vs

AR1+V) showing that the addition of the BRAF inhibitor does not potentiate the effect of eIF4E silencing in the resistant cell lines (Figure 3a).

Silencing of eIF4E can inhibit the proliferation of vemurafenib resistant cells. We investigated the integrity of the eIF4F complex in order to provide mechanistic insight towards this observation. Cap-binding analysis demonstrated that, compared to the parental A375, vemurafenib resistant lines AR1, AR2, AR1WO and AR2WO cell lines exhibited decreased eIF4E:4E-BP1 complex formation, leading to increased eIF4E:eIF4G1 association (Figure 3b). Furthermore, compared to the parental A375 cell line, vemurafenib resistant lines overexpressed cyclin D3 and VEGF, two well-documented eIF4E downstream targets (159, 244). (Figure 3c). Our results suggest an increased role of eIF4E in the survival of cells with acquired resistance to vemurafenib.

2.4.4 4E-BP1/2 stable knockdown contributes to vemurafenib resistance in A375 cells

The data we have shown support the hypothesis that acquired resistance to vemurafenib is facilitated by hyperphosphorylation of 4E-BP1, leading to increased cap-dependent mRNA translation, relative to parental A375. To further investigate the role of 4E-BP1 in resistance to vemurafenib, we transduced cells with retroviral particles expressing sh4E-BP1 and sh4E-BP2 RNAs. Knockdown of 4E-BP1/2 would have a similar effect on eIF4E activity as a 4E-BP1/2 hyperphosphorylation. Following puromycin selection and immunoblot confirmation, positive 4E-BP1/2 stable knockdown clones were established (Figure 4a). Consistent with increased eIF4E activity, the 4E-

BP1/2 double knockdown cell line expressed elevated levels of eIF4E downstream targets c-Myc compared to the control scrambled knockdown (shCTL) cell line (Figure 4a). To determine the sensitivity to vemurafenib in the 4E-BP1/2 knockdown cell line we assessed cell proliferation. While the proliferation rates between A375 shCTL and A375 shBP1/2 cell lines were similar, the 4E-BP1/2 double knockdown cells were more resistant to vemurafenib compared to their control knockdown counterparts (Figure 4b). Furthermore, in long-term clonogenic (proliferation) assays, we showed that the A375 shBP1/2 cell line is more resistant to vemurafenib compared to the A375 shCTL cell line (Figure 4c). To summarize, these data demonstrate that depletion of 4E-BP1/2 can cause a partial rescue of vemurafenib-induced inhibition of proliferation.

2.5 Discussion

Gain-of-function BRAF mutations are common in melanoma, and although patients with tumors harboring mutant BRAF initially respond to targeted agents, resistance develops in most cases (236, 246, 247). Significant efforts have been made to understand sensitivity and resistance to vemurafenib in this context, with several investigations focusing on the ERK and PI3K-Akt/mTOR pathways in melanoma progression (134, 136). Interestingly, the profiles of downstream events, such as Mnk phosphorylation (directly upstream of eIF4E) and specifically, eIF4E expression remain poorly documented in melanoma.

We found that a subset of cell lines expressed high levels of phospho-Akt, which correlated with elevated expression of hyperphosphorylated 4E-BP1 (Figure 1b). This

led us to reason that the survival of this subset of melanoma cells (A375M, MM117, MM102, MM111, BLM and SKMel28) would be driven by less sequestered, and more bioavailable eIF4E (233). The proliferation of these cell lines was significantly decreased when eIF4E was silenced, suggesting that this translation factor helps drive melanoma progression (Figure 1c, Supplementary Figure S1b). Our data show that treatment of A375 cells with vemurafenib causes: (1) a time dependent reduction in phosphorylation of 4E-BP1 (Figure 2a), (2) increased eIF4E:4E-BP1 association (Figure 2c), and (3) decreased abundance of light and heavy polysome fractions, as well as the reduced loading of eIF4E-sensitive mRNA cyclin D3 in heavy polysomes (Figures 2d, 2e, and Supplementary Figure S2); these results point to a role of vemurafenib in inhibiting eIF4E-mediated mRNA translation.

Conversely, in terms of resistance to chemotherapeutics, overexpression of eIF4E has been documented following anthracycline treatment in breast cancer (248), rapamycin treatment in murine lymphoma models (249, 250), and here, upon vemurafenib resistance in melanoma. Significant work by other groups has been put forward to address chemotherapy resistance in melanoma cells. Specifically, the observance of elevated phospho-4E-BP1, has been documented in cross-resistance to BRAF or MEK inhibitors, which could be overcome by treating resistant cells with the mTOR inhibitor rapamycin (241). Furthermore, the use of second-generation mTOR inhibitors, such as everolimus and temsirolimus, alongside vemurafenib has come to fruition in clinical trials (see NCT01596140). Although targeting mTOR in such cases has the potential to regress and/or eradicate tumors, this may be insufficient, as

elevated phospho-4E-BP1 levels are often associated with relatively high levels of eIF4E. Thus examining the eIF4E/4E-BP ratio upon administration of mTOR inhibitors (243), or perhaps more effectively, directly targeting eIF4E should provide a more pronounced effect clinically.

During preparation of this manuscript, a mechanism of resistance to anti-BRAF and anti-MEK treatment of melanomas was shown to involve heightened activation of the eIF4F complex (236). As a means of targeting the eIF4F complex in response to standards of care, flavagline derivatives were developed, and were shown to depress translation of exogenous 5'-capped mRNA, and reduce tumor volume in a Mel624 xenograft model (in concert with anti-BRAF). Although this investigation is promising in terms of targeting eIF4A, further examination of the effect of flavaglines on known eIF4E translational targets (e.g. c-Myc, cyclin D3), and their effect on multiple melanoma cell lines and xenograft models would add to this approach.

In our study of genetically blocking eIF4E, rather then chemical inhibition of eIF4A with flavaglines (251), we observed the most pronounced inhibition of proliferation in cell lines with elevated phospho-4E-BP1 levels (Figure 1d). Exploring the effect of flavaglines within our panel of cell lines, in terms of proliferation inhibition and eIF4E target expression would further support the clinical delivery of flavaglines in concert with anti-MEK and anti-BRAF therapies.

Overall, our data demonstrate that eIF4E promotes melanoma cell proliferation and may play a role in developing acquired resistance to the BRAF V600E inhibitor vemurafenib. Thus, targeting eIF4E in melanoma may be a novel therapeutic option geared towards cells expressing high basal levels of phospho-4E-BP1, and/or eIF4E upon acquired resistance to vemurafenib. Moreover, we hypothesize that eIF4E may promote vemurafenib resistance by promoting translation initiation of specific mRNAs, such as those intimately linked to cell survival. The literature supports this hypothesis, showing that proliferation and pro-survival mRNAs are less efficiently translated when cap dependent (eIF4E-mediated) translation is blocked (252, 253). Future work in our lab will also focus on isolating translating ribosomes (polysomes) to define specific mRNAs, whereby translation is dependent on activated eIF4E in cells with acquired resistance to vemurafenib. Identification of specific mRNAs that are essential for eIF4E-mediated resistance to vemurafenib may suggest novel therapies, in addition to eIF4E inhibitors, to prevent or overcome resistance.

The work presented herein supports the importance of validating phospho-4E-BP1 and eIF4E as markers of resistance to BRAF inhibitors, using patient derived pre- and post-relapse melanoma samples. We anticipate that a combinatorial drug treatment approach involving vemurafenib and novel eIF4E-targeting therapies will significantly reduce melanoma progression.

2.6 Figures and Supplementary Figures

Figure 1

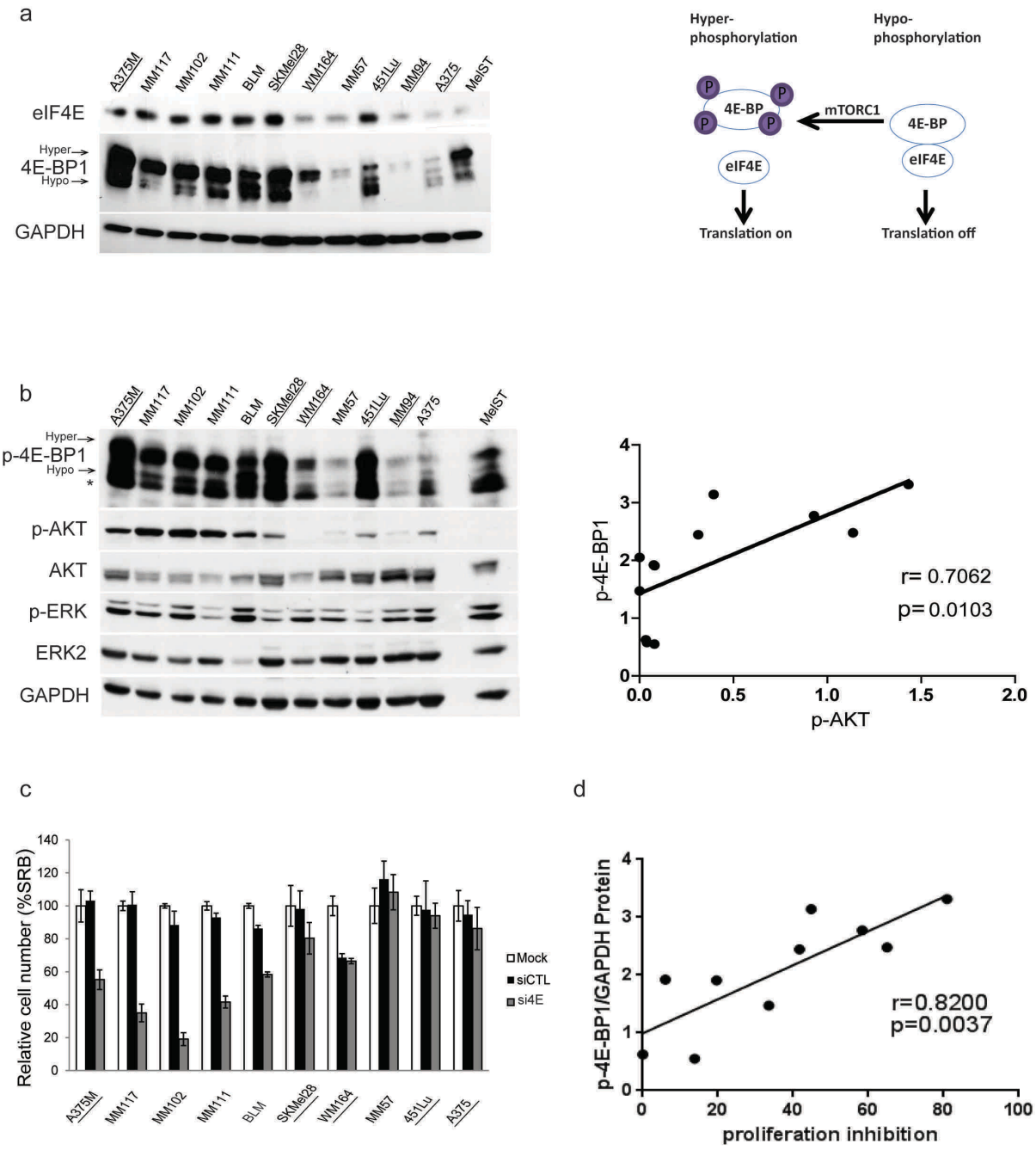

Figure 2.1. eIF4E knockdown inhibits proliferation in melanoma cell lines that highly express eIF4E, p-AKT, and hyperphosphorylated 4E-BP1.

(a) Western blots displaying eIF4E and 4E-BP1 protein expression in a panel of melanoma cell lines compared to immortalized melanocytes (MelST). Underlined are the cell lines that possess a BRAF V600E mutation. The schematic (right) shows the relationship between the phosphorylation status of 4E-BP and its ability to bind and inhibit eIF4E. (b) Western blot of p-AKT, AKT, p-ERK, ERK2, and p-4E-BP1 in melanoma cell lines versus immortalized melanocytes (MelST). GAPDH is a loading control in all immunoblots. Four bands can be seen on p-4E-BP1 blot: the upper band represents the hyperphosphorylated form, whereas the lower band represents the hypophosphorylated form. The lowest band identified with an asterisk shows the phosphorylation of 4E-BP2. Correlation between the expression of p-AKT and p-4E-BP1 in the melanoma cell lines is shown (right). Pearson correlation statistics have been employed. (c) Cell proliferation assay plot following four-day eIF4E siRNA treatment, assessed by sulforhodamine B (SRB) staining. Error bars were defined as mean +/- SD, n=3. (d) Correlation between the levels of proliferation inhibition upon eIF4E siRNA silencing versus p-4E-BP1 expression. Pearson correlation statistics have been employed. Note: p-4E-BP1 and p-AKT protein levels were normalized to corresponding GAPDH levels.

Figure 2

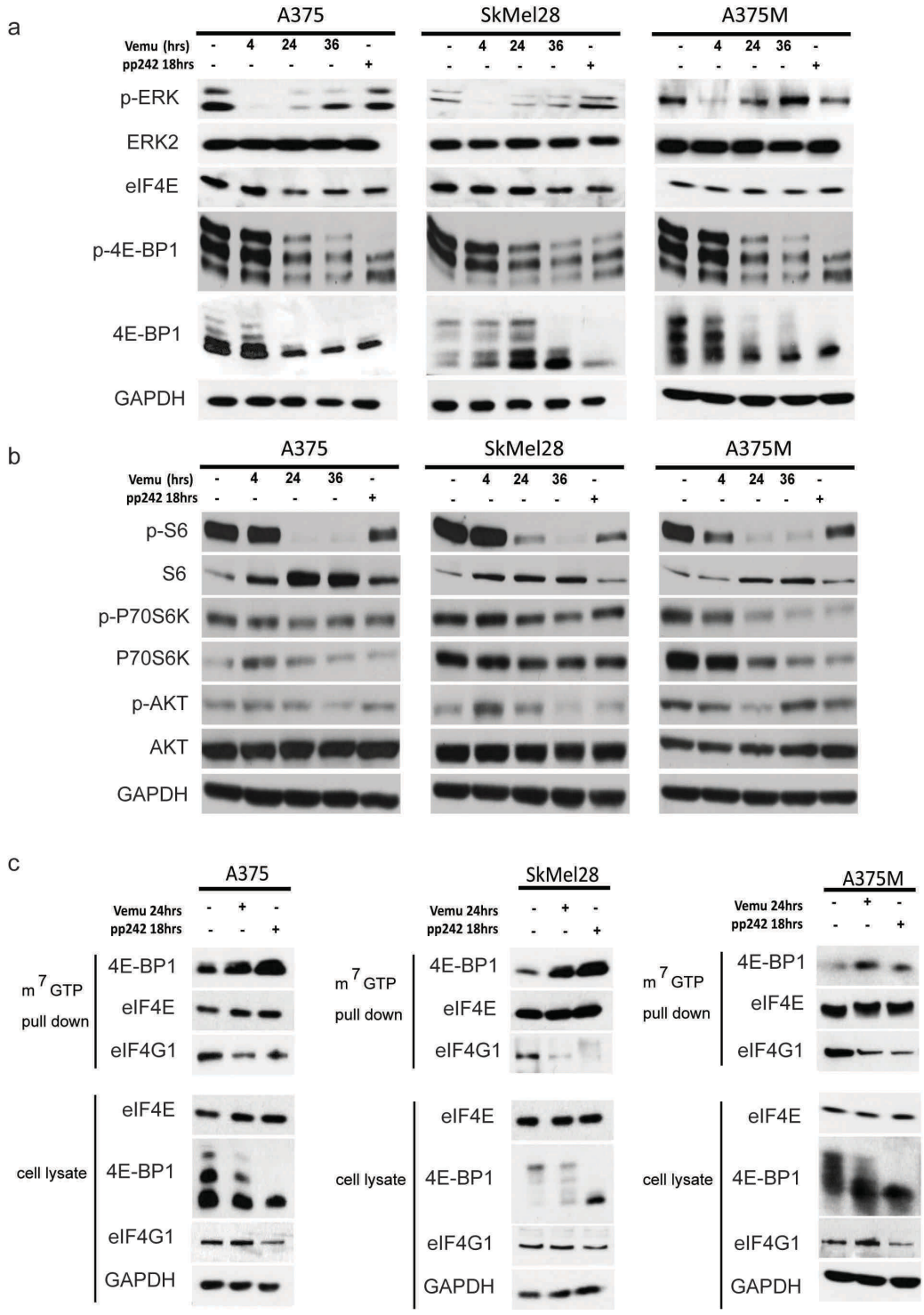
a
A375
SkMel28
A375M
Vemu (hrs) - 4 24 36 -
pp242 18hrs - - - - +
p-ERK
ERK2
eIF4E
p-4E-BP1
4E-BP1
GAPDH
b
A375
SkMel28
A375M
Vemu (hrs) - 4 24 36 -
pp242 18hrs - - - - +
p-S6
S6
p-P70S6K
P70S6K
p-AKT
AKT
GAPDH
c
A375
SkMel28
A375M
Vemu 24hrs - + -
pp242 18hrs - - +
m7GTP pull down
4E-BP1
eIF4E
eIF4G1
cell lysate
eIF4E
4E-BP1
eIF4G1
GAPDH

Figure 2 continued

d

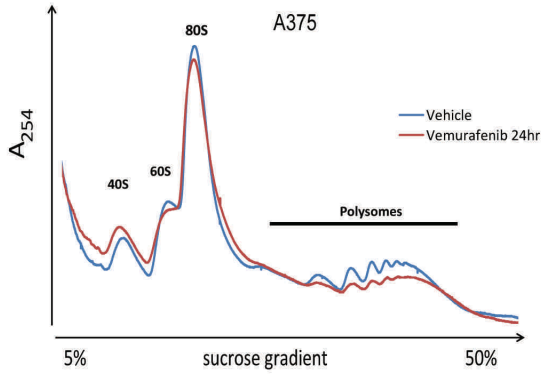

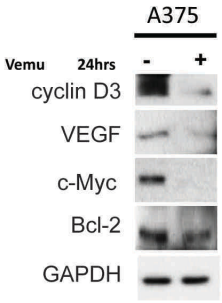

e

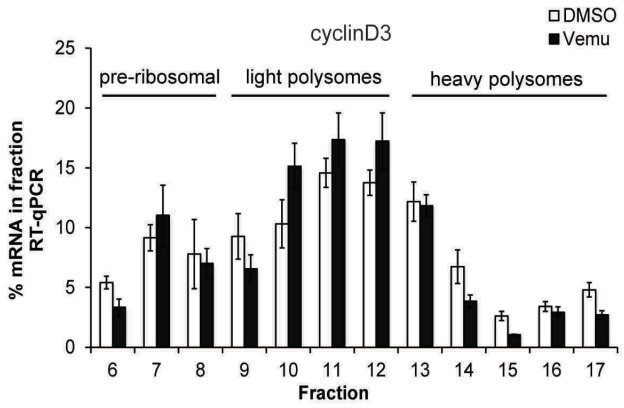

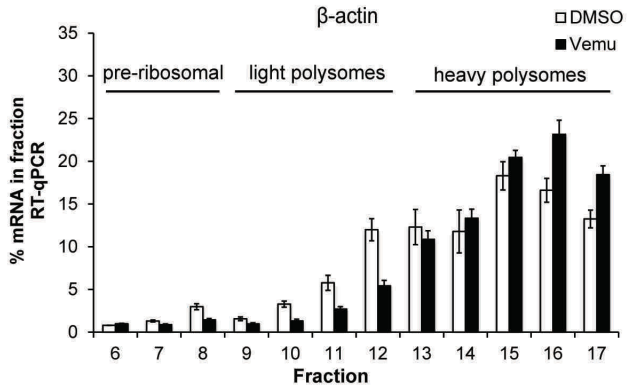

Figure 2.2. Vemurafenib drastically inhibits the phosphorylation of the eIF4E inhibitory protein, 4E-BP1, in $BRAF^{V600E}$ melanomas.

(a) Western blot of eIF4E, p-4E-BP1, 4E-BP1 and p-ERK and ERK2 in A375, SkMel28 and A375M upon 2.5μM vemurafenib treatment at the times indicated. 1μM PP242 was used as a positive control to promote 4E-BP1 hypophosphorylation. (b) Western blot of p-S6, S6, p-P70S6K, P70S6K and p-AKT and AKT in A375, SkMel28 and A375M upon 2.5μM vemurafenib treatment at the times indicated. (c) Cap-binding assay in A375, SkMel28 and A375M upon 2.5μM vemurafenib treatment. (d) Polysome profile (% sucrose gradient vs 254 nm rRNA absorbance) in A375 cells in the absence and presence of 2.5μM vemurafenib for 24 hours (left panel). Western blot analysis of cyclin D3, VEGF, c-Myc, and Bcl-2 following treatment with 2.5μM vemurafenib for 24 hours (right panel). (e) qRT-PCR was used to determine the distribution of cyclin D3 and β-actin mRNAs in polysome fractions (heavy versus light polysomes) isolated from A375 cells treated with DMSO or 2.5μM vemurafenib for 24 hours.

Figure 3

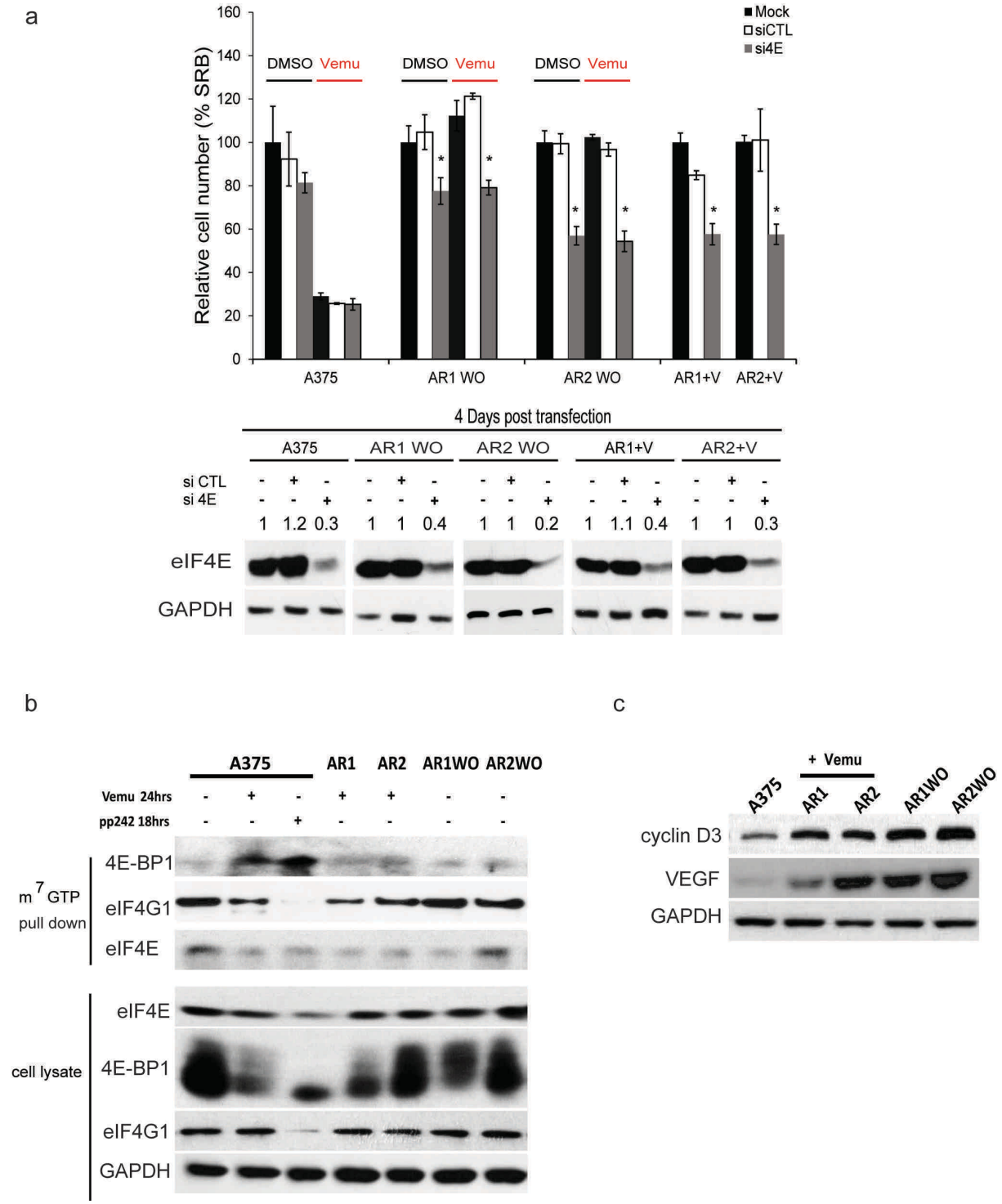
a
Relative cell number (% SRB)
Mock
siCTL
si4E
DMSO Vemu
A375
AR1 WO
AR2 WO
AR1+V
AR2+V
4 Days post transfection
si CTL
si 4E
1 1.2 0.3 1 1 0.4 1 1 0.2 1 1.1 0.4 1 1 0.3
eIF4E
GAPDH
b
A375
AR1
AR2
AR1WO
AR2WO
Vemu 24hrs
pp242 18hrs
m7GTP pull down
4E-BP1
eIF4G1
eIF4E
cell lysate
eIF4E
4E-BP1
eIF4G1
GAPDH
c
+ Vemu
A375
AR1
AR2
AR1WO
AR2WO
cyclin D3
VEGF
GAPDH

Figure 2.3. eIF4E plays a key role in vemurafenib resistance in A375 $BRAF^{V600E}$ human melanoma cell lines.

(a) Cell proliferation assessment by SRB staining four days-post si4E transfection with either vehicle (DMSO) or 2.5μM vemurafenib co-treatment in A375, AR1 WO and AR2 WO, AR1, and AR2, Note: AR1 and AR2 are continuously maintained in 2.5μM vemurafenib. Error bars were defined as mean +/- SD, n=3. Statistical significance was determined by the Student's *t*-test. * < 0.05. (b) Cap-binding assay in parental A375 and resistant lines AR1, AR2 (maintained in 2.5 μM vemurafenib), and corresponding vemurafenib wash off lines AR1WO and AR2WO. PP242 is a positive control, for 4E-BP1 hypophosphorylation. (c) Western blot of cyclin D3, VEGF, and GAPDH in A375 parental, resistant lines AR1 and AR2, and corresponding wash-offs, AR1WO and AR2 WO, respectively.

Figure 4

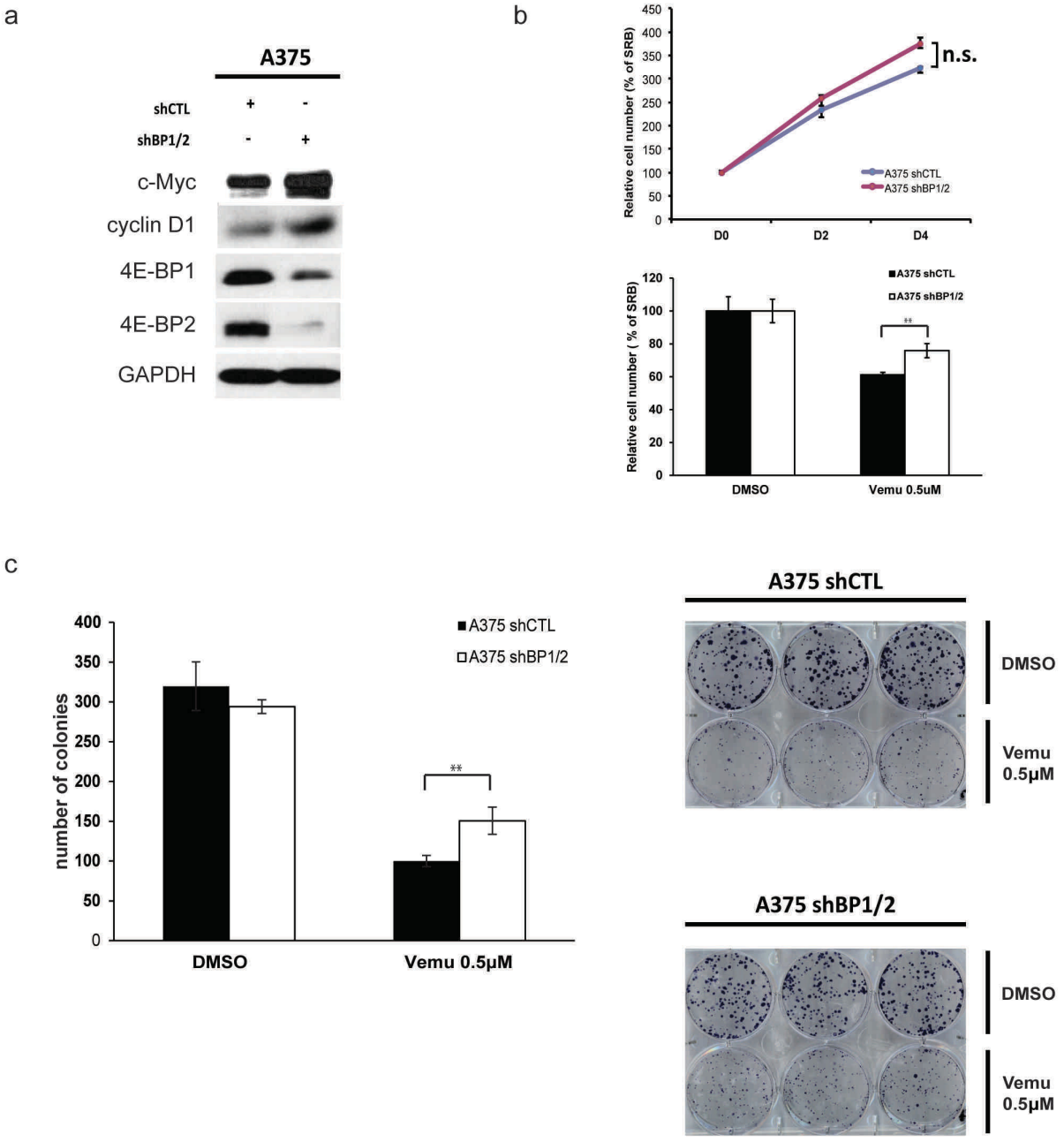
a
A375
shCTL + -
shBP1/2 - +
c-Myc
cyclin D1
4E-BP1
4E-BP2
GAPDH
b
Relative cell number (% of SRB)
n.s.
A375 shCTL
A375 shBP1/2
D0
D2
D4
Relative cell number (% of SRB)
**
DMSO
Vemu 0.5uM
c
number of colonies
A375 shCTL
A375 shBP1/2
**
DMSO
Vemu 0.5μM
A375 shCTL
DMSO
Vemu 0.5μM
A375 shBP1/2
DMSO
Vemu 0.5μM

Figure 2.4. Stable knockdown of 4E-BP1/2 contributes to the development of vemurafenib resistance in A375 cells.

(a) Western blot of c-Myc, 4E-BP1, 4E-BP2, and GAPDH (loading control) in A375 shCTL and shBP1/2 cell lines. (b) Cell proliferation assay after four days with or without 0.5μM vemurafenib treatment in A375 shCTL and shBP1/2 stable cell lines. Error bars were defined as mean +/- SD, n=3. Statistical significance was determined by one-way analysis of variance followed by the Newman–Keuls post-hoc test using Prism version 3.0 (GraphPad Software, San Diego, CA). * $p < 0.05$. (c) Clonogenic assay after 14 days with or without 0.5μM vemurafenib treatment in A375 shCTL and shBP1/2 stable cell lines. The number of colonies was counted manually and graphed. Error bars were defined as mean +/- SD, n=3. Statistical significance was determined by one-way analysis of variance followed by the Newman–Keuls post-hoc test using Prism version 3.0 (GraphPad Software, San Diego, CA). ** $p < 0.01$. Representative pictures are shown on the right.

Figure S1

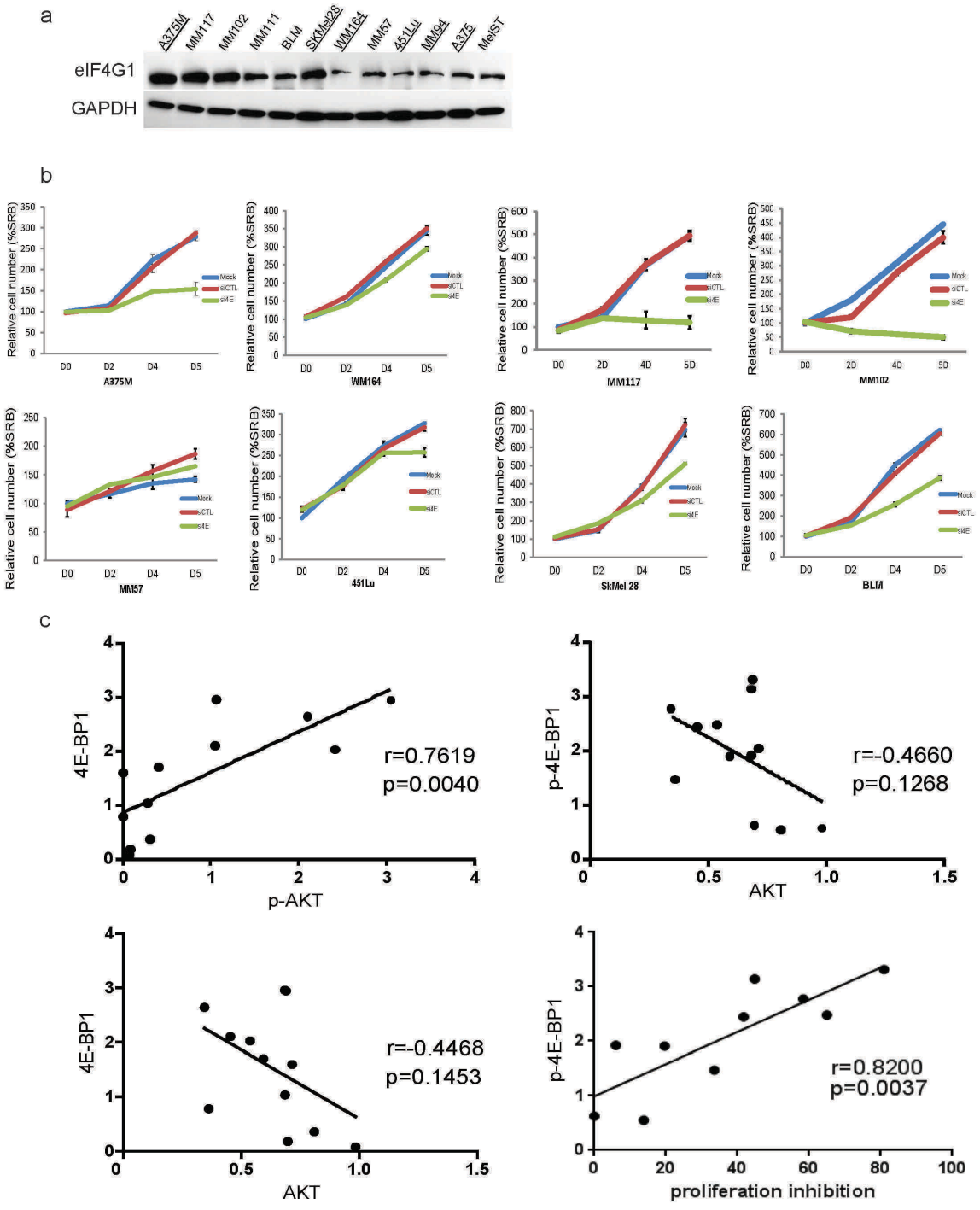
a
A375M
MM117
MM102
MM111
BLM
SkMel28
WM164
MM57
451Lu
MM94
A375
MelST
eIF4G1
GAPDH
b
Relative cell number (%SRB)
Mock
siCTL
siE
A375M
WM164
MM117
MM102
MM57
451Lu
SkMel 28
BLM
c
4E-BP1
p-AKT
r=0.7619
p=0.0040
p-4E-BP1
AKT
r=-0.4660
p=0.1268
4E-BP1
AKT
r=-0.4468
p=0.1453
p-4E-BP1
proliferation inhibition
r=0.8200
p=0.0037

Figure S1

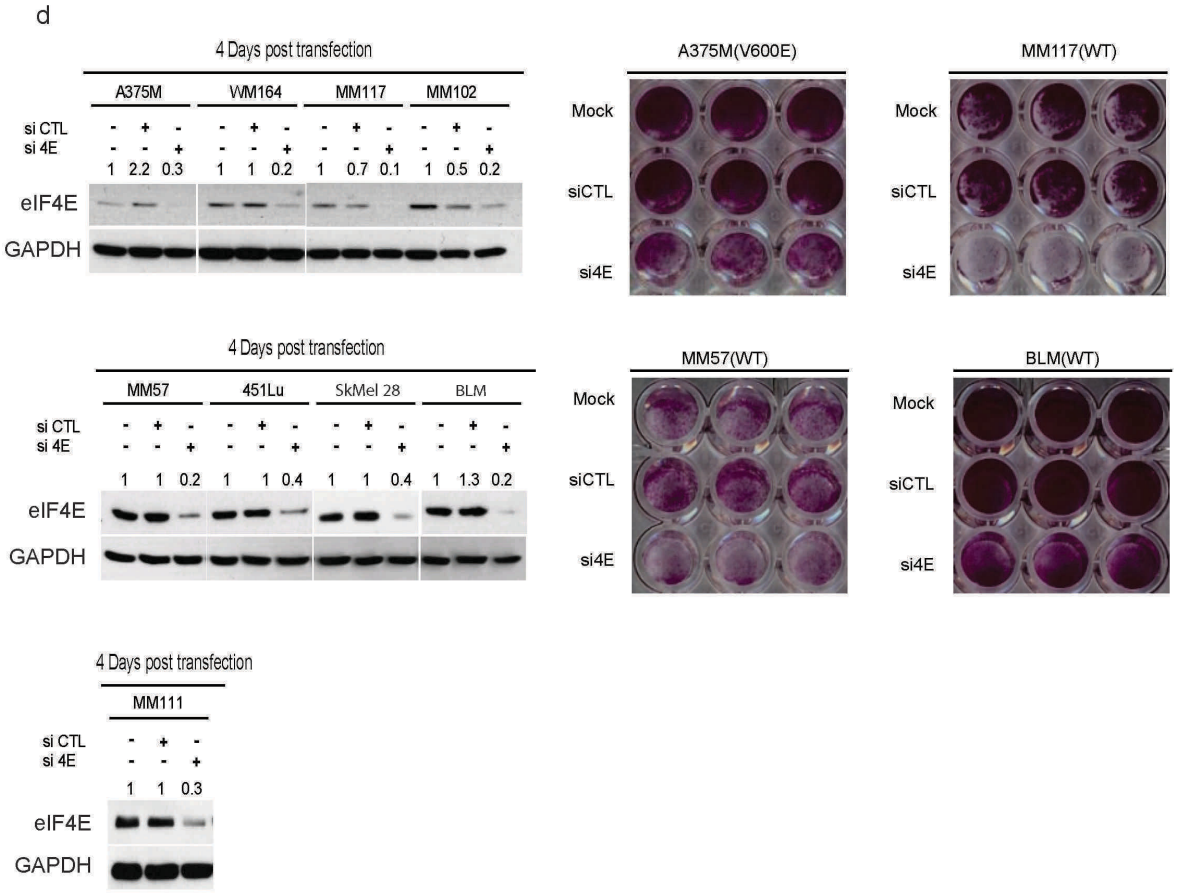
d
4 Days post transfection
A375M
WM164
MM117
MM102
si CTL
si 4E
1 2.2 0.3 1 1 0.2 1 0.7 0.1 1 0.5 0.2
eIF4E
GAPDH
A375M(V600E)
MM117(WT)
Mock
siCTL
si4E
4 Days post transfection
MM57
451Lu
SkMel 28
BLM
1 1 0.2 1 1 0.4 1 1 0.4 1 1.3 0.2
MM57(WT)
BLM(WT)
4 Days post transfection
MM111
1 1 0.3

Figure 2S1. The effect of eIF4E knockdown in a panel of human melanoma cell lines, and the correlation between (p)-AKT and (p)-4E-BP1 expression.

(a) Western blot of eIF4G1 in a panel of melanoma cell lines. (b) Growth curves of various melanoma cell lines from either siCTL or eIF4E siRNA treated for four days. (c) The correlation between the expression of (p) -AKT and (p)-4E-BP1 in melanoma cell lines as well as the correlation between proliferation inhibition by silencing eIF4E versus the expression of p-4E-BP1 in melanoma cell lines. (d) Western blot of eIF4E depletion and images of corresponding SRB staining, following four-day knockdown. Protein densitometry was employed by Image J software to quantify the efficiency of eIF4E knockdown. The relative value of eIF4E density in each lane was normalized to the GAPDH value as indicated.

Figure S2

a

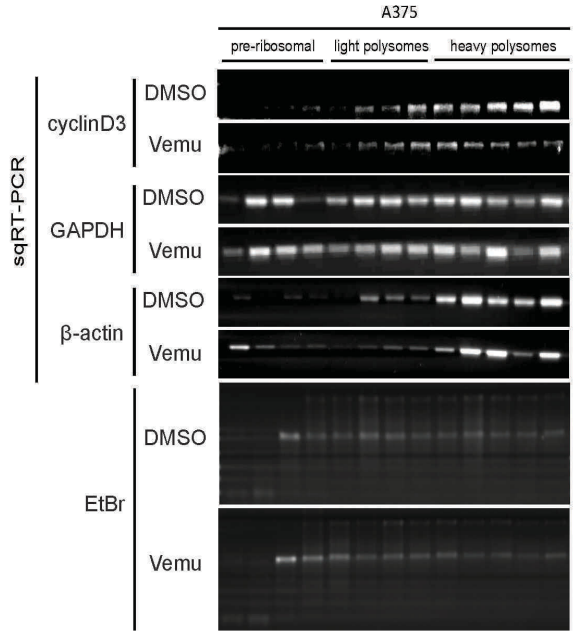
A375
pre-ribosomal
light polysomes
heavy polysomes
sqRT-PCR
cyclinD3
DMSO
Vemu
GAPDH
DMSO
Vemu
β-actin
DMSO
Vemu
EtBr
DMSO
Vemu

b

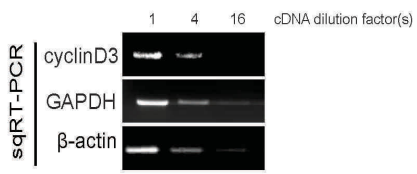
1
4
16
cDNA dilution factor(s)
sqRT-PCR
cyclinD3
GAPDH
β-actin

Figure 2S2. Vemurafenib inhibits the translation of eIF4E-sensitive mRNA cyclinD3.

(a) RNA was visualized by ethidium bromide (EtBr). Semiquantitative reverse polymerase chain reaction (sqRT-PCR) was used to determine the distribution of cyclin D3, GAPDH and β-actin mRNAs in polysome fractions isolated from A375 cells treated with DMSO or 2.5μM vemurafenib for 24 hours.

(b) The sqRT-PCR reactions were in the linear range.

Figure S3

a

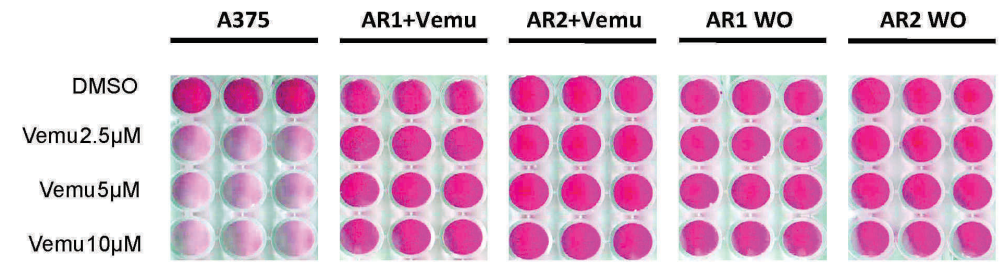
A375
AR1+Vemu
AR2+Vemu
AR1 WO
AR2 WO
DMSO
Vemu2.5μM
Vemu5μM
Vemu10μM

b

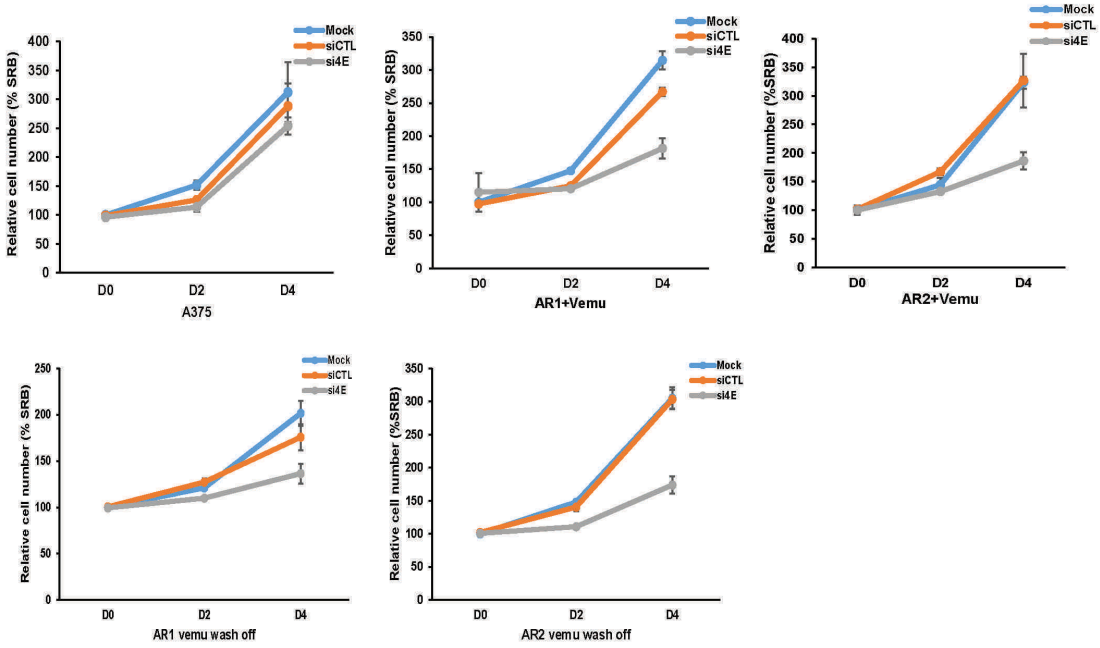
Mock
siCTL
si4E
Relative cell number (% SRB)
Relativve cell number (% SRB)
Relative cell number (%SRB)
D0
D2
D4
A375
AR1+Vemu
AR2+Vemu
AR1 vemu wash off
AR2 vemu wash off

Figure 2S3. The role of eIF4E in developing acquired resistance to vemurafenib. (a) SRB assay under escalating doses of vemurafenib in A375 and vemurafenib resistant cell lines AR1, AR2 , AR1 wash off (WO) and AR2 WO lines for four days. (b)Growth curves of A375 and vemurafenib resistant cell lines AR1, AR2 , AR1 WO and AR2 WO lines upon four days of eIF4E knockdown.

Chapter 3

Mnk1/2 are a therapeutic target in cKit mutant melanoma.

3.1 Abstract

cKit is activated in 20-30% of acral, mucosal and chronically damaged skin (CSD) melanomas. cKit mutant melanomas are often resistant, or quickly develop resistance, to cKit inhibitors, thus more effective therapies are desperately needed. Signalling pathways activated downstream of oncogenic cKit include the MAPK and PI3K-AKT-mTOR cascades, which ultimately impinge upon the known oncogene and eukaryotic translation initiation factor eIF4E, to cause its phosphorylation. eIF4E is exclusively phosphorylated by Mnk1/2 kinases (MAP kinase-interacting serine/threonine-protein kinase 1/2), and this modification is essential for its oncogenicity. We evaluated the role of the Mnk/eIF4E axis downstream of oncogenic c-Kit, and found that Mnk1/2 can be therapeutically targeted in melanomas with cKit mutations (D820Y and L576P). Biopsies from patients with acral, mucosal and CSD melanomas, showed that Mnk1 and eIF4E are both highly phosphorylated in those melanomas with cKit aberrations, versus wild-type cKit. Moreover, pharmacologic or genetic inhibition of cKit reduces cell proliferation, coincident with repression of phospho-Mnk and phospho-eIF4E. Consistent with the importance of Mnk1/2 downstream of mutated cKit, we show that the proliferation, migration, invasion and melanoma outgrowth are attenuated when Mnk1/2 are silenced in cKit mutant melanoma cells. Polysome profiling of melanomas lacking Mnk1/2 define the molecular

mechanisms underlying the oncogenic activities of the Mnk/eIF4E axis, downstream of mutant cKit. Combined, these studies support inhibiting Mnk1/2 as a novel therapeutic strategy for these incurable cKit-driven melanomas and emphasize the need for clinical development of Mnk1/2 inhibitors.

3.2 Introduction

Melanoma is a cancer that originates from dysfunctional melanocytes. Melanoma arising on acral and mucosal anatomical sites account for about 5%-60% of melanoma cases, varying largely between races (254-256), have a much poorer prognoses, and effective therapeutic options are lacking.

Curtin and colleagues first found that melanomas arising in acral, mucosal and chronic sun-damaged regions harbour a high frequency of activating mutations in *KIT* gene (126). More recently, the 'The Cancer Genome Atlas (TCGA)' Network classified cutaneous melanoma into BRAF, NRAS, NF1 and triple-wild type groups. About 22% of triple wild type melanomas harbour cKit aberrations (78). The *KIT* gene encodes the cKit tyrosine kinase receptor, and constitutive activation of cKit, via mutation or amplification, leads to the co-activation of downstream MAPK and PI3K-AKT-mTOR pathways, and subsequent promotion of tumorigenesis (150, 257-260). Current therapeutic strategies for treating cKit aberrant melanomas include various tyrosine kinase inhibitors (TKIs) such as imatinib, dasatinib and nilotinib (58). However, as with many chemotherapeutics, patients with cKit aberrant melanoma quickly develop acquired resistance to these TKIs, often due to the acquisition of secondary mutations in cKit (131, 151).

One potential novel therapeutic target that has not been well defined in melanomas harbouring cKit mutations or amplifications is the Mnk/eIF4E axis. eIF4E is part of the eIF4F complex, which also consists of the helicase eIF4A, and scaffolding protein eIF4G. eIF4E is overexpressed in a wide variety of human malignancies including melanoma (194, 195) and facilitates the translation of pro-survival mRNAs, such as VEGF, cyclin D3, E1 and Mcl-1.

Prior to its phosphorylation on serine 209 by mitogen-activated protein kinase (MAPK)-interacting kinases (Mnk) 1 and 2, eIF4E is incorporated into the eIF4F complex, comprising eIF4G and eIF4A (218). Although Mnk activity and the phosphorylation of eIF4E are dispensable for normal development (187, 188), eIF4E phosphorylation is required for tumorigenesis, lymphomagenesis and tumor metastasis, thus making Mnk1/2 kinases ideal therapeutic targets (187-189). In metastatic melanomas, eIF4E is highly phosphorylated and this is strongly associated with a reduced life expectancy (195). These data, and phospho-eIF4E being the convergence point of aberrant cKit signalling, provide support for the prospect of targeting Mnk1/2 therapeutically in melanomas harbouring cKit mutations and amplifications.

Our data show that the Mnk/eIF4E axis is a major downstream effector of oncogenic cKit. Our findings provide the groundwork for targeting Mnk/eIF4E axis in cKit melanomas.

3.3 Material and Methods

3.3.1 Reagents

Dasatinib was purchased from LC Laboratories (MA, US). Drug was dissolved in DMSO and 10mM aliquots of Dasatinib were stored at -80°C. The following commercially available antibodies were used: phospho-Mnk1 (Thr197/202), phospho-eIF4E (Ser209), phospho-ERK (T202/Y204), phospho-cKit (Tyr 703), cKit, cleaved PARP, phospho-AKT (Ser 473) AKT, phospho-4E-BP1 (T37/46), 4E-BP1, phospho-S6 (S240/244), S6, phospho-P70S6K (Thr 389), P70S6K and GAPDH were purchased from Cell Signalling Technology. eIF4E antibody was purchased from BD Bioscience. Mnk2 antibody was purchased from Santa Cruz Biotechnology. Transfection reagents Lipofectamine 2000 or Lipofectamine RNAiMax were purchased from Invitrogen.

3.3.2 Cell Culture

All cell lines used in this paper, except A375, were kindly provided by Dr. Ghanem Ghanem (Institute Jules Bordet, Bruxelles). A375 cell line was a gift from Dr. Gideon Bollag. A375 was cultured in Dulbecco's modified Eagle medium (DMEM) containing 10% fetal bovine serum (FBS) and 1% Penicillin/Streptomycin; MM61, MM111, and HBL cells were cultured in HAM's F10 containing 10% FBS and 1% Penicillin/Streptomycin. M230 cells was cultured in RPMI-164 containing 10% FBS and 1% Penicillin/Streptomycin. Stable cell lines (HBL pBABE, ca-Mnk, shCTL, shMnk1+2) were cultured in HAM's F10 containing 10% FBS and 1% Penicillin/Streptomycin supplemented with 1ug/ml of puromycin for selection. All cell lines were maintained at 37°C in a humidified incubator with 5% CO_2.

3.3.3 Proliferation assay

Cell proliferation was tested by sulforhodamine B (SRB) assay. Cells were plated in 96-well plates 24 h before treatment, andthen treated with vemurafenib, for 24, 48, and 96 hours. After each treatment, 96-well plates were harvested and fixed with 10% trichloroacetic acid (TCA) for 1 hour. Plates were then washed and sterilized with water three times and allowed to air-dry overnight. Once the fixation was completed, each well was stained with 100 µl of 0.4% (w/v) SRB dissolved in 1% acetic acid. for at least 30 minutes. After staining, plates were washed with 1% acetic acid three times and air-dried overnight. Bound SRB was solubilized by adding 100 µl/well of 10mM unbuffered Tris base, pH 10.5 for 10 minutes. Absorbance at 564 nm was read using FLUOstar OPTIMA plate reader.

3.3.4 Plasmids, Virus Production, Stable Cell Selection

Human shMnk1 and shMnk2 plasmids were obtained from Dr. Sid Huang's group. (Sigma MISSION shRNAs), shRNAs were co-transfected with PLP1, VSVG and PLP2 packaging constructs into 293FT cells using Lipofectamine 2000 (Invitrogen) to generate viral particles. Viral supernatants were harvested 48 hours post-transfection and spun at 1000 rpm for five minutes. Control or shMnk1+2 viral supernatants were added to HBL cells overnight to establish shMNK1 and shMNK2 stable knockdown cell lines. After two rounds of infection, cells were treated with puromycin (1µg/ml) for 48 hours for subclone selection.

3.3.5 Polysome profiling

Polysome profiling was performed as previously described by (238) . For sucrose gradient fractionation and polysome isolation, HBL shCTL and HBL shMnk1+2 cells were used. Cells were treated with cycloheximide (100 microgram/ml) five minutes prior to harvesting, then washed in cold PBS containing 100 microgram/ml cycloheximide, followed by centrifugation for 5 minutes at 1500 rpm. Cell pellets were lysed in hypotonic buffer (5 mM Tris-HCl (pH 7.5), 2.5 mM $MgCl_2$, 1.5 mM KCl and 1X protease inhibitor cocktail (EDTA-free), containing 1mM DTT and RNAse inhibitor (100 units). Samples were kept on ice for 12 minutes, then centrifuged at 12, 200 rpm for 7 minutes. The supernatants were loaded on to 10–50% sucrose gradient followed by centrifugation at 39,000 rpm for 2 hours at 4°C. Fractions were collected (24 fractions, 12 drops each) using a Foxy JR ISCO collector and data (absorbance, 254 nm) were collected.

3.3.6 Western blot analysis

Cells were treated with dasatinib, imatinib or SEL201 at the indicated times, and pellets were harvested to obtain protein extracts. Briefly, cell pellets were lysed in RIPA buffer (50 mM Tris-HCl, pH 8.0, with 150 mM sodium chloride, 1.0% Igepal CA-630 (NP-40), 0.5% sodium deoxycholate, and 0.1% sodium dodecyl sulphate). After sonication, cell lysates were centrifuged at 13,000 rpm for 15 minutes. The supernatants were collected and protein concentrations were quantified. Equal amounts of protein were loaded and separated]on a 10% SDS-PAGE. After transferring to a nitrocellulose membrane (BioRad), 5% milk/TBS was used to block for 1 hour, and then probed for target antibodies overnight at 4°C. After incubation with horseradish

peroxidase (HRP) conjugated secondary antibodies for 1 hour at room temperature, the signals of targeted protein were developed with chemiluminescence substrate (Amersham).

3.3.7 RNA interference

Cells were seeded in 10 cm dishes at 80% confluency. cKit,eIF4E siRNA or control siRNA was added into dishes 20 minutes after incubation with transfection reagent Lipofectamine RNAiMAX following manufacturer's instructions. After 16 hours, cells were washed with 1X PBS and fresh medium was added. At day 4 of transfection, cell pellets were harvested for western blotting. The sequences of the previously validated cKit siRNA pair were as follows: #1 5′-AGC AGG AAA UAA AGU AUA GGU UUAG -3′and 5′-CUA AAC CUA UAC UUU AUU UCC UGC UAC -3′; #2 5′-CGA UUC UAA GUU CUA CAA GAU GATC -3′and 5′-GAU CAU CUU GUA GAA CUU AGA AUC GAC -3′. AllStars Negative Control siRNA (Qiagen) was used as non-silencing control.

3.3.8 RNA isolation

To isolate mRNAs from each polysome fraction, Trizol (Invitrogen) was added in each fraction tubefollowed by 5 minutes of incubation at room temperature. Then 200µl of chloroform was added to each tube and mixed well for 15 seconds. Following centrifugation at 12,000 x g for 15 minutes at 4°C, the clear phase was carefully obtained and placed into an RNAse-free tube. 500µl of isopropanol was added to the clear phase and the mixture was centrifuged for 30 minutes (12,000 x g, 4°C). The isopropanol was then removed and the remaining pellets were washed with 1ml of 75%

ethanol (in DEPC water) followed by centrifugation for 5 minutes (12,000 x g, 4°C). The remaining liquid was then carefully aspirated and the pellets were allowed to air-dry. 20µl of DEPC water were added to dissolve RNA pellets, which were then quantitated (Thermo scientific Nanodrop 1000).

3.3.9 Clonogenic assay

1000 cells per well were plated in 6-well plates and the cells were allowed to adhere overnight. After overnight incubation, the cells were treated with either DMSO (control) or SEL201 at the indicated concentrations. After 14 days, media were removed from the wells, and the cells were stained with 0.5% (W/V) crystal violet in 70% ethanol. After one hour of incubation at room temperature, staining dye was washed and the colony numbers were counted manually. The experiment was done in triplicates.

3.3.10 Animal study

4-6 weeks old female Scid Beige (strain code 250) mice were purchased from Charles River Laboratories. For mice xenografts, 5×10^6 HBL shCTL or shMnk1+2 cells were suspended in PBS and injected subcutaneously in female Scid Beige mice. Tumors were allowed to form palpable tumors and the size was measured every two days using a caliper. Tumor volume was derived using the following formula: (LxWxW)/2, in which L refers to the diameter of the longest axis and W refers to the diameter of the shortest axis. At endpoint, tumors were harvested for either western blotting analysis or fixed in 10% formalin for immunohistochemistry (IHC) assessment.

3.3.11 Immunohistochemistry and scoring

Human melanoma tissue samples were acquired from 24 patients hospitalized during January 2013 and January 2016 at the Peking Cancer Hospital & Institute, Beijing, China. These paraffin-embedded samples were stained with hematoxylin and eosin (H&E) and tested for melanoma markers (S-100, HMB-45, or MART-1) to confirm the diagnosis of melanoma by the pathology department in Peking Cancer Hospital, or by the pathology department of hospitals where patients were initially diagnosed. Clinical data, including age, sex, thickness (Breslow), ulceration were collected in 16 out of 24 patients.

Immunohistochemistry (IHC) analysis for phospho-eIF4E (phospho S209, abcam), phospho-Mnk1 (phospho Thr 197/202, cell signalling) and total Mnk1(Sigma-Aldaich) were conducted on formalin fixed, paraffin embedded tumor sections at 1:50 dilution, followed by a standard avidin–biotin detection protocol. Hematoxylin counterstained slides were mounted with cover slips and staining intensity was determined by Dr. Dong, a clinically certified pathologist in Beijing Cancer Hospital & Institute. Staining intensity was scored as 0, 1, 2, and 3 ("0" as negative staining, and "3" as the strongest staining intensity). Representative images of the intensity scores were shown in Figure 1B. Five images of melanoma lesions were taken from each stained slide and the scoring was given according to the intensity of the red staining in these images. Less than 10% of positive (red) staining for the targeted protein in a sample was considered negative staining, and was scored as 0; score 1 was given to those samples that showed weak red staining; score 2 was given to the samples that

revealed mild red staining; and score 3 was given to those samples that had the darkest red staining.

3.3.12 Statistical analysis

All *in vitro* experiments were triplicated and quantitative data were shown as the average of all biological replicates. Each *in vivo* experiment was repeated twice with the number of animals indicated in the figures. Statistical analyses were performed using GraphPad Prism. The details of each statistical test used were given in the figure legends.

3.3.13 Study Approval

All animal care and experiments were carried out according to rules and regulations established by the Canadian Council of Animal Care and protocols were approved by the McGill University Animal Care Committee. Consent was obtained for human tissue acquisition according to guidelines set by Peking Cancer Hospital & Institute, Beijing, China and their affiliated local medical authorities. And the IHC study on human melanoma sample was approved by the medical ethics committee of the Beijing Cancer Hospital & Institute and was conducted according to the Declaration of Helsinki Principles.

3.4 Results

Mnk1 and eIF4E are phosphorylated in human melanomas harbouring cKit aberrations.

Although Mnk1/2 expression and phosphorylation have been previously demonstrated in human cancer (183, 261, 262), their expression and phosphorylation status in melanoma cell lines and melanoma tissues has not been previously reported. We used immunohistochemistry (IHC) to evaluate Mnk1, phospho-Mnk1 and phospho-eIF4E expression in archival surgical specimens of melanomas wherein cKit was either wild type or mutated (Supplemental Table 1). We found that melanomas from patients harbouring mutant cKit expressed significantly higher levels of phospho-Mnk1 (trend test via chi square, p=0.0446), compared to patients whose melanomas were cKit wild type (Figure 1A). cKit mutant melanomas also expressed higher levels of Mnk1 compared to cKit wild-type melanomas (Supplementary Figure 1A). As readout for increased Mnk1/2 activity, we also determined the phosphorylation state of eIF4E, one of the best-described substrates of Mnk1/2. In keeping with higher Mnk1/2 activity in melanomas driven by oncogenic cKit, phospho-eIF4E (trend test via chi square, p=0.0404) was also higher in cKit mutant melanomas versus wild-type cKit melanomas (Figure 1A). Furthermore, phospho-Mnk1 and phospho-eIF4E levels positively-correlate within a given patient sample (trend test via pearson correlation, p=0.002), which lends confidence to using phospho-eIF4E as a biological outcome for increased Mnk1/2 activation (Figure 1B).

Next, we determined whether cKit mutant melanoma cell lines could be used as in vitro tumour model to study the role of the Mnk/eIF4E pathway downstream of oncogenic cKit. We profiled the expression and phosphorylation of Mnk1, in a panel of melanoma cell lines harbouring different oncogenic mutations in *NRAS, BRAF, and KIT (*Supplementary Figure 1B). As shown in Figure 1C, there is a striking correlation in

melanomas with aberrant cKit, either with cKit point mutations or amplification, and increased expression of phospho-Mnk1 and phospho-eIF4E. These data are in line with the patient data that activation of the Mnk/eIF4E axis lies downstream of oncogenic cKit signaling.

Inhibiting cKit, pharmacologically or genetically, blocks the phosphorylation of Mnk1 and eIF4E.

Recent clinical trials report the potential of cKit inhibitors in melanoma, however their mechanism of action remains poorly developed (128, 131, 147, 263). To test whether the Mnk/eIF4E axis resides in the same molecular pathway downstream of activated cKit, we looked at the phosphorylation of Mnk1 and eIF4E in response to two cKit inhibitors dasatinib and imatinib. As shown in Figure 2A, dasatinib significantly inhibited cell proliferation of both D820Y (HBL, MM61, MM111) and L576P (M230) cKit mutant melanoma cell lines, but not in cKit wild-type A375 cells. Western blot analysis revealed that dasatinib treatment repressed the expression of phospho-Mnk1 and phospho-eIF4E in either cKit mutant melanoma cell lines (Figure 2B). Imatinib on the other hand, only repressed proliferation of the L576P mutant cell line (supplementary Figure 2A), consistent with previous reports showing that imatinib is refractory in cells expressing the cKit D820Y mutation (151). Similar with the cell proliferation data, imatinib only inhibited the phosphorylation of Mnk1 and eIF4E in cKit L576P mutant M230 cells (supplementary Figure 2B). We also generated HBL cells stably expressing either a constitutively activated Mnk1 construct (CA-Mnk1) or control vector (pBABE). Overexpression of CA-Mnk1 had little effect on cell proliferation compared to pBABE

HBL cells, however the IC50 of dasatinib increased in CA-Mnk HBL cells compared to their pBABE counterparts (Supplemental Figure 2C, 2D). Collectively, these data support our hypothesis that the activity of dasatinib acts through repressing Mnk1 activity.

In addition to inhibiting cKit, dasatinib can also inhibits src and platelet derived growth factor receptor (PDGFR) (264), thus we next silenced the expression of cKit using siRNA and examined the effect of cKit depletion on cell proliferation. As shown in Figure 2C, cKit knock down results in an inhibition of proliferation of cKit mutant melanoma cell lines. Moreover, genetically inhibiting cKit expression also suppresses the phosphorylation of Mnk1 and eIF4E (Figure 2D). These data suggest that Mnk1 is activated and eIF4E phosphorylated downstream of cKit activating mutations.

Pharmacologically or genetically blocking Mnk1/2 inhibits oncogenic properties in cKit mutant melanoma.

We next investigated the role of Mnk1/2 in oncogenic signaling and characterized the effects of blocking these kinases pharmacologically and genetically in cKit mutant melanomas. Unlike CGP57380 and cercosporamide, which are not being pursued clinically, Sel201 has low nM potency on the target combined with high selectivity against other kinases. SEL201 potently suppressed Mnk1/2 activity in our panel of cKit mutant melanoma cell lines, as determined by repressed phosphorylation of its substrate eIF4E, in addition, SEL201 significantly decreased the colony forming ability of both cKit D820Y and L576P mutant melanoma cell lines (Figure 3A). To confirm the results we obtained with SEL201, we stably silenced Mnk1 and Mnk2 in HBL cells using

shRNAs. As shown in Figure 3B (left hand panel), Mnk1 and its substrate phospho-eIF4E, were all suppressed in the shMnk1+2 stable cell line compared to the shRNA control HBL cell line. Due to the low specificity of the currently available Mnk2 antibodies, we used RT-qPCR to demonstrate the depletion Mnk2 status in shMnk1+2 HBL cells (Figure 3B, middle panel). Furthermore, we found there was a significant reduction in the number of colonies formed in the shMnk1+2 stable cell line, compared to the control shRNA, single shMnk1 or shMnk2 knock down HBL cells (Figure 3B, right hand panel).

We next established an *in vivo* xenograft model to identify whether Mnk1/2 activity is required for cKit mutant melanoma tumorigenic potential. HBL cells that were stably silenced, or not, for Mnk1 and Mnk2 expression (Figure 3B) were injected into SCID Beige mice. As shown in Figure 3C-3D, we monitored tumor outgrowth over 29 days after the injection, and demonstrate that shCTL tumors grow significantly larger than tumors lacking Mnk1 and Mnk2. Our *in vivo* data suggests that the Mnk activation, downstream of oncogenic cKit, is indispensible for cKit melanoma tumor outgrowth. These *in vitro* and *in vivo* data indicate that Mnk1/2 have a critical function in the survival of cKit mutant melanoma and suggest that these kinases are a therapeutic target in this hard-to-treat disease.

The migration and invasive characteristics of cKit mutant melanoma cells is dependant on the Mnk/eIF4E axis.

As the Mnk/eIF4E axis is a known facilitator of cell migration and invasion (187, 189), we next wanted to examine whether inhibition of Mnk1/2 could be used as a

strategy to block these properties in cKit mutant melanomas. We performed the Boyden Chamber assay, wherein HBL cells were seeded on top of the trans-well (coated with or without collagen I) and subsequently treated with various doses of the Mnk1/2 inhibitor SEL201. As shown in Figure 4A, the number of HBL cells that migrated through the trans-well was significantly reduced after a 72-hour treatment with SEL201. Next, we tested the ability of HBL cells to invade through Collagen I. Similarly; we found the invasive ability of HBL cells was significantly inhibited by pharmacologic inhibition of Mnk1/2 (Figure 4B). The effects of SEL201 were validated using our HBL cells that are devoid of both Mnk1 and Mnk2. Genetic silencing of Mnk1 and Mnk2 reduced cell migration and invasive abilities of cKit mutant HBL melanoma cells (Figure 4C). Collectively, our data show that Mnk1/2 inhibition reduces migration and invasion of cKit mutant melanoma cells.

mRNA translation of pro-oncogenic proteins is regulated downstream of oncogenic cKit/Mnk/eIF4E

We have mapped that Mnk1/2 are major downstream effectors of oncogenic cKit. The phosphorylation of eIF4E by Mnk1/2 engenders translation of mRNAs that encode proteins that promote invasion and metastasis (187-189). We hypothesize that one biological outcome in cells with activating cKit mutations is aberrant mRNA translation. To uncover the molecular mechanisms underlying the oncogenic activities of the Mnk/eIF4E axis downstream of mutant cKit, we sought to identify the translational targets of phospho-eIF4E by performing polysome profiling in shMnk1/2 dual depleted versus control shRNA HBL cells (Figure 5A). Polysome profiling curves of both Mnk

knock down or control group substantially overlapped with each other, consistent with previous findings that Mnk regulates only a subset of pro-survival and pro-metastatic mRNA candidates (187, 252). HBL cells devoid of Mnk1/2 expressed less cyclin E1 protein, compared to shCTL HBL cells (Figure 5B). The decrease in cyclin E1 protein is not attributed to a block in transcription, as cyclin E1 mRNA levels are similar in shCTL and shMnk1/2 HBL cells (Figure 5C). RT-qPCR analysis of RNA isolated from heavy and light polysome-bound fractions in shCTL and shMNK1/2-HBL cells indicated that blocking Mnk activity leads to a redistribution of cyclin E1 mRNA from heavy (efficiently translated) to light (poorly translated) polysomes. This is consistent with the Mnk/eIF4E axis controlling the translation initiation of cyclin E1 mRNA. In conclusion, our data suggest that Mnk1/2 may suppress cell proliferation, at least in part, by blocking mRNA translation initiation.

3.5 Discussion

cKit mutant melanomas are often resistant, or quickly develop resistance, to cKit inhibitors, thus more effective therapies are desperately needed. The convergence point of MAPK and PI3K-AKT-mTOR signalling, activated downstream of oncogenic cKit, is the Mnk/eIF4E axis that has not been characterized in cKit aberrant human melanoma. In this report, we show that cKit aberrant melanomas cell lines and patient specimens, express elevated phospho-Mnk and phospho-eIF4E (Figure 1A-1C). We then provide ample evidence that cKit melanomas are driven by high Mnk1/2 activity, suggesting that therapeutically blocking activity of these kinases represents an innovative therapeutic approach in cKit mutant melanoma. Moreover, we present strong data in support of pre-

clinical development of a novel Mnk1/2 inhibitor, SEL201. SEL201 suppressed cell survival, cell migration and invasion in melanomas driven by cKit. Last year, a new clinical phase I/II trial opened (NCT02605083), which aims to study the efficacy of the Mnk1/2 inhibitor eFT508 in advanced cancers, including melanoma.

Importantly, the Mnk1/2 targeting approach may not be limited to cKit mutant melanomas. Two BRAFV600E/PTEN null melanoma cell lines analyzed in our cohort also overexpressed phospho-eIF4E (Figure 1C, Supplementary Figure 1B). This is consistent with the data we observe in cKit mutant melanoma cells, as mutant BRAF and loss of PTEN results in activation of MAPK and PI3K downstream signalling pathways. Recently, melanoma with Loss-of-function mutations in the tumor suppressor neurofibromin 1 (NF1) has been found accounting for 15% in the patients with cutaneous melanoma(78). Although the role of targeting Mnk1/2 activites have not been explored yet in NF1 aberrant melanomas, however a recent research does report that Mnk kinases are therapeutic targets for NF1-deficient malignancies malignant peripheral nerve sheath tumors (MPNSTs) (265), implying that Mnk1/2 may be targetable in NF1 mutant melanoma. Moreover, our work highlights the need to test Mnk1/2 inhibitors in diseases wherein cKit is commonly mutated, such as GIST (Gastrointestinal stromal tumors) cancer. In GIST, secondary mutations or amplification of cKit contributes to resistance to cKit inhibitors, and in these cases Mnk1/2 therapeutic intervention would be predicted to overcome resistance (147, 151) .

eIF4E is one of the best studied substrates of Mnk1/2 (266-268). Our profiling of Mnk1/2 activity in patient melanomas, suggest that the phosphorylation state of eIF4E phosphorylation can be used as a biomarker to screen for tumors that are driven by

Mnk1/2 kinases. eIF4E is the rate-limiting factor of regulating mRNA translation initiation (161). Inhibition of eIF4E function leads to reduction of cell survival and tumor growth and predicts responsiveness to BRAF and MEK inhibitors in human melanomas (143, 144, 194). Our data show that inhibiting cKit signaling, genetically or pharmacologically: (1) suppresses phospho-Mnk and phospho-eIF4E (Figure 2B, 2D), (2) decreased phosphorylation of 4E-BP1, which then has the capacity to tightly bind to and inhibit eIF4E function (Data not shown), and (3) reduced the abundance of heavy polysome distribution (Data not shown). We predict that activating mutations in cKit alter mRNA translation. In future work, it will be important to uncover the molecular mechanisms underlying the oncogenic activities of the Mnk/eIF4E axis, downstream of mutant cKit. We are currently identifying, genome-wide translational targets of phospho-eIF4E in cKit mutant melanomas, with the goal of translating basic research findings into potential therapeutic targets for correcting the defects caused by mutant cKit. Here we report that cyclin E1 mRNA translation is regulated downstream of Mnk1/2 kinase activation in cKit mutant melanoma. Cyclin E1, the activator of CDK2, is required for the G1- to S-phase cell cycle transition (269). In breast cancer, cyclin E1 overexpression is linked with poor patient survival (270), and in malignant melanoma, although cyclin E is not detected in benign naevi, it is easily detected in most metastatic melanomas (271). Moreover, cyclin E expressing melanoma cells display increased abilities to metastasize to the lung (272).

Our findings provide evidence for increased Mnk1/2 kinase activity in cKit mutant melanoma, and that blocking Mnk1/2 exerts potent anti-melanoma effects in vitro and in

vivo. Our study, and the work of others (273-276), urgently supports the pre-clinical development of Mnk1/2 inhibitors for the treatment of patients with cKit aberrations.

3.6 Figures and Supplementary Figures

Figure 1

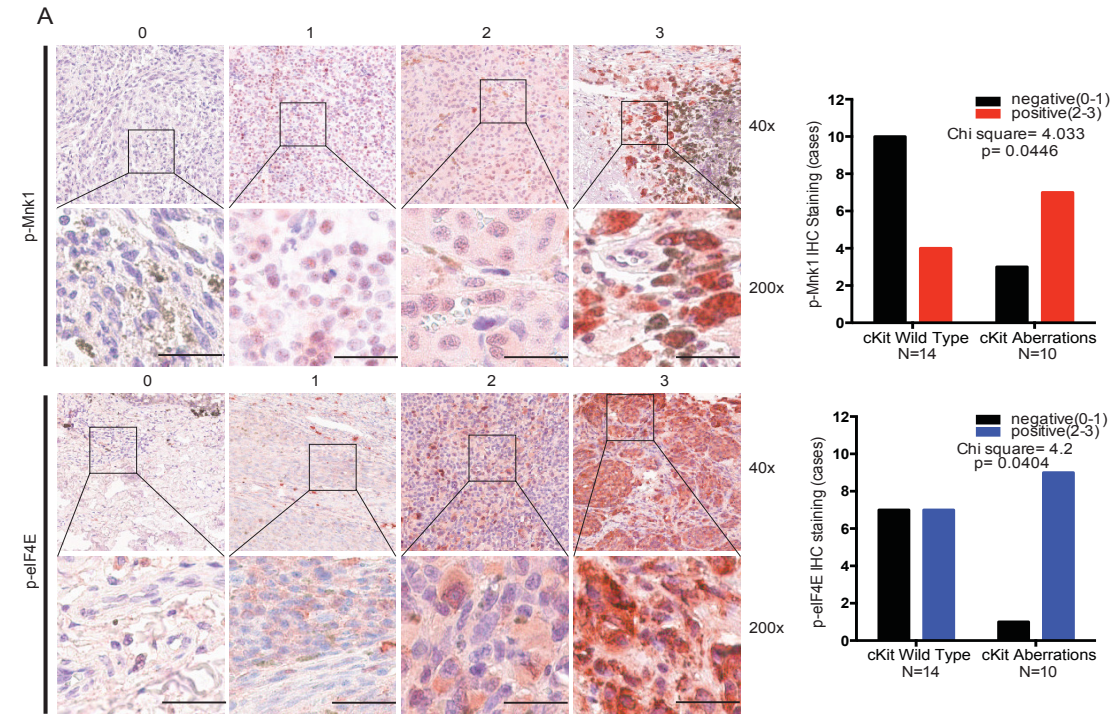

Figure 3.1. cKit mutant melanoma patients overexpress high phospho-Mnk and phospho-eIF4E.

(A) Representative images of phospho-Mnk1 and phospho-eIF4E IHC staining. Bar graphs of phospho-Mnk1 and phospho-eIF4E IHC scores in melanoma patients were shown on the right hand panel. (Chi-squared test, p values shown in the figure, scale bar; 40 micrometer). (B) The correlation between phospho-eIF4E and phospho-Mnk1 IHC scores in melanoma patients. (Pearson correlation test, r and p value shown in the figure). (C) phospho-Mnk1 and phospho-eIF4E levels were assessed by protein densitometry, values were normalized to corresponding protein levels in non malignant mel-ST (* $p < 0.05$, ** $p < 0.01$, NS= Not significant, one-way ANOVA variance test).

Figure 2

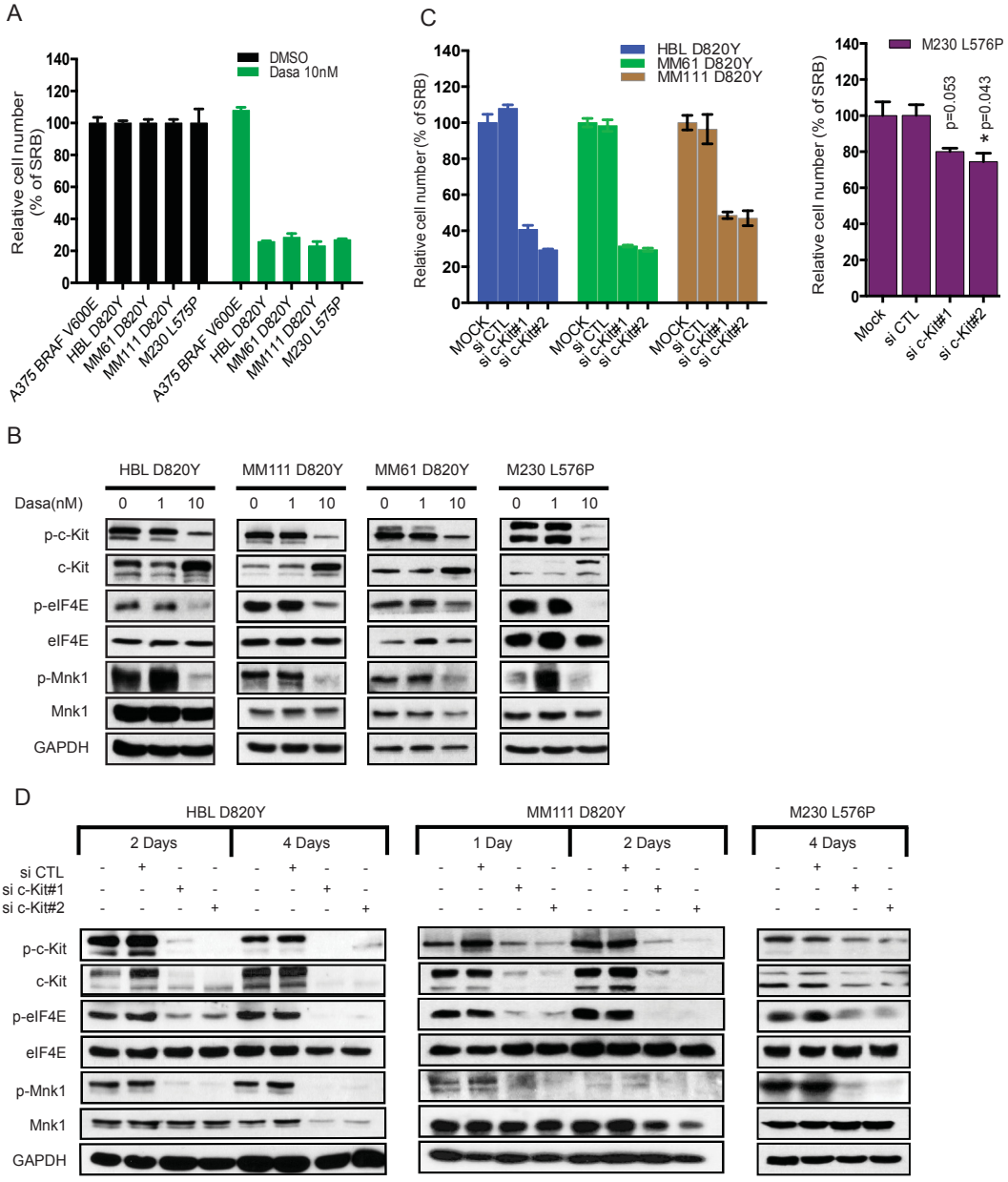
A
Relative cell number (% of SRB)
DMSO
Dasa 10nM
A375 BRAF V600E
HBL D820Y
MM61 D820Y
MM111 D820Y
M230 L575P
C
HBL D820Y
MM61 D820Y
MM111 D820Y
MOCK
si CTL
si c-Kit#1
si c-Kit#2
M230 L576P
p=0.053
* p=0.043
Mock
B
HBL D820Y
MM111 D820Y
MM61 D820Y
M230 L576P
Dasa(nM)
0 1 10
p-c-Kit
c-Kit
p-eIF4E
eIF4E
p-Mnk1
Mnk1
GAPDH
D
HBL D820Y
MM111 D820Y
M230 L576P
2 Days
4 Days
1 Day
si CTL
si c-Kit#1
si c-Kit#2

Figure 3.2. cKit inhibitor dasaatinib suppresses cell proliferation and the activation of Mnk/eIF4E axis in cKit melanomas.

(A) Cell proliferation was assessed by SRB staining 72 hours after either vehicle (DMSO) or 10nM of dasatinib treatment in A375, HBL, MM61, MM111 and M230 melanoma cell lines. (Error bars were defined as mean +/- SD, n=3). (B) Western blot of phospho-cKit, cKit, phospho-eIF4E, eIF4E, phospho-Mnk1, Mnk1 in HBL, MM111, MM61, and M230 melanoma cells lines with dasatinib treatment for 24 hours. GAPDH is the loading control for all the immunoblots. (C) Cell proliferation assay plot following cKit siRNA treatment for four days, as assessed by sulforhodamine B (SRB) staining. (Error bars were defined as mean +/- SD, n=3).

(D) Western blot of phospho-cKit, cKit, phospho-eIF4E, eIF4E, phospho-Mnk1, Mnk1 in HBL ,MM111 and M230 cell lines with cKit siRNA treatment at the time points indicated.

Figure 3

A

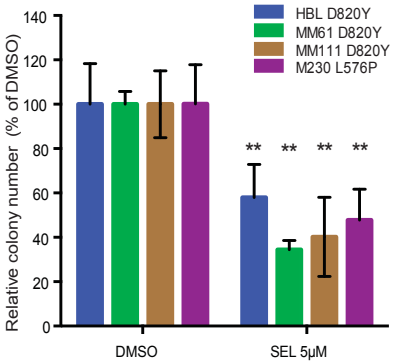

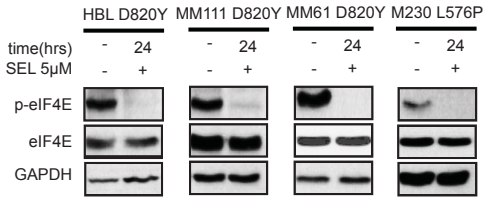

B

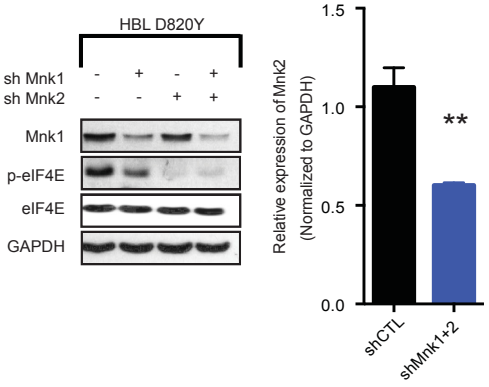

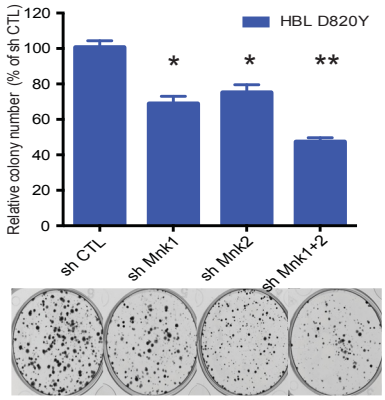

C

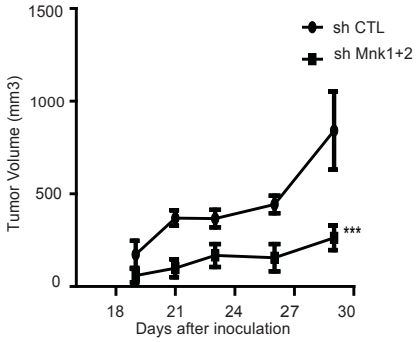

D

Figure 3.3. Stable knockdown or inhibition of Mnk1/2 in HBL cells suppresses clonogenicity and tumor growth.

(A) Clonogenic assay after 14 days with or without 5μM of Mnk inhibitor SEL201 treatment in HBL, MM61, MM111, M230 cell lines. Colonies were counted by GelCounter. (Error bars were defined as mean +/- SD, n=3. Statistical significance was determined by unpaired Student's t-test. ** $p < 0.01$). Western blot of phospho-eIF4E, eIF4E and GAPDH (loading control) following SEL201 treatment in HBL, MM61, MM111, M230 cell lines were shown. (B) Western blot of Mnk1, phospho-eIF4E, eIF4E and GAPDH (loading control) in HBL shCTL and shMnk1+2 cell lines (left). RT-qPCR of Mnk2 mRNA level in HBL shCTL and shMnk1+2 cell lines (middle). Clonogenic assay following 14 days of growth in HBL shCTL and shMnk1+2 stable cell lines (right). Colonies were counted by GelCounter. (Error bars were defined as mean +/- SD, n=3. Statistical significance was determined by unpaired Student's t-test. * $p < 0.05$, ** $p < 0.01$). Representative pictures are shown on the bottom. (C) $5X10^6$ cells were inoculated subcutaneously in SCID Beige mice, tumor size was measured every two days. Error bars were defined as standard error of the mean (SEM), n=5 per group. Statistical significance was determined by two-way ANOVA. ***$P<0.001$ (** $p<0.01$, N=2 experiment). (D) Representative pictures of HBL shCTL versus shMnk1+2 tumors.

Figure 4

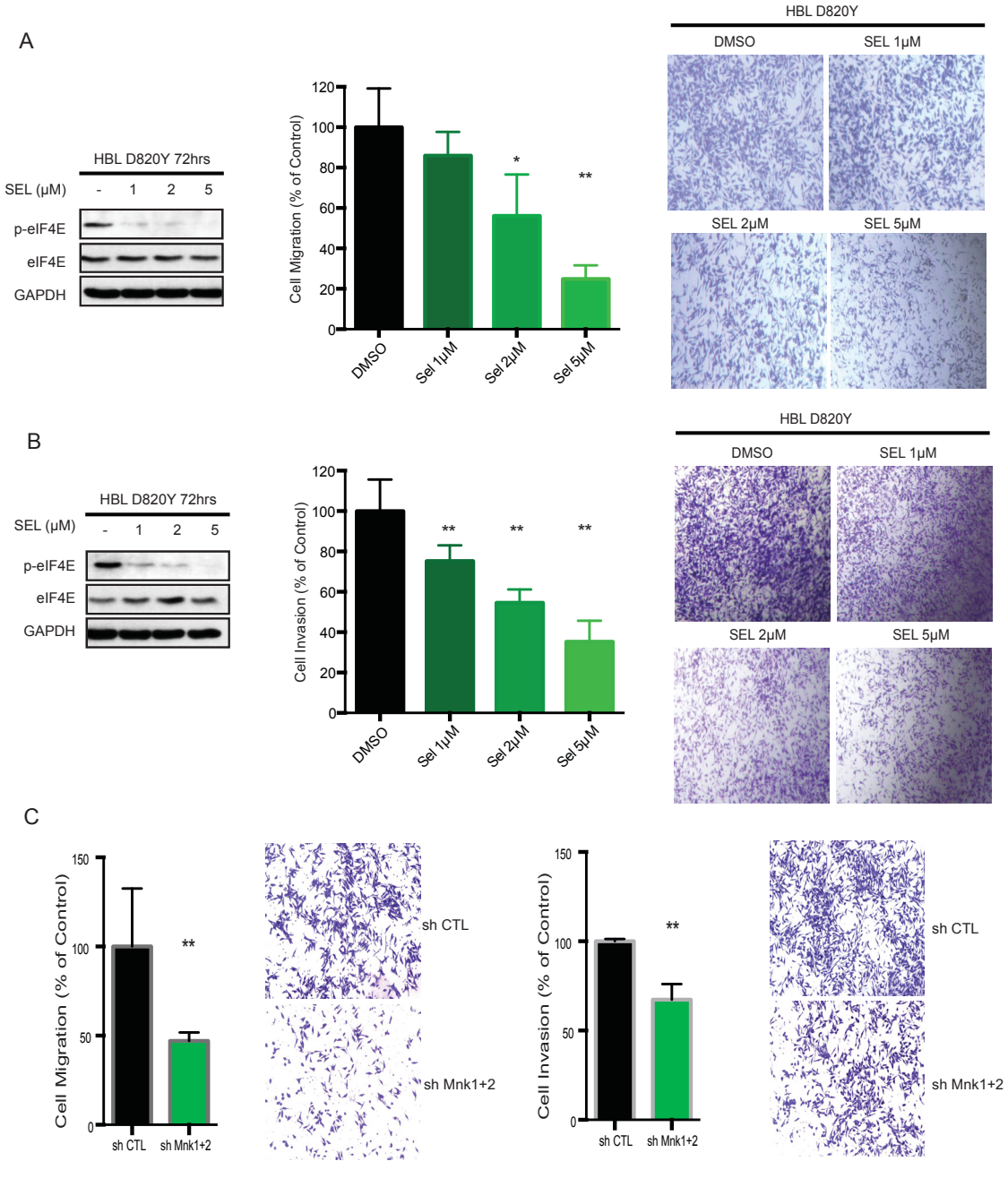
A
HBL D820Y 72hrs
SEL (μM) - 1 2 5
p-eIF4E
eIF4E
GAPDH
Cell Migration (% of Control)
120
100
80
60
40
20
0
DMSO
Sel 1μM
Sel 2μM
Sel 5μM
*
**
HBL D820Y
DMSO
SEL 1μM
SEL 2μM
SEL 5μM
B
HBL D820Y 72hrs
SEL (μM) - 1 2 5
p-eIF4E
eIF4E
GAPDH
Cell Invasion (% of Control)
120
100
80
60
40
20
0
DMSO
Sel 1μM
Sel 2μM
Sel 5μM
**
**
**
HBL D820Y
DMSO
SEL 1μM
SEL 2μM
SEL 5μM
C
Cell Migration (% of Control)
150
100
50
0
sh CTL
sh Mnk1+2
**
sh CTL
sh Mnk1+2
Cell Invasion (% of Control)
150
100
50
0
sh CTL
sh Mnk1+2
**
sh CTL
sh Mnk1+2

Figure 3.4. Mnk inhibition reduces cell migration and invasion capacities in cKit mutant HBL melanoma cells.

(A) Western blot of phospho-eIF4E, eIF4E and GAPDH (loading control) in HBL cell lines following 72hours of treatment with SEL201 (left panel). Cell migration was assessed by transwell assay. Representative pictures are shown on the right hand panel. (Statistical significance was determined by unpaired Student's t-test. * $p < 0.05$, ** $p < 0.01$) (B) Western blot of phospho-eIF4E, eIF4E and GAPDH (loading control) in HBL cell lines with 72-hour treatment of SEL201 (left panel). Cell invasion was assessed by transwell assay. Representative pictures are shown on the right hand panel. (Statistical significance was determined by unpaired Student's t-test. ** $p < 0.01$). (C) Cell migration and invasion were assessed by trans-well assay in shCTL versus shMnk1+2 HBL cells. Representative pictures are shown on the right hand panel. (Statistical significance was determined by unpaired Student's t-test. ** $p < 0.01$).

Figure 5

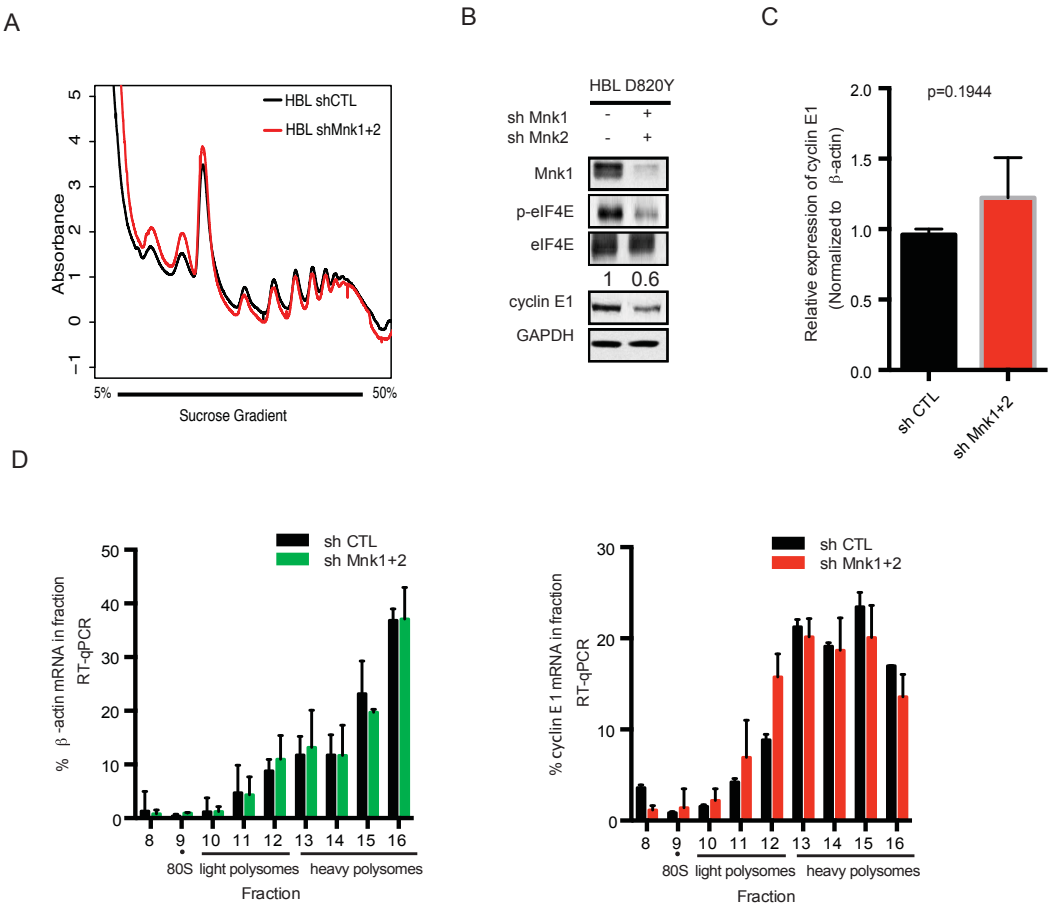
A
HBL shCTL
HBL shMnk1+2
Absorbance
5%
50%
Sucrose Gradient
B
HBL D820Y
sh Mnk1
sh Mnk2
Mnk1
p-eIF4E
eIF4E
1 0.6
cyclin E1
GAPDH
C
p=0.1944
Relative expression of cyclin E1 (Normalized to β-actin)
sh CTL
sh Mnk1+2
D
sh CTL
sh Mnk1+2
% β -actin mRNA in fraction RT-qPCR
80S
light polysomes
heavy polysomes
Fraction
% cyclin E 1 mRNA in fraction RT-qPCR

Figure 3.5. cKit and Mnk1/2 inhibition impairs cyclin E1 mRNA translation in cKit mutant melanoma cells.

(A) Polysome profile (% sucrose gradient versus 254 nm rRNA absorbance) in HBL shCTL and shMnk1+2 cells. (B) Western blot of phospho-eIF4E, eIF4E, Mnk1, cyclin E1 and GAPDH (loading control) in HBL shCTL and shMnk1+2 cells. Densitometry of cyclin E1 levels were shown in the figure. (C) RT-qPCR of cyclin E1 mRNA level in HBL shCTL and shMnk1+2 cell lines. (Error bars were defined as mean +/- SD, n=3) (D) RT–qPCR was used to determine the distribution of b-actin and cyclin E1 mRNAs in polysome fractions (heavy versus light polysomes) isolated from HBL shCTL or HBL shMnk1+2 cells.

Supplementary Table 1

Patient	cKit status	subtype	Gender	Age	Thickness(mm)	Ulceration	p-Mnk1(N/C)	p-eIF4E(N/C)	Mnk1(N/C)
1	cKit WT	Acral	Female	27	2.5	No	2(+/+)	2(+/+)	1(+/+)
2	cKit WT	Mucosal	Female	52	-	-	3(-/+)	2(-/+)	3(-/+)
3	cKit WT	Acral	Female	65	8	No	1(-/+)	2(+/+)	1(-/+)
4	cKit WT	Acral	Male	41	8	Yes	0(-/-)	2(+/+)	1(+/+)
5	cKit WT	Acral	Male	59	5	Yes	1(-/+)	1(-/+)	0(-/+)
6	cKit WT	CSD	Male	66	6	Yes	0(-/-)	1(-/+)	1(+/+)
7	cKit WT	CSD	Female	42	3.9	-	0(-/-)	1(-/+)	1(-/+)
8	cKit WT	Acral	Male	45	1.3	No	2(-/+)	0(-/-)	1(-/+)
9	cKit WT	Acral	Male	44	5	Yes	0(-/-)	1(-/+)	1(-/+)
10	cKit WT	Acral	Female	61	3	Yes	0(-/-)	1(-/+)	0(-/-)
11	cKit WT	Mucosal	Male	65	7	No	1(+/+)	2(+/+)	1(+/+)
12	cKit WT	Mucosal	Female	26	-	Yes	1(-/+)	1(-/+)	0(-/-)
13	cKit WT	Mucosal	Female	45	-	-	2(+/+)	3(-/+)	2(+/+)
14	cKit WT	Mucosal	Female	35	8	Yes	1(+/-)	2(+/+)	3(+/+)
15	cKit K642E	Acral	Female	61	3	Yes	1(-/+)	2(-/+)	0(-/-)
16	cKit L576P	Acral	Female	57	2	No	1(-/+)	2(-/+)	2(-/+)
17	cKit L576P	Mucosal	Female	56	2	Yes	2(+/+)	3(-/+)	2(+/+)
18	cKit L576P	Mucosal	Male	51	5	Yes	0(-/-)	1(-/+)	0(-/-)
19	cKit L576P	Acral	Male	64	2.2	No	2(+/+)	2(-/+)	2(+/-)
20	cKit K642E	Acral	Male	62	4	Yes	2(+/+)	3(-/+)	2(+/+)
21	cKit L576P	Mucosal	Male	56	3	Yes	2(+/+)	3(-/+)	0(-/-)
22	cKit L576P	CSD	Male	66	3	No	3(-/+)	3(-/+)	2(-/+)
23	cKit L576P	CSD	Male	71	3.1	Yes	2(+/+)	3(-/+)	2(+/+)
24	cKit L576P	Mucosal	Male	63	-	No	2(+/+)	3(+/+)	2(+/+)

Supplementary Figure 1

A

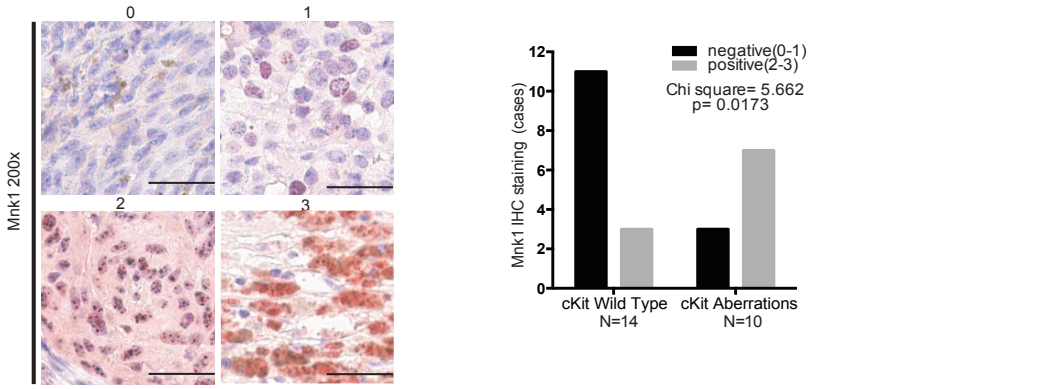

B

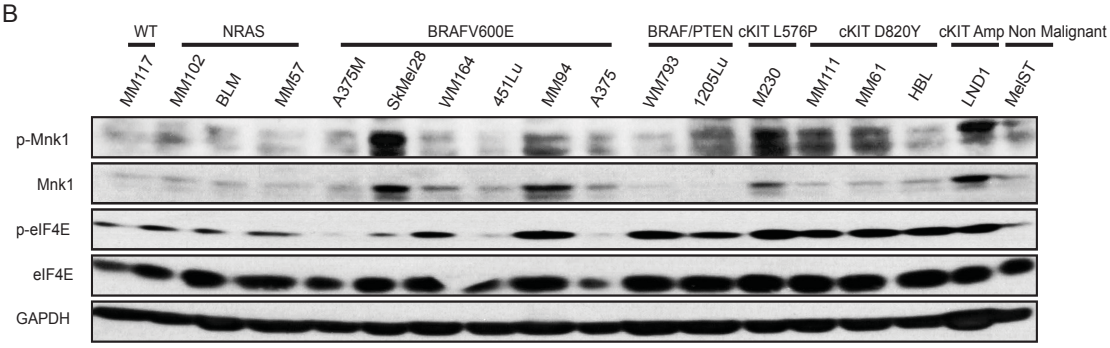

Supplementary Table 3.1

Clinical information, including age, sex, thickness (Breslow), ulceration (The scores of phospho-eIF4E, phospho-Mnk1 and Mnk1 IHC staining were provided.)

Figure 3S1. Mnk1 expression detected by IHC in cKit wild type and mutant patient samples.

(A) Representative images of Mnk1 IHC staining. Bar graph of Mnk1 IHC scores in melanoma patients was showed on the left panel

(B) Western blots displaying phopho/total Mnk and phopho/total eIF4E protein levels in a panel of melanoma cell lines. GAPDH is a loading control.

Figure 2 supplementary

A

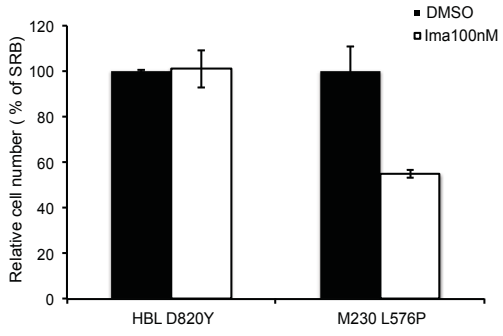

B

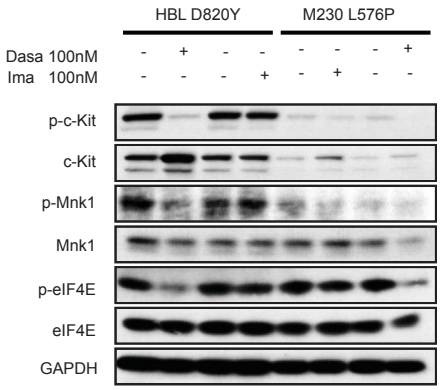

C

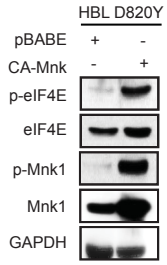

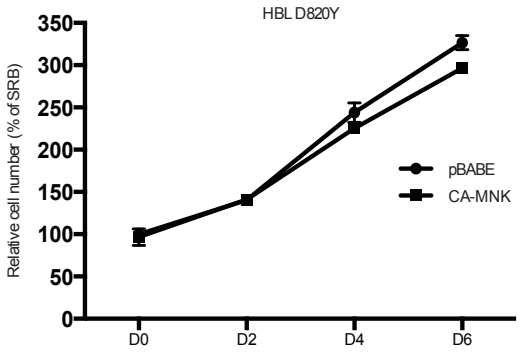

D

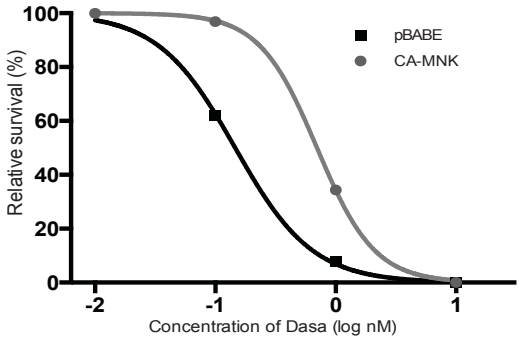

Figure 3S2. Imatinib only inhibits the Mnk/eIF4E axis in cKit L576 aberrant M230 melanoma cells. Overexpressing Mnk partially increases the resistance to Dasatinib in cKit mutant HBL cells.

(A) Cell proliferation assessment by SRB staining 72 hours after treatment with either vehicle (DMSO), 100nM dasatinib or 100nM imatinib treatment in HBL and M230. (Error bars were defined as mean +/- SD, n=3). (B) Western blot of phospho-cKit, cKit, phospho-Mnk1, Mnk1, phospho-eIF4E, eIF4E and GAPDH in HBL and M230 cells with 24- hour dasatinib or imatinib treatment. (C) Western blot of phospho-Mnk1, Mnk1, phospho-eIF4E, eIF4E and GAPDH (loading control) in HBL pBABE and CA-Mnk cell lines (left). Cell proliferation assessed by SRB staining in HBL pBABE and CA-Mnk (right). (D) Cell proliferation assessment by SRB staining at 72 hours with either vehicle (DMSO) or 0.1,1 and 10nM of dasatinib treatment in HBL pBABE and CA-Mnk cells. IC50 was determined using Prism version 3.0 (GraphPad Software, San Diego, CA).

Chapter 4

Discussion & Future directions.

Melanoma is often found in different anatomic sites such as: the skin with non-chronic sun induced damaged region (cutaneous melanoma), the skin with chronic sun induced damaged, acral and mucosal sites and the eye (18-20). Mutations in the BRAF gene have been identified in over 50% of cutaneous melanoma, in which the BRAF V600E mutant is the most dominant genetic alteration (23). Melanomas arising from acral, mucosal and chronic sun induced damage harbour cKit activating alterations (58). Last year, the TCGA reported that cutaneous melanoma could be defined into subgroups according to distinct genetic mutations, with BRAF mutations being the most prevalent. Moreover, NRAS and NF1 have been identified as mutational hotspots in cutaneous melanoma. Surprisingly, in melanomas which have no BRAF, NRAS and NF1 mutation, termed “triple-wild type” cutaneous melanoma, cKit aberrations are enriched (78). The work of defining these characteristic genetic alterations into melanoma subgroups, not only facilitates our current understanding of the molecular biology of melanoma tumorigenesis, but more importantly, increases the potential to guide the development of novel drugs for the treatment of this devastating disease.

For BRAF mutant melanoma, current targeted therapeutic interventions include the usage of BRAF and MEK inhibitors. Although patients initially respond dramatically to these drugs, unfortunately after 7-8 months from their first response, acquired resistance ensues. This lead to the combination therapy of BRAF plus MEK inhibitors

for the treatment of BRAF mutant melanoma. However, increasing clinical reports support that this combination therapy is still not the best cure for BRAF mutant melanoma patients, again because acquired resistance develops, and increased adverse side effects also presented in these patients. Therefore, finding new therapeutic targets in BRAF melanoma is urgently needed. By investigating the mechanisms underlying the development of acquired resistance to BRAF and MEK, it is clear that a common event is the reactivation of MAPK signalling and the activation of PI3K-AKT-mTOR signalling. The dual activation of these two critical signalling pathways finally converge on the activation of eIF4E, resulting in the formation of the eIF4F complex to facilitate mRNA translation. In this thesis work we explored the role of the eukaryotic translation initiation factor eIF4E in the response and resistance to the BRAF inhibitor vemurafenib in BRAF mutant melanomas. We found that inhibition of eIF4E activity is essential for BRAF mutant melanomas to respond to BRAF targeted therapy. We demonstrated that melanomas with acquired resistance to vemurafenib, showed elevated eIF4E activity, a finding validated by another group in BRAF mutant melanoma patients (REF boussemart). This finding is important for providing guidance for targeting mRNA translation to suppress melanoma, and to also overcome, or delay, acquired resistance to targeted therapeutic inhibitors in clinical settings.

Currently, there is no effective cure for NRAS mutant melanoma. MEK inhibitors shows some response in NRAS melanoma patients, but the effect is modest, with 20%-30% overall response(110, 277, 278). This may be due to the ability of aberrant NRAS to co-activate the MAPK and PI3K pathways, thus only inhibiting the

MAPK signalling, by using MEK inhibitors, is not sufficient to suppress oncogenic NRAS induced tumorigenesis. NRAS downstream signalling does ultimately impinge on the activation of eIF4E; thus targeting eIF4E activity may also hold promise in NRAS mutant melanomas.

For NF1 aberrant melanoma, there are currently no approved drugs that are used in the clinic. The ability of NF1 to negatively regulate the activity of the RAS-GTPase, is lost in NF1 mutant melanoma, thus MEK inhibitors have been used to suppress these melanoma. The signalling pathways activated downstream of NF1 converge on eIF4E. Recently, Lock and colleagues demonstrated that targeting eIF4E activity, via blocking Mnk1/2, synergized with MEK inhibition to suppress NF1 deficient malignant peripheral nerve sheath tumors (MPNSTs) (265). This data strongly support the potential for blocking the Mnk/eIF4E axis in NF1 mutant melanoma.

cKit genetic alterations are enriched preferentially in acral, mucosal and chronically damaged skin (CSD) melanomas, as well as in the “triple wild type” cutaneous melanomas. cKit mutant melanomas are often resistant, or quickly develop resistance to clinical tyrosine kinase inhibitors (TKIs). Signalling pathways activated downstream of oncogenic cKit include the MAPK and PI3K-AKT-mTOR cascades, which ultimately impinge upon eIF4E, to cause its phosphorylation. In this thesis work, we found patients with acral, mucosal and CSD melanomas, showed that Mnk1 and eIF4E are both highly phosphorylated in those melanomas with cKit aberrations, versus wild-type cKit. Moreover, we showed that inhibiting Mnk1/2 in cKit mutant melanoma

cells attenuates the proliferation, migration, invasion and melanoma outgrowth. Collectively, Mnk1/2 can be therapeutically targeted in melanomas with cKit mutations (D820Y and L576P).

In conclusion, melanomas with BRAF, NRAS, NF1 or cKit aberrations all activate the MAPK and PI3K signalling pathways, and these converge on the activation of eIF4E. Targeting eIF4E, and/or its kinases Mnk1/2, may be a viable means of suppressing melanomas with different leading genetic alterations. Importantly, our findings may not be limited to melanoma, considering the high mutation frequency of cKit in human gastrointestinal stromal tumours (GISTs), and NRAS, BRAF in colorectal cancers (45, 279-282).

Some future directions that have stemmed from this body of work are discussed below:

1. Characterizing the translatome of cKit mutant melanomas

If we are to correct the defects caused by mutant cKit, it will be important to gain an understanding of the mRNAs that are preferentially translated in melanomas harbouring cKit aberrations. To this end, we will characterize the Mnk/eIF4E-dependent translational targets in cKit driven melanomas. In Gastrointestinal stromal tumours (GISTs), over 60% of patients harbour activating mutations in the *KIT* gene. cKit activating mutations lead to up-regulating cyclin D, whose regulation is in part dependent on eIF4E associated increased translation efficiency and reduced

degradation of cyclin D protein (283). In cKit mutant melanomas, we predict the translatome to be aberrant. In collaboration with Dr.Topisirovic's lab, we first performed polysome profiling in cKit mutant HBL cells treated with 1) DMSO and 2) Dasatinib to define those mRNAs that are dependent on cKit activation. Additionally, to identify mRNAs that are aberrantly translated in both a cKit and Mnk/eIF4E dependent manner, we included the profiling of 1) shControl (shCTL) and 2) shMnk1+2 HBL stable cell lines described in (part of thesis). RNA extracted from polysomal fractions of both dasatinib treated and shCTL/shMnk1/2 stable knock down in HBL cells will be analyzed by RNA-seq to identify mRNAs that

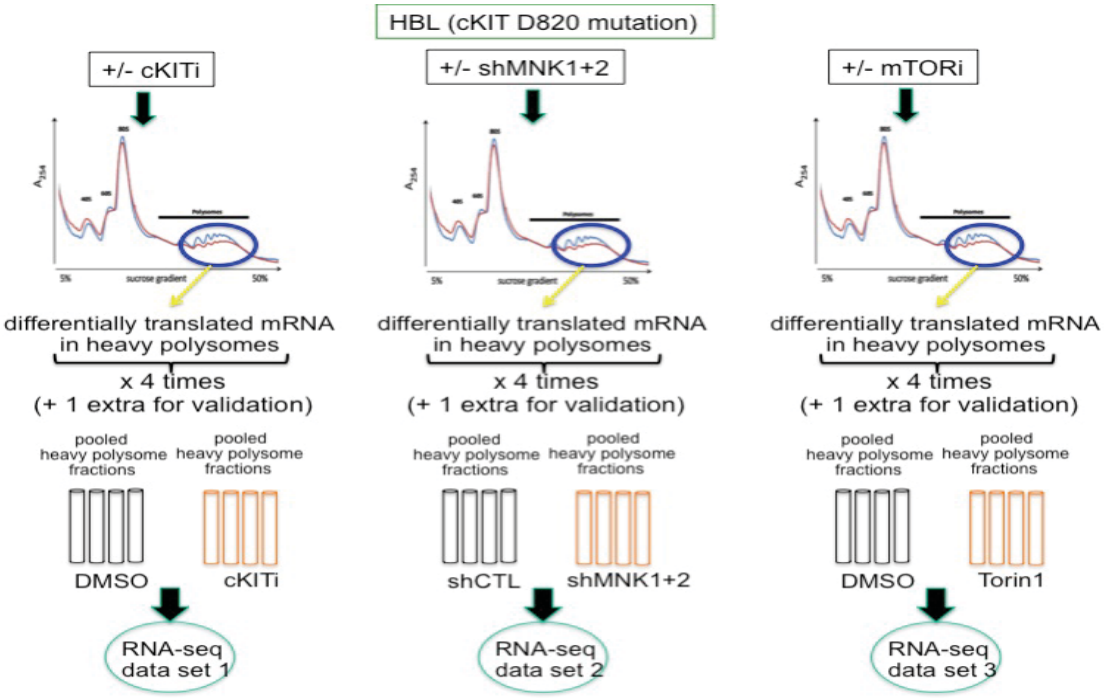

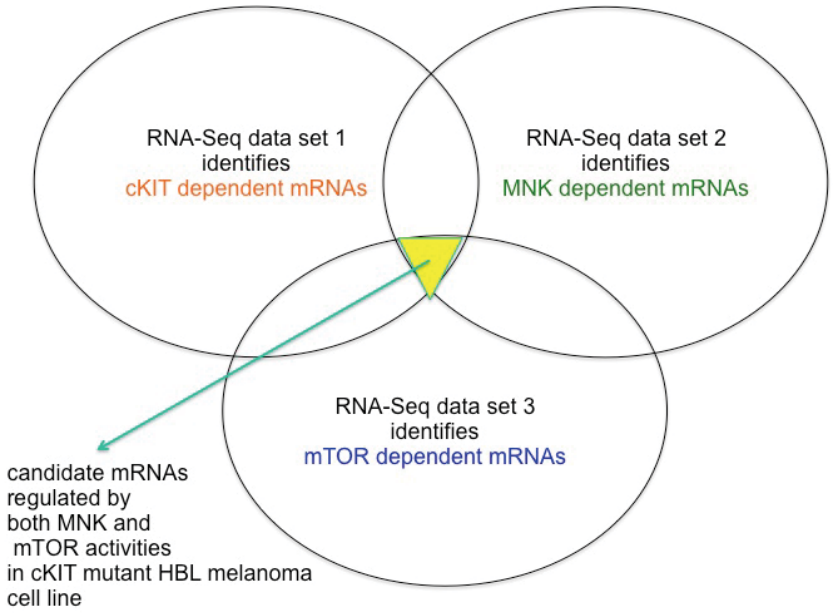

Figure 4.1 Schematic workflow of isolating polysomes fractions and performing RNAseq

are suppressed in both dasatinib and Mnk1/2 silenced group. Active site mTOR inhibitors, such as PP242 and Torin1, sequester eIF4E from binding eIF4G, and therefore inhibit the phosphorylation of eIF4E by Mnk kinases. As a control, we will also include polysome fractions isolated from Torin 1 treated HBL cells. To understand how mutant cKit mediates melanoma cell survival, we will prioritize validation of mRNAs that encode for proteins functioning in proliferation, invasion and known to be regulated by eIF4E. We will compare protein expression candidates in cKit mutant versus cKit wild type cells. We then are going to test whether increased protein level is due to translational regulation, by testing the distribution of corresponding mRNAs in polysomes using QPCR. On the other hand, we will also assess the biological impact of the validated mRNA targets in cKit mutant cells. Specifically, we will monitor the

proliferation of cKit mutant cells lacking validated mRNA targets and study their sensitivity to Mnk1/2 and cKit inhibitors.

2. Identify effective drug combinations co-targeting Mnk1/2 using a shRNA library screen.

Although Mnk activity and the phosphorylation of eIF4E are dispensable for normal development (187, 188), it is evident that eIF4E phosphorylation is required for full tumorigenesis, lymphomagenesis and tumor metastasis, thus making Mnk1/2 kinases ideal therapeutic targets (187-189). In melanoma, phosphorylated eIF4E is associated with advanced stages and worse survival (194, 195). The Mnk inhibitor cercosporamide inhibited eIF4E phosphorylation and reduced melanoma metastasis to the lung (196). Depletion of Mnk1 and Mnk2 kinases in the glioma cell line U87MG reduced xenograft outgrowth in nude mice (188). Mechanistically, previous studies showed that mRNAs involved in apoptosis, cell cycle, metastasis and ribosome biogenesis were sensitive to Mnk inhibition(187, 252).

Not only Mnk inhibition alone, but also its combination with other targeted inhibitors is promising in suppressing cancer. For instance, malignant gliomas activate mTORC1 signalling to facilitate tumor progression, whereas, mTORC inhibitors have a minimal effect in treating gliomas. Surprisingly, Grizmil and colleagues demonstrated that the Mnk inhibitor CGP57380 synergized with mTORC inhibitor RAD001 to reduce glioma cell protein synthesis, proliferation and tumor growth in a mouse model (284). In cutaneous T-cell lymphoma (CTCL) cells, Mnk inhibition in combination with the

mTORC inhibitor rapamycin achieved the maximum suppression of cell proliferation as well as promoting apoptosis in CTCL cells, compared to Mnk or mTORC inhibitor alone (285). Furthermore, in acute myeloid leukemia (AML), it has been shown that the Mnk inhibitor cercosporamide increased the sensitivity to mTORC inhibitor rapamycin and chemotherapy drug cytarabine in both cell lines, and the combination therapies enhanced the anti-tumor effect in a mouse xenograft model (286). The application of mTORC inhibitors is limited due to the negative mTOR/S6K/IRS-1 feedback loop, but Mnk inhibitor helps circumventing this pitfall of mTORC inhibtors. Therefore, we are interested in investigating whether Mnk inhibition in combining with other drug targets would be a superior therapeutic option for treating melanomas.

RNA interference (RNAi) technology is a powerful tool in functional genomics, because it allows rapid drug target discovery and validation in cultured cells. There are two commonly used methods for silencing target genes: 1. by using double-stranded (ds) interfering RNA oligonucleotides (siRNA) and 2. by using short hairpin RNA (shRNA) to stably knock down target genes. Because this technology requires highly charged oligonucleotides to pass the lipid bilayer of the cell membrane, the shRNA method, which is delivered by viral transduction, is more widely used.

In human melanoma, shRNA library based RNA interference (RNAi) technology has been widely used for identifying novel therapeutic targets. For instance, CDDO-Me [2-cyano-3,12-dioxooleana-1,9(11)-dien-28-oic acid methyl ester], a first-in-class antioxidant inflammation modulator, has been used for its antitumor activity in

various human malignancies, including human melanoma. In order to increase the drug response to CDDO-Me in melanoma, Qin and colleagues performed a large-scale synthetic lethal screen, which targets 6,000 human genes, to identify targets that would sensitize melanoma cells to CDDO-Me. In that report, they identified 5 five genes (GNPAT, SUMO1, SPINT2, FLI1, and SSX1), which when down-regulated, led to significantly decreased ERK and AKT activation and synergized with the CDDO-Me to kill melanoma (287). In another study, a siRNA library targeting 635 kinases was used in a screen for novel therapeutic targets in melanoma (288). The authors identified GSK3α as crucial for melanoma development, and importantly, when inhibited, it sensitized melanoma cells to apoptosis inducing drugs (288).

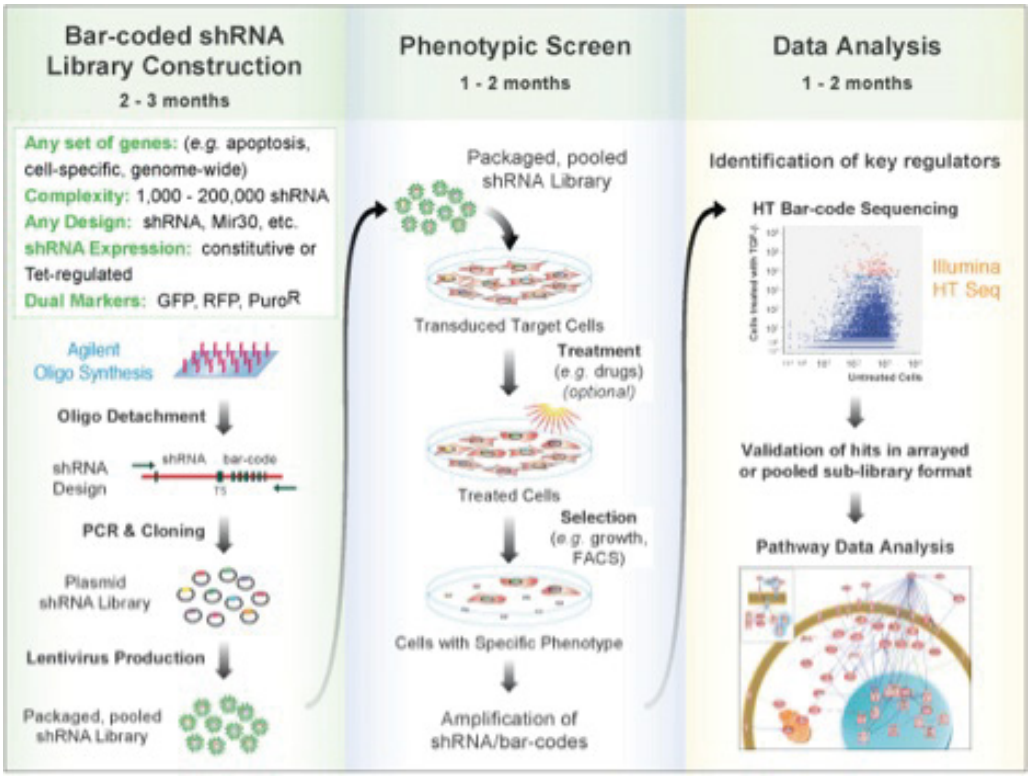

Figure 4.2 Schematic workflow of shRNA library based synthetic lethality screen

In collaboration with Dr. Sid Huang's lab, we will perform an unbiased shRNA screening approach to identify effective drug combinations with the Mnk1/2 inhibitor SEL201 in cKit melanomas. The lentiviral shRNA knockdown library consists of ~8000 shRNAs against ~1200 known targets of FDA approved or clinically active drugs. This library targets ~85 kinase and kinase related, and ~1100 non-kinase genes. By using this library screen in HBL cells, we will identify druggable targets, which when inhibited will enhance drug sensitivity to the Mnk inhibitor SEL201. As shown in Figure 4.2, HBL cells will be infected with lentiviral shRNA pools and cultured with or without SEL201. After selection, the relative abundance of shRNA vectors in the absence, or presence, of SEL201 will be determined by next generation sequencing of the barcode identifiers present in each shRNA vector. To minimize "off target" effects in the shRNA screens, we will prioritize candidates that are targeted by multiple shRNAs, or candidates that act in the same linear pathway. Then, in the subsequent validation steps, we will test whether the "candidate" pathway is activated in cKit mutant melanoma cell lines and patient samples. Also, we will test the activity of the candidates in cells treated with SEL201 and silenced for Mnk1/2. The identified targets in this screen correspond to a FDA approved or clinically active drug, thus we can also test the effects of the identified drug *in vitro* and *in vivo* for the ability to cooperate with SEL201 in inhibition of the proliferation of mutant cKit melanomas.

3. Validate Mnk1/2 inhibitor (SEL201) in an *in vivo* model of cKit activated melanoma.

In melanomas, Mnk inhibitor cercosporamide successfully inhibited the capacity of melanoma cells B16 metastasizing to the lung in a mouse xenograft model (196). Mnk inhibition also showed efficacy in suppressing the tumor growth of glioma, lymphoma and leukemia animal xenografts (284-286). Furthermore, there are two clinical phase I/II trials (NCT02605083, NCT02439346) testing the efficacy of Mnk inhibitors in advanced human cancers.

We have shown previously that Mnk inhibition or depletion decrease the clonogenicity, cell migration and invasion capacities and inhibit the tumor outgrowth in a cKit mutant melanoma xenograft model. Thus, in order to improve the clinical application of Mnk inhibitor SEL201, we will test the ability of SEL201 to block the initiation and progression of cKit-activated melanomas *in vivo*. 1) Mice will be injected with HBL cKit mutant cells and be administrated with SEL201 by gavage at a dose of 50mg/kg/day, which is well tolerated and inhibits phospho-eIF4E *in vivo*; 2) dasatinib by gavage at a dose of 1mg/kg twice daily; 3) SEL201 +dasatinib; or 4) a vehicle, after palpable tumors are detected. Melanoma samples will be harvested to determine whether dual inhibition of Mnk1/2 and cKit is more effective than single agents at inhibiting the initiation of cKit melanomas. This experiment is clinical relevant considering the low response rate of cKit melanoma patients to current tyrosine kinase inhibitors. Therefore it is important and worth to try if it will be beneficial in terms of improving the overall survival and responsiveness when inhibitors of the Mnk/eIF4E axis are combined with cKit targeted therapies in cKit mutant melanoma settings.

In conclusion, our group and others demonstrated that targeting eIF4E-dependent mRNA translation initiation suppresses the melanoma survival *in vitro* and *in vivo* (143, 144, 217). Importantly, blocking the eIF4F translation initiation complex, either by directly inhibiting eIF4E or indirectly by suppressing eIF4A or eIF4G, overcomes resistance to BRAF targeted inhibitors (143, 144). Furthermore, we showed inhibiting the activity of Mnk kinases in melanoma suppresses cell survival and tumor outgrowth. Therefore, this thesis provided the fundamental investigation of targeting mRNA translation initiation as a viable means of treating melanoma. Another research hotspot in the melanoma field is immune checkpoint inhibitors that are targeting PD-L1, PD-1, and CTLA-4. Although the overall patient response rates to checkpoint inhibitors is generally lower than that of targeted therapeutic inhibitors, immuno-therapeutic inhibitors showed sustained anti-tumor efficacy in treating melanoma patients. Furthermore, immune therapy opens a door for melanoma patients who lack BRAF, NRAS, NF1, cKit genetic mutations and thus are ineligible for targeted therapies. The role of eIF4E dependent mRNA translation initiation in response and resistance to immunotherapies is still elusive, therefore, it will also be interesting in the future to investigate the function of eIF4E and Mnk kinases in the immune micro-environment in melanoma.

Contributions to original knowledge

Translation initiation factor eIF4E has been reported overexpressed in various human cancers including melanoma. We demonstrated that melanoma cell lines overexpress eIF4E compared to immortalized melanocytes. Furthermore, for the first time, we identified cell lines with differential sensitivity to the effects of eIF4E silencing: those melanoma cell lines that expressed hyper-phosphorylated 4E-BP1 were more sensitive to eIF4E depletion. Importantly, we showed that eIF4E activity is elevated compared to their parental counterparts in a model of acquired resistance to vemurafenib. Elevation of eIF4E availability by stably knocking down its repressor proteins 4E-BP1, 4E-BP2 increased the resistance to the BRAF inhibitor vemurafenib in A375 melanoma cells. In cKit mutant melanoma, It has been reported that downstream signalling MAPK and PI3K-AKT mTOR pathways are activated. However, the role of the Mnk/eIF4E axis in the biology of cKit mutant melanoma remains obscure. We illustrated that melanoma cells harbouring cKit aberrations express high levels of phospho-Mnk and phospho-eIF4E. cKit genetic depletion or application of cKit inhibitor suppressed cell proliferation and reduced phospho-Mnk and phospho-eIF4E expression. Mnk1/2 knockdown in cKit mutant HBL cells significantly decreased its clonogenicity in vitro and curtailed melanoma outgrowth in vivo. Moreover, the novel Mnk1/2 inhibitor SEL201 drastically reduced the migration and invasion of cKit mutant melanoma cells.

In summary, our findings provided the fundamental investigation of targeting mRNA translation initiation as a viable means of treating melanomas with BRAF or cKit aberrations.

Chapter 5. References

1. Proksch E, Brandner JM, & Jensen JM (2008) The skin: an indispensable barrier. *Exp Dermatol* 17(12):1063-1072.
2. Lippens S, Hoste E, Vandenabeele P, Agostinis P, & Declercq W (2009) Cell death in the skin. *Apoptosis* 14(4):549-569.
3. Asahina M, Poudel A, & Hirano S (2015) Sweating on the palm and sole: physiological and clinical relevance. *Clin Auton Res* 25(3):153-159.
4. Dubey S & Roulin A (2014) Evolutionary and biomedical consequences of internal melanins. *Pigment Cell Melanoma Res* 27(3):327-338.
5. Simpson CL, Patel DM, & Green KJ (2011) Deconstructing the skin: cytoarchitectural determinants of epidermal morphogenesis. *Nat Rev Mol Cell Biol* 12(9):565-580.
6. Lomas A, Leonardi-Bee J, & Bath-Hextall F (2012) A systematic review of worldwide incidence of nonmelanoma skin cancer. *Br J Dermatol* 166(5):1069-1080.
7. Alam M & Ratner D (2001) Cutaneous squamous-cell carcinoma. *N Engl J Med* 344(13):975-983.
8. Rubin AI, Chen EH, & Ratner D (2005) Basal-cell carcinoma. *N Engl J Med* 353(21):2262-2269.
9. Porceddu SV, Veness MJ, & Guminski A (2015) Nonmelanoma Cutaneous Head and Neck Cancer and Merkel Cell Carcinoma: Current Concepts, Advances, and Controversies. *J Clin Oncol*.
10. Miller AJ & Mihm MC, Jr. (2006) Melanoma. *N Engl J Med* 355(1):51-65.
11. Brantsch KD*, et al.* (2008) Analysis of risk factors determining prognosis of cutaneous squamous-cell carcinoma: a prospective study. *Lancet Oncol* 9(8):713-720.
12. Mourouzis C*, et al.* (2009) Cutaneous head and neck SCCs and risk of nodal metastasis - UK experience. *J Craniomaxillofac Surg* 37(8):443-447.
13. Holmes D (2014) The cancer that rises with the sun. *Nature* 515(7527):S110-111.
14. Siegel RL, Miller KD, & Jemal A (2015) Cancer statistics, 2015. *CA Cancer J Clin* 65(1):5-29.
15. Del Bino S*, et al.* (2015) Chemical analysis of constitutive pigmentation of human epidermis reveals constant eumelanin to pheomelanin ratio. *Pigment Cell Melanoma Res*.
16. Alaluf S*, et al.* (2002) The impact of epidermal melanin on objective measurements of human skin colour. *Pigment Cell Res* 15(2):119-126.
17. Taylor SC (2002) Skin of color: biology, structure, function, and implications for dermatologic disease. *J Am Acad Dermatol* 46(2 Suppl Understanding):S41-62.
18. Kong Y*, et al.* (2011) Large-scale analysis of KIT aberrations in Chinese patients with melanoma. *Clin Cancer Res* 17(7):1684-1691.
19. Ashida A*, et al.* (2012) Assessment of BRAF and KIT mutations in Japanese melanoma patients. *Journal of dermatological science* 66(3):240-242.
20. Chi Z*, et al.* (2011) Clinical presentation, histology, and prognoses of malignant melanoma in ethnic Chinese: a study of 522 consecutive cases. *BMC Cancer* 11:85.
21. Hanahan D & Weinberg RA (2011) Hallmarks of cancer: the next generation. *Cell* 144(5):646-674.

22. Clark WH, Jr., *et al.* (1984) A study of tumor progression: the precursor lesions of superficial spreading and nodular melanoma. *Hum Pathol* 15(12):1147-1165.
23. Tsao H, Chin L, Garraway LA, & Fisher DE (2012) Melanoma: from mutations to medicine. *Genes Dev* 26(11):1131-1155.
24. Roh MR, Eliades P, Gupta S, & Tsao H (2015) Genetics of Melanocytic Nevi. *Pigment Cell Melanoma Res*.
25. Braig M & Schmitt CA (2006) Oncogene-induced senescence: putting the brakes on tumor development. *Cancer research* 66(6):2881-2884.
26. Thompson JF, Scolyer RA, & Kefford RF (2005) Cutaneous melanoma. *Lancet* 365(9460):687-701.
27. Kamb A, *et al.* (1994) Analysis of the p16 gene (CDKN2) as a candidate for the chromosome 9p melanoma susceptibility locus. *Nature genetics* 8(1):23-26.
28. Burkhart DL & Sage J (2008) Cellular mechanisms of tumour suppression by the retinoblastoma gene. *Nat Rev Cancer* 8(9):671-682.
29. Blais A & Dynlacht BD (2007) E2F-associated chromatin modifiers and cell cycle control. *Curr Opin Cell Biol* 19(6):658-662.
30. Soufir N, *et al.* (1998) Prevalence of p16 and CDK4 germline mutations in 48 melanoma-prone families in France. The French Familial Melanoma Study Group. *Hum Mol Genet* 7(2):209-216.
31. Hussussian CJ, *et al.* (1994) Germline p16 mutations in familial melanoma. *Nature genetics* 8(1):15-21.
32. Zuo L, *et al.* (1996) Germline mutations in the p16INK4a binding domain of CDK4 in familial melanoma. *Nature genetics* 12(1):97-99.
33. Pomerantz J, *et al.* (1998) The Ink4a tumor suppressor gene product, p19Arf, interacts with MDM2 and neutralizes MDM2's inhibition of p53. *Cell* 92(6):713-723.
34. Harris SL & Levine AJ (2005) The p53 pathway: positive and negative feedback loops. *Oncogene* 24(17):2899-2908.
35. Daud A & Bastian BC (2012) Beyond BRAF in melanoma. *Curr Top Microbiol Immunol* 355:99-117.
36. Stahl JM, *et al.* (2004) Deregulated Akt3 activity promotes development of malignant melanoma. *Cancer research* 64(19):7002-7010.
37. Maehama T & Dixon JE (1998) The tumor suppressor, PTEN/MMAC1, dephosphorylates the lipid second messenger, phosphatidylinositol 3,4,5-trisphosphate. *J Biol Chem* 273(22):13375-13378.
38. Li J, *et al.* (1997) PTEN, a putative protein tyrosine phosphatase gene mutated in human brain, breast, and prostate cancer. *Science* 275(5308):1943-1947.
39. Hsu M, Andl T, Li G, Meinkoth JL, & Herlyn M (2000) Cadherin repertoire determines partner-specific gap junctional communication during melanoma progression. *J Cell Sci* 113 (Pt 9):1535-1542.
40. Hsu MY, Wheelock MJ, Johnson KR, & Herlyn M (1996) Shifts in cadherin profiles between human normal melanocytes and melanomas. *J Investig Dermatol Symp Proc* 1(2):188-194.
41. Blackburn JS, Liu I, Coon CI, & Brinckerhoff CE (2009) A matrix metalloproteinase-1/protease activated receptor-1 signaling axis promotes melanoma invasion and metastasis. *Oncogene* 28(48):4237-4248.

42. Jiao Y, *et al.* (2012) Matrix metalloproteinase-2 promotes alphavbeta3 integrin-mediated adhesion and migration of human melanoma cells by cleaving fibronectin. *PloS one* 7(7):e41591.
43. Curtin JA, *et al.* (2005) Distinct sets of genetic alterations in melanoma. *N Engl J Med* 353(20):2135-2147.
44. Hodis E, *et al.* (2012) A landscape of driver mutations in melanoma. *Cell* 150(2):251-263.
45. Davies H, *et al.* (2002) Mutations of the BRAF gene in human cancer. *Nature* 417(6892):949-954.
46. Jakob JA, *et al.* (2012) NRAS mutation status is an independent prognostic factor in metastatic melanoma. *Cancer* 118(16):4014-4023.
47. Menzies AM, *et al.* (2012) Distinguishing clinicopathologic features of patients with V600E and V600K BRAF-mutant metastatic melanoma. *Clin Cancer Res* 18(12):3242-3249.
48. Lovly CM, *et al.* (2012) Routine multiplex mutational profiling of melanomas enables enrollment in genotype-driven therapeutic trials. *PloS one* 7(4):e35309.
49. Wan PT, *et al.* (2004) Mechanism of activation of the RAF-ERK signaling pathway by oncogenic mutations of B-RAF. *Cell* 116(6):855-867.
50. Fedorenko IV, Gibney GT, & Smalley KS (2013) NRAS mutant melanoma: biological behavior and future strategies for therapeutic management. *Oncogene* 32(25):3009-3018.
51. Hocker T & Tsao H (2007) Ultraviolet radiation and melanoma: a systematic review and analysis of reported sequence variants. *Hum Mutat* 28(6):578-588.
52. Kelleher FC & McArthur GA (2012) Targeting NRAS in melanoma. *Cancer J* 18(2):132-136.
53. Giehl K (2005) Oncogenic Ras in tumour progression and metastasis. *Biol Chem* 386(3):193-205.
54. Posch C, *et al.* (2013) Combined targeting of MEK and PI3K/mTOR effector pathways is necessary to effectively inhibit NRAS mutant melanoma in vitro and in vivo. *Proceedings of the National Academy of Sciences of the United States of America* 110(10):4015-4020.
55. Bello DM, *et al.* (2013) Prognosis of acral melanoma: a series of 281 patients. *Ann Surg Oncol* 20(11):3618-3625.
56. Shoo BA & Kashani-Sabet M (2009) Melanoma arising in African-, Asian-, Latino- and Native-American populations. *Semin Cutan Med Surg* 28(2):96-102.
57. Lian B & Guo J (2014) Adjuvant therapy of mucosal melanoma. *Chin Clin Oncol* 3(3):33.
58. Carvajal RD, *et al.* (2011) KIT as a therapeutic target in metastatic melanoma. *JAMA* 305(22):2327-2334.
59. Yarden Y, *et al.* (1987) Human proto-oncogene c-kit: a new cell surface receptor tyrosine kinase for an unidentified ligand. *EMBO J* 6(11):3341-3351.
60. Grabbe J, Welker P, Dippel E, & Czarnetzki BM (1994) Stem cell factor, a novel cutaneous growth factor for mast cells and melanocytes. *Arch Dermatol Res* 287(1):78-84.

61. Galli SJ, Tsai M, Wershil BK, Tam SY, & Costa JJ (1995) Regulation of mouse and human mast cell development, survival and function by stem cell factor, the ligand for the c-kit receptor. *Int Arch Allergy Immunol* 107(1-3):51-53.
62. Wehrle-Haller B (2003) The role of Kit-ligand in melanocyte development and epidermal homeostasis. *Pigment Cell Res* 16(3):287-296.
63. Mauro MJ, O'Dwyer M, Heinrich MC, & Druker BJ (2002) STI571: a paradigm of new agents for cancer therapeutics. *J Clin Oncol* 20(1):325-334.
64. Beadling C, *et al.* (2008) KIT gene mutations and copy number in melanoma subtypes. *Clin Cancer Res* 14(21):6821-6828.
65. Webster JD, Kiupel M, & Yuzbasiyan-Gurkan V (2006) Evaluation of the kinase domain of c-KIT in canine cutaneous mast cell tumors. *BMC Cancer* 6:85.
66. Singh AD, Turell ME, & Topham AK (2011) Uveal melanoma: trends in incidence, treatment, and survival. *Ophthalmology* 118(9):1881-1885.
67. Onken MD, *et al.* (2008) Oncogenic mutations in GNAQ occur early in uveal melanoma. *Invest Ophthalmol Vis Sci* 49(12):5230-5234.
68. Van Raamsdonk CD, *et al.* (2009) Frequent somatic mutations of GNAQ in uveal melanoma and blue naevi. *Nature* 457(7229):599-602.
69. Van Raamsdonk CD, Fitch KR, Fuchs H, de Angelis MH, & Barsh GS (2004) Effects of G-protein mutations on skin color. *Nature genetics* 36(9):961-968.
70. Van Raamsdonk CD, *et al.* (2010) Mutations in GNA11 in uveal melanoma. *N Engl J Med* 363(23):2191-2199.
71. Nikolaou VA, Stratigos AJ, Flaherty KT, & Tsao H (2012) Melanoma: new insights and new therapies. *J Invest Dermatol* 132(3 Pt 2):854-863.
72. Nikolaev SI, *et al.* (2012) Exome sequencing identifies recurrent somatic MAP2K1 and MAP2K2 mutations in melanoma. *Nature genetics* 44(2):133-139.
73. Bernards A & Settleman J (2005) GAPs in growth factor signalling. *Growth Factors* 23(2):143-149.
74. Cancer Genome Atlas Research N (2008) Comprehensive genomic characterization defines human glioblastoma genes and core pathways. *Nature* 455(7216):1061-1068.
75. Ding L, *et al.* (2008) Somatic mutations affect key pathways in lung adenocarcinoma. *Nature* 455(7216):1069-1075.
76. Maertens O, *et al.* (2013) Elucidating distinct roles for NF1 in melanomagenesis. *Cancer Discov* 3(3):338-349.
77. Krauthammer M, *et al.* (2015) Exome sequencing identifies recurrent mutations in NF1 and RASopathy genes in sun-exposed melanomas. *Nature genetics* 47(9):996-1002.
78. Cancer Genome Atlas N (2015) Genomic Classification of Cutaneous Melanoma. *Cell* 161(7):1681-1696.
79. Schlessinger J (2000) Cell signaling by receptor tyrosine kinases. *Cell* 103(2):211-225.
80. Ulivieri A, *et al.* (2015) Molecular characterization of a selected cohort of patients affected by pulmonary metastases of malignant melanoma: Hints from BRAF, NRAS and EGFR evaluation. *Oncotarget* 6(23):19868-19879.

81. Katunaric M, *et al.* (2014) EGFR and cyclin D1 in nodular melanoma: correlation with pathohistological parameters and overall survival. *Melanoma Res* 24(6):584-591.
82. Niu HT, *et al.* (2013) Identification of anaplastic lymphoma kinase break points and oncogenic mutation profiles in acral/mucosal melanomas. *Pigment Cell Melanoma Res* 26(5):646-653.
83. Diaz A, *et al.* (2007) Functional expression of human-epidermal-growth-factor receptor in a melanoma cell line. *Biotechnol Appl Biochem* 48(Pt 1):21-27.
84. Ueno Y, *et al.* (2008) Heregulin-induced activation of ErbB3 by EGFR tyrosine kinase activity promotes tumor growth and metastasis in melanoma cells. *Int J Cancer* 123(2):340-347.
85. Bardeesy N, *et al.* (2005) Role of epidermal growth factor receptor signaling in RAS-driven melanoma. *Mol Cell Biol* 25(10):4176-4188.
86. Furge KA, *et al.* (2001) Suppression of Ras-mediated tumorigenicity and metastasis through inhibition of the Met receptor tyrosine kinase. *Proceedings of the National Academy of Sciences of the United States of America* 98(19):10722-10727.
87. Dankort D, *et al.* (2009) Braf(V600E) cooperates with Pten loss to induce metastatic melanoma. *Nature genetics* 41(5):544-552.
88. Nathanson KL, *et al.* (2013) Tumor genetic analyses of patients with metastatic melanoma treated with the BRAF inhibitor dabrafenib (GSK2118436). *Clin Cancer Res* 19(17):4868-4878.
89. Hawryluk EB & Tsao H (2014) Melanoma: clinical features and genomic insights. *Cold Spring Harb Perspect Med* 4(9):a015388.
90. Griewank KG, *et al.* (2014) Genetic alterations and personalized medicine in melanoma: progress and future prospects. *Journal of the National Cancer Institute* 106(2):djt435.
91. FitzGerald MG, *et al.* (1996) Prevalence of germ-line mutations in p16, p19ARF, and CDK4 in familial melanoma: analysis of a clinic-based population. *Proceedings of the National Academy of Sciences of the United States of America* 93(16):8541-8545.
92. Goldstein AM, *et al.* (2006) High-risk melanoma susceptibility genes and pancreatic cancer, neural system tumors, and uveal melanoma across GenoMEL. *Cancer research* 66(20):9818-9828.
93. Lin JY & Fisher DE (2007) Melanocyte biology and skin pigmentation. *Nature* 445(7130):843-850.
94. Ward KA, Lazovich D, & Hordinsky MK (2012) Germline melanoma susceptibility and prognostic genes: a review of the literature. *J Am Acad Dermatol* 67(5):1055-1067.
95. Garraway LA, *et al.* (2005) Integrative genomic analyses identify MITF as a lineage survival oncogene amplified in malignant melanoma. *Nature* 436(7047):117-122.
96. Tee AR, *et al.* (2002) Tuberous sclerosis complex-1 and -2 gene products function together to inhibit mammalian target of rapamycin (mTOR)-mediated downstream signaling. *Proceedings of the National Academy of Sciences of the United States of America* 99(21):13571-13576.
97. Ma L, Chen Z, Erdjument-Bromage H, Tempst P, & Pandolfi PP (2005) Phosphorylation and functional inactivation of TSC2 by Erk implications for tuberous sclerosis and cancer pathogenesis. *Cell* 121(2):179-193.

98. Roux PP, Ballif BA, Anjum R, Gygi SP, & Blenis J (2004) Tumor-promoting phorbol esters and activated Ras inactivate the tuberous sclerosis tumor suppressor complex via p90 ribosomal S6 kinase. *Proceedings of the National Academy of Sciences of the United States of America* 101(37):13489-13494.
99. Carriere A, *et al.* (2008) Oncogenic MAPK signaling stimulates mTORC1 activity by promoting RSK-mediated raptor phosphorylation. *Curr Biol* 18(17):1269-1277.
100. Tsao H, Atkins MB, & Sober AJ (2004) Management of cutaneous melanoma. *N Engl J Med* 351(10):998-1012.
101. Atkins MB, *et al.* (1999) High-dose recombinant interleukin 2 therapy for patients with metastatic melanoma: analysis of 270 patients treated between 1985 and 1993. *J Clin Oncol* 17(7):2105-2116.
102. Middleton MR, *et al.* (2000) Randomized phase III study of temozolomide versus dacarbazine in the treatment of patients with advanced metastatic malignant melanoma. *J Clin Oncol* 18(1):158-166.
103. Chapman PB, *et al.* (2011) Improved survival with vemurafenib in melanoma with BRAF V600E mutation. *N Engl J Med* 364(26):2507-2516.
104. Flaherty KT, *et al.* (2010) Inhibition of mutated, activated BRAF in metastatic melanoma. *N Engl J Med* 363(9):809-819.
105. Sosman JA, *et al.* (2012) Survival in BRAF V600-mutant advanced melanoma treated with vemurafenib. *N Engl J Med* 366(8):707-714.
106. McArthur GA, *et al.* (2014) Safety and efficacy of vemurafenib in BRAF(V600E) and BRAF(V600K) mutation-positive melanoma (BRIM-3): extended follow-up of a phase 3, randomised, open-label study. *Lancet Oncol* 15(3):323-332.
107. Falchook GS, *et al.* (2012) Dabrafenib in patients with melanoma, untreated brain metastases, and other solid tumours: a phase 1 dose-escalation trial. *Lancet* 379(9829):1893-1901.
108. Ascierto PA, *et al.* (2013) Phase II trial (BREAK-2) of the BRAF inhibitor dabrafenib (GSK2118436) in patients with metastatic melanoma. *J Clin Oncol* 31(26):3205-3211.
109. Hauschild A, *et al.* (2012) Dabrafenib in BRAF-mutated metastatic melanoma: a multicentre, open-label, phase 3 randomised controlled trial. *Lancet* 380(9839):358-365.
110. Falchook GS, *et al.* (2012) Activity of the oral MEK inhibitor trametinib in patients with advanced melanoma: a phase 1 dose-escalation trial. *Lancet Oncol* 13(8):782-789.
111. Infante JR, *et al.* (2012) Safety, pharmacokinetic, pharmacodynamic, and efficacy data for the oral MEK inhibitor trametinib: a phase 1 dose-escalation trial. *Lancet Oncol* 13(8):773-781.
112. Kim KB, *et al.* (2013) Phase II study of the MEK1/MEK2 inhibitor Trametinib in patients with metastatic BRAF-mutant cutaneous melanoma previously treated with or without a BRAF inhibitor. *J Clin Oncol* 31(4):482-489.
113. Flaherty KT, *et al.* (2012) Improved survival with MEK inhibition in BRAF-mutated melanoma. *N Engl J Med* 367(2):107-114.
114. Flaherty KT, *et al.* (2012) Combined BRAF and MEK inhibition in melanoma with BRAF V600 mutations. *N Engl J Med* 367(18):1694-1703.

115. Long GV, *et al.* (2014) Combined BRAF and MEK inhibition versus BRAF inhibition alone in melanoma. *N Engl J Med* 371(20):1877-1888.
116. Larkin J, *et al.* (2014) Combined vemurafenib and cobimetinib in BRAF-mutated melanoma. *N Engl J Med* 371(20):1867-1876.
117. Robert C, *et al.* (2015) Improved overall survival in melanoma with combined dabrafenib and trametinib. *N Engl J Med* 372(1):30-39.
118. Wolchok JD, *et al.* (2009) Guidelines for the evaluation of immune therapy activity in solid tumors: immune-related response criteria. *Clin Cancer Res* 15(23):7412-7420.
119. O'Day SJ, *et al.* (2010) Efficacy and safety of ipilimumab monotherapy in patients with pretreated advanced melanoma: a multicenter single-arm phase II study. *Ann Oncol* 21(8):1712-1717.
120. McDermott D, *et al.* (2013) Efficacy and safety of ipilimumab in metastatic melanoma patients surviving more than 2 years following treatment in a phase III trial (MDX010-20). *Ann Oncol* 24(10):2694-2698.
121. Robert C, *et al.* (2011) Ipilimumab plus dacarbazine for previously untreated metastatic melanoma. *N Engl J Med* 364(26):2517-2526.
122. Robert C, *et al.* (2014) Anti-programmed-death-receptor-1 treatment with pembrolizumab in ipilimumab-refractory advanced melanoma: a randomised dose-comparison cohort of a phase 1 trial. *Lancet* 384(9948):1109-1117.
123. Weber JS, *et al.* (2015) Nivolumab versus chemotherapy in patients with advanced melanoma who progressed after anti-CTLA-4 treatment (CheckMate 037): a randomised, controlled, open-label, phase 3 trial. *Lancet Oncol* 16(4):375-384.
124. Robert C, *et al.* (2015) Nivolumab in previously untreated melanoma without BRAF mutation. *N Engl J Med* 372(4):320-330.
125. Larkin J, *et al.* (2015) Combined Nivolumab and Ipilimumab or Monotherapy in Untreated Melanoma. *N Engl J Med* 373(1):23-34.
126. Curtin JA, Busam K, Pinkel D, & Bastian BC (2006) Somatic activation of KIT in distinct subtypes of melanoma. *J Clin Oncol* 24(26):4340-4346.
127. Kim KB, *et al.* (2008) Phase II trial of imatinib mesylate in patients with metastatic melanoma. *Br J Cancer* 99(5):734-740.
128. Wyman K, *et al.* (2006) Multicenter Phase II trial of high-dose imatinib mesylate in metastatic melanoma: significant toxicity with no clinical efficacy. *Cancer* 106(9):2005-2011.
129. Kluger HM, *et al.* (2011) A phase 2 trial of dasatinib in advanced melanoma. *Cancer* 117(10):2202-2208.
130. Buchbinder EI, *et al.* (2015) Phase 2 study of sunitinib in patients with metastatic mucosal or acral melanoma. *Cancer* 121(22):4007-4015.
131. Guo J, *et al.* (2011) Phase II, open-label, single-arm trial of imatinib mesylate in patients with metastatic melanoma harboring c-Kit mutation or amplification. *J Clin Oncol* 29(21):2904-2909.
132. Carvajal RD (2013) Another option in our KIT of effective therapies for advanced melanoma. *J Clin Oncol* 31(26):3173-3175.
133. Shi H, *et al.* (2014) Acquired resistance and clonal evolution in melanoma during BRAF inhibitor therapy. *Cancer Discov* 4(1):80-93.
134. Nazarian R, *et al.* (2010) Melanomas acquire resistance to B-RAF(V600E) inhibition by RTK or N-RAS upregulation. *Nature* 468(7326):973-977.

135. Girotti MR, *et al.* (2013) Inhibiting EGF receptor or SRC family kinase signaling overcomes BRAF inhibitor resistance in melanoma. *Cancer Discov* 3(2):158-167.
136. Villanueva J, *et al.* (2010) Acquired resistance to BRAF inhibitors mediated by a RAF kinase switch in melanoma can be overcome by cotargeting MEK and IGF-1R/PI3K. *Cancer cell* 18(6):683-695.
137. Straussman R, *et al.* (2012) Tumour micro-environment elicits innate resistance to RAF inhibitors through HGF secretion. *Nature* 487(7408):500-504.
138. Poulikakos PI, *et al.* (2011) RAF inhibitor resistance is mediated by dimerization of aberrantly spliced BRAF(V600E). *Nature* 480(7377):387-390.
139. Shi H, *et al.* (2012) Melanoma whole-exome sequencing identifies (V600E)B-RAF amplification-mediated acquired B-RAF inhibitor resistance. *Nat Commun* 3:724.
140. Johannessen CM, *et al.* (2010) COT drives resistance to RAF inhibition through MAP kinase pathway reactivation. *Nature* 468(7326):968-972.
141. Trunzer K, *et al.* (2013) Pharmacodynamic effects and mechanisms of resistance to vemurafenib in patients with metastatic melanoma. *J Clin Oncol* 31(14):1767-1774.
142. Wagle N, *et al.* (2011) Dissecting therapeutic resistance to RAF inhibition in melanoma by tumor genomic profiling. *J Clin Oncol* 29(22):3085-3096.
143. Boussemart L, *et al.* (2014) eIF4F is a nexus of resistance to anti-BRAF and anti-MEK cancer therapies. *Nature* 513(7516):105-109.
144. Zhan Y, *et al.* (2015) The role of eIF4E in response and acquired resistance to vemurafenib in melanoma. *J Invest Dermatol* 135(5):1368-1376.
145. Blanke CD, *et al.* (2008) Long-term results from a randomized phase II trial of standard- versus higher-dose imatinib mesylate for patients with unresectable or metastatic gastrointestinal stromal tumors expressing KIT. *J Clin Oncol* 26(4):620-625.
146. Mar VJ, *et al.* (2013) BRAF/NRAS wild-type melanomas have a high mutation load correlating with histologic and molecular signatures of UV damage. *Clin Cancer Res* 19(17):4589-4598.
147. Hodi FS, *et al.* (2013) Imatinib for melanomas harboring mutationally activated or amplified KIT arising on mucosal, acral, and chronically sun-damaged skin. *J Clin Oncol* 31(26):3182-3190.
148. Yoshida H, *et al.* (2001) Review: melanocyte migration and survival controlled by SCF/c-kit expression. *J Investig Dermatol Symp Proc* 6(1):1-5.
149. Roskoski R, Jr. (2005) Signaling by Kit protein-tyrosine kinase--the stem cell factor receptor. *Biochem Biophys Res Commun* 337(1):1-13.
150. Alexeev V & Yoon K (2006) Distinctive role of the cKit receptor tyrosine kinase signaling in mammalian melanocytes. *J Invest Dermatol* 126(5):1102-1110.
151. Todd JR, Becker TM, Kefford RF, & Rizos H (2013) Secondary c-Kit mutations confer acquired resistance to RTK inhibitors in c-Kit mutant melanoma cells. *Pigment Cell Melanoma Res* 26(4):518-526.
152. Alkalaeva EZ, Pisarev AV, Frolova LY, Kisselev LL, & Pestova TV (2006) In vitro reconstitution of eukaryotic translation reveals cooperativity between release factors eRF1 and eRF3. *Cell* 125(6):1125-1136.
153. Song H, *et al.* (2000) The crystal structure of human eukaryotic release factor eRF1--mechanism of stop codon recognition and peptidyl-tRNA hydrolysis. *Cell* 100(3):311-321.

154. Weixlbaumer A, *et al.* (2008) Insights into translational termination from the structure of RF2 bound to the ribosome. *Science* 322(5903):953-956.
155. Sonenberg N & Hinnebusch AG (2009) Regulation of translation initiation in eukaryotes: mechanisms and biological targets. *Cell* 136(4):731-745.
156. Aitken CE & Lorsch JR (2012) A mechanistic overview of translation initiation in eukaryotes. *Nat Struct Mol Biol* 19(6):568-576.
157. Carroll M & Borden KL (2013) The oncogene eIF4E: using biochemical insights to target cancer. *J Interferon Cytokine Res* 33(5):227-238.
158. Gallie DR (1991) The cap and poly(A) tail function synergistically to regulate mRNA translational efficiency. *Genes Dev* 5(11):2108-2116.
159. Topisirovic I, Svitkin YV, Sonenberg N, & Shatkin AJ (2011) Cap and cap-binding proteins in the control of gene expression. *Wiley Interdiscip Rev RNA* 2(2):277-298.
160. Duncan R, Milburn SC, & Hershey JW (1987) Regulated phosphorylation and low abundance of HeLa cell initiation factor eIF-4F suggest a role in translational control. Heat shock effects on eIF-4F. *J Biol Chem* 262(1):380-388.
161. Gingras AC, Raught B, & Sonenberg N (1999) eIF4 initiation factors: effectors of mRNA recruitment to ribosomes and regulators of translation. *Annu Rev Biochem* 68:913-963.
162. Matsuo H, *et al.* (1997) Structure of translation factor eIF4E bound to m7GDP and interaction with 4E-binding protein. *Nat Struct Biol* 4(9):717-724.
163. Fraser CS, Hershey JW, & Doudna JA (2009) The pathway of hepatitis C virus mRNA recruitment to the human ribosome. *Nat Struct Mol Biol* 16(4):397-404.
164. Kapp LD & Lorsch JR (2004) GTP-dependent recognition of the methionine moiety on initiator tRNA by translation factor eIF2. *J Mol Biol* 335(4):923-936.
165. Schmitt E, Naveau M, & Mechulam Y (2010) Eukaryotic and archaeal translation initiation factor 2: a heterotrimeric tRNA carrier. *FEBS Lett* 584(2):405-412.
166. Shin BS, *et al.* (2011) Initiation factor eIF2gamma promotes eIF2-GTP-Met-tRNAi(Met) ternary complex binding to the 40S ribosome. *Nat Struct Mol Biol* 18(11):1227-1234.
167. Villa N, Do A, Hershey JW, & Fraser CS (2013) Human eukaryotic initiation factor 4G (eIF4G) protein binds to eIF3c, -d, and -e to promote mRNA recruitment to the ribosome. *J Biol Chem* 288(46):32932-32940.
168. Majumdar R, Bandyopadhyay A, & Maitra U (2003) Mammalian translation initiation factor eIF1 functions with eIF1A and eIF3 in the formation of a stable 40 S preinitiation complex. *J Biol Chem* 278(8):6580-6587.
169. Marintchev A, *et al.* (2009) Topology and regulation of the human eIF4A/4G/4H helicase complex in translation initiation. *Cell* 136(3):447-460.
170. Jackson RJ (2013) The current status of vertebrate cellular mRNA IRESs. *Cold Spring Harb Perspect Biol* 5(2).
171. Cheung YN, *et al.* (2007) Dissociation of eIF1 from the 40S ribosomal subunit is a key step in start codon selection in vivo. *Genes Dev* 21(10):1217-1230.
172. Nanda JS, Saini AK, Munoz AM, Hinnebusch AG, & Lorsch JR (2013) Coordinated movements of eukaryotic translation initiation factors eIF1, eIF1A, and eIF5 trigger phosphate release from eIF2 in response to start codon recognition by the ribosomal preinitiation complex. *J Biol Chem* 288(8):5316-5329.

173. Feoktistova K, Tuvshintogs E, Do A, & Fraser CS (2013) Human eIF4E promotes mRNA restructuring by stimulating eIF4A helicase activity. *Proceedings of the National Academy of Sciences of the United States of America* 110(33):13339-13344.
174. Truitt ML, *et al.* (2015) Differential Requirements for eIF4E Dose in Normal Development and Cancer. *Cell* 162(1):59-71.
175. De Benedetti A & Harris AL (1999) eIF4E expression in tumors: its possible role in progression of malignancies. *Int J Biochem Cell Biol* 31(1):59-72.
176. Graff JR, *et al.* (1995) Reduction of translation initiation factor 4E decreases the malignancy of ras-transformed cloned rat embryo fibroblasts. *Int J Cancer* 60(2):255-263.
177. Kevil CG, *et al.* (1996) Translational regulation of vascular permeability factor by eukaryotic initiation factor 4E: implications for tumor angiogenesis. *Int J Cancer* 65(6):785-790.
178. Li S, *et al.* (2003) Translation factor eIF4E rescues cells from Myc-dependent apoptosis by inhibiting cytochrome c release. *J Biol Chem* 278(5):3015-3022.
179. Rosenwald IB, *et al.* (1995) Eukaryotic translation initiation factor 4E regulates expression of cyclin D1 at transcriptional and post-transcriptional levels. *J Biol Chem* 270(36):21176-21180.
180. von Der Haar T, Ball PD, & McCarthy JE (2000) Stabilization of eukaryotic initiation factor 4E binding to the mRNA 5'-Cap by domains of eIF4G. *J Biol Chem* 275(39):30551-30555.
181. Richter JD & Sonenberg N (2005) Regulation of cap-dependent translation by eIF4E inhibitory proteins. *Nature* 433(7025):477-480.
182. Gingras AC, *et al.* (2001) Hierarchical phosphorylation of the translation inhibitor 4E-BP1. *Genes Dev* 15(21):2852-2864.
183. Graff JR, *et al.* (2009) eIF4E activation is commonly elevated in advanced human prostate cancers and significantly related to reduced patient survival. *Cancer research* 69(9):3866-3873.
184. O'Reilly KE, *et al.* (2009) Phosphorylated 4E-BP1 is associated with poor survival in melanoma. *Clin Cancer Res* 15(8):2872-2878.
185. Rojo F, *et al.* (2007) 4E-binding protein 1, a cell signaling hallmark in breast cancer that correlates with pathologic grade and prognosis. *Clin Cancer Res* 13(1):81-89.
186. Buxade M, Parra-Palau JL, & Proud CG (2008) The Mnks: MAP kinase-interacting kinases (MAP kinase signal-integrating kinases). *Front Biosci* 13:5359-5373.
187. Furic L, *et al.* (2010) eIF4E phosphorylation promotes tumorigenesis and is associated with prostate cancer progression. *Proceedings of the National Academy of Sciences of the United States of America* 107(32):14134-14139.
188. Ueda T, *et al.* (2010) Combined deficiency for MAP kinase-interacting kinase 1 and 2 (Mnk1 and Mnk2) delays tumor development. *Proceedings of the National Academy of Sciences of the United States of America* 107(32):13984-13990.
189. Robichaud N, *et al.* (2015) Phosphorylation of eIF4E promotes EMT and metastasis via translational control of SNAIL and MMP-3. *Oncogene* 34(16):2032-2042.
190. Jones RM, *et al.* (1996) An essential E box in the promoter of the gene encoding the mRNA cap-binding protein (eukaryotic initiation factor 4E) is a target for activation by c-myc. *Mol Cell Biol* 16(9):4754-4764.

191. Topisirovic I, *et al.* (2009) Stability of eukaryotic translation initiation factor 4E mRNA is regulated by HuR, and this activity is dysregulated in cancer. *Mol Cell Biol* 29(5):1152-1162.
192. Murata T & Shimotohno K (2006) Ubiquitination and proteasome-dependent degradation of human eukaryotic translation initiation factor 4E. *J Biol Chem* 281(30):20788-20800.
193. Yang SX, Hewitt SM, Steinberg SM, Liewehr DJ, & Swain SM (2007) Expression levels of eIF4E, VEGF, and cyclin D1, and correlation of eIF4E with VEGF and cyclin D1 in multi-tumor tissue microarray. *Oncol Rep* 17(2):281-287.
194. Khosravi S, *et al.* (2015) eIF4E is an adverse prognostic marker of melanoma patient survival by increasing melanoma cell invasion. *J Invest Dermatol* 135(5):1358-1367.
195. Carter JH, *et al.* (2016) Phosphorylation of eIF4E serine 209 is associated with tumour progression and reduced survival in malignant melanoma. *Br J Cancer* 114(4):444-453.
196. Konicek BW, *et al.* (2011) Therapeutic inhibition of MAP kinase interacting kinase blocks eukaryotic initiation factor 4E phosphorylation and suppresses outgrowth of experimental lung metastases. *Cancer research* 71(5):1849-1857.
197. Shain AH, *et al.* (2015) Exome sequencing of desmoplastic melanoma identifies recurrent NFKBIE promoter mutations and diverse activating mutations in the MAPK pathway. *Nature genetics* 47(10):1194-1199.
198. Margolin K, *et al.* (2005) CCI-779 in metastatic melanoma: a phase II trial of the California Cancer Consortium. *Cancer* 104(5):1045-1048.
199. Davies MA, *et al.* (2012) Phase I study of the combination of sorafenib and temsirolimus in patients with metastatic melanoma. *Clin Cancer Res* 18(4):1120-1128.
200. Margolin KA, *et al.* (2012) Randomized phase II trial of sorafenib with temsirolimus or tipifarnib in untreated metastatic melanoma (S0438). *Clin Cancer Res* 18(4):1129-1137.
201. Hainsworth JD, *et al.* (2010) Bevacizumab and everolimus in the treatment of patients with metastatic melanoma: a phase 2 trial of the Sarah Cannon Oncology Research Consortium. *Cancer* 116(17):4122-4129.
202. Dronca RS, *et al.* (2014) Phase II study of temozolomide (TMZ) and everolimus (RAD001) therapy for metastatic melanoma: a North Central Cancer Treatment Group study, N0675. *Am J Clin Oncol* 37(4):369-376.
203. O'Reilly KE, *et al.* (2006) mTOR inhibition induces upstream receptor tyrosine kinase signaling and activates Akt. *Cancer research* 66(3):1500-1508.
204. Markman B, Dienstmann R, & Tabernero J (2010) Targeting the PI3K/Akt/mTOR pathway--beyond rapalogs. *Oncotarget* 1(7):530-543.
205. Ogita S & Lorusso P (2011) Targeting phosphatidylinositol 3 kinase (PI3K)-Akt beyond rapalogs. *Target Oncol* 6(2):103-117.
206. Marone R, *et al.* (2009) Targeting melanoma with dual phosphoinositide 3-kinase/mammalian target of rapamycin inhibitors. *Mol Cancer Res* 7(4):601-613.
207. Eberle J, Fecker LF, Bittner JU, Orfanos CE, & Geilen CC (2002) Decreased proliferation of human melanoma cell lines caused by antisense RNA against translation factor eIF-4A1. *Br J Cancer* 86(12):1957-1962.

208. Jansen AP, Camalier CE, & Colburn NH (2005) Epidermal expression of the translation inhibitor programmed cell death 4 suppresses tumorigenesis. *Cancer research* 65(14):6034-6041.
209. Graff JR, *et al.* (2007) Therapeutic suppression of translation initiation factor eIF4E expression reduces tumor growth without toxicity. *J Clin Invest* 117(9):2638-2648.
210. Hong DS, *et al.* (2011) A phase 1 dose escalation, pharmacokinetic, and pharmacodynamic evaluation of eIF-4E antisense oligonucleotide LY2275796 in patients with advanced cancer. *Clin Cancer Res* 17(20):6582-6591.
211. Assouline S, *et al.* (2009) Molecular targeting of the oncogene eIF4E in acute myeloid leukemia (AML): a proof-of-principle clinical trial with ribavirin. *Blood* 114(2):257-260.
212. Pettersson F, *et al.* (2011) Ribavirin treatment effects on breast cancers overexpressing eIF4E, a biomarker with prognostic specificity for luminal B-type breast cancer. *Clin Cancer Res* 17(9):2874-2884.
213. Pettersson F, *et al.* (2015) Genetic and pharmacologic inhibition of eIF4E reduces breast cancer cell migration, invasion, and metastasis. *Cancer research* 75(6):1102-1112.
214. Moerke NJ, *et al.* (2007) Small-molecule inhibition of the interaction between the translation initiation factors eIF4E and eIF4G. *Cell* 128(2):257-267.
215. Chen L, *et al.* (2012) Tumor suppression by small molecule inhibitors of translation initiation. *Oncotarget* 3(8):869-881.
216. Willimott S, Beck D, Ahearne MJ, Adams VC, & Wagner SD (2013) Cap-translation inhibitor, 4EGI-1, restores sensitivity to ABT-737 apoptosis through cap-dependent and -independent mechanisms in chronic lymphocytic leukemia. *Clin Cancer Res* 19(12):3212-3223.
217. Feng Y, *et al.* (2015) SBI-0640756 Attenuates the Growth of Clinically Unresponsive Melanomas by Disrupting the eIF4F Translation Initiation Complex. *Cancer research* 75(24):5211-5218.
218. Pyronnet S, *et al.* (1999) Human eukaryotic translation initiation factor 4G (eIF4G) recruits mnk1 to phosphorylate eIF4E. *EMBO J* 18(1):270-279.
219. Scheper GC, Morrice NA, Kleijn M, & Proud CG (2001) The mitogen-activated protein kinase signal-integrating kinase Mnk2 is a eukaryotic initiation factor 4E kinase with high levels of basal activity in mammalian cells. *Mol Cell Biol* 21(3):743-754.
220. Ueda T, Watanabe-Fukunaga R, Fukuyama H, Nagata S, & Fukunaga R (2004) Mnk2 and Mnk1 are essential for constitutive and inducible phosphorylation of eukaryotic initiation factor 4E but not for cell growth or development. *Mol Cell Biol* 24(15):6539-6549.
221. Bastian BC (2014) The molecular pathology of melanoma: an integrated taxonomy of melanocytic neoplasia. *Annual review of pathology* 9:239-271.
222. Maurer G, Tarkowski B, & Baccarini M (2011) Raf kinases in cancer-roles and therapeutic opportunities. *Oncogene* 30(32):3477-3488.
223. Young K, Minchom A, & Larkin J (2012) BRIM-1, -2 and -3 trials: improved survival with vemurafenib in metastatic melanoma patients with a BRAF(V600E) mutation. *Future Oncol* 8(5):499-507.
224. Chapman PB, *et al.* (2011) Improved survival with vemurafenib in melanoma with BRAF V600E mutation. *N Engl J Med* 364(26):2507-2516.

225. Sun C, *et al.* (2014) Reversible and adaptive resistance to BRAF(V600E) inhibition in melanoma. *Nature* 508(7494):118-122.
226. Romano E, *et al.* (2013) Identification of multiple mechanisms of resistance to vemurafenib in a patient with BRAFV600E-mutated cutaneous melanoma successfully rechallenged after progression. *Clin Cancer Res* 19(20):5749-5757.
227. Greger JG, *et al.* (2012) Combinations of BRAF, MEK, and PI3K/mTOR inhibitors overcome acquired resistance to the BRAF inhibitor GSK2118436 dabrafenib, mediated by NRAS or MEK mutations. *Mol Cancer Ther* 11(4):909-920.
228. Lazaris-Karatzas A, Montine KS, & Sonenberg N (1990) Malignant transformation by a eukaryotic initiation factor subunit that binds to mRNA 5' cap. *Nature* 345(6275):544-547.
229. Avdulov S, *et al.* (2004) Activation of translation complex eIF4F is essential for the genesis and maintenance of the malignant phenotype in human mammary epithelial cells. *Cancer cell* 5(6):553-563.
230. Ruggero D, *et al.* (2004) The translation factor eIF-4E promotes tumor formation and cooperates with c-Myc in lymphomagenesis. *Nature medicine* 10(5):484-486.
231. Soni A, *et al.* (2008) eIF4E knockdown decreases breast cancer cell growth without activating Akt signaling. *Mol Cancer Ther* 7(7):1782-1788.
232. Mamane Y, *et al.* (2004) eIF4E--from translation to transformation. *Oncogene* 23(18):3172-3179.
233. Pause A, *et al.* (1994) Insulin-dependent stimulation of protein synthesis by phosphorylation of a regulator of 5'-cap function. *Nature* 371(6500):762-767.
234. Gingras AC, Kennedy SG, O'Leary MA, Sonenberg N, & Hay N (1998) 4E-BP1, a repressor of mRNA translation, is phosphorylated and inactivated by the Akt(PKB) signaling pathway. *Genes Dev* 12(4):502-513.
235. Lawrence JC, Jr. & Abraham RT (1997) PHAS/4E-BPs as regulators of mRNA translation and cell proliferation. *Trends in biochemical sciences* 22(9):345-349.
236. Boussemart L, *et al.* (2014) eIF4F is a nexus of resistance to anti-BRAF and anti-MEK cancer therapies. *Nature*.
237. Kozlowski JM, Hart IR, Fidler IJ, & Hanna N (1984) A human melanoma line heterogeneous with respect to metastatic capacity in athymic nude mice. *Journal of the National Cancer Institute* 72(4):913-917.
238. Gandin V, *et al.* (2014) Polysome fractionation and analysis of mammalian translatomes on a genome-wide scale. *J Vis Exp* (87).
239. Gupta PB, *et al.* (2005) The melanocyte differentiation program predisposes to metastasis after neoplastic transformation. *Nature genetics* 37(10):1047-1054.
240. Corcoran RB, *et al.* (2013) TORC1 suppression predicts responsiveness to RAF and MEK inhibition in BRAF-mutant melanoma. *Science translational medicine* 5(196):196ra198.
241. Atefi M, *et al.* (2011) Reversing melanoma cross-resistance to BRAF and MEK inhibitors by co-targeting the AKT/mTOR pathway. *PloS one* 6(12):e28973.
242. Sonenberg N, Rupprecht KM, Hecht SM, & Shatkin AJ (1979) Eukaryotic mRNA cap binding protein: purification by affinity chromatography on sepharose-coupled m7GDP. *Proceedings of the National Academy of Sciences of the United States of America* 76(9):4345-4349.

243. Alain T, *et al.* (2012) eIF4E/4E-BP ratio predicts the efficacy of mTOR targeted therapies. *Cancer research* 72(24):6468-6476.
244. Dowling RJ, *et al.* (2010) mTORC1-mediated cell proliferation, but not cell growth, controlled by the 4E-BPs. *Science* 328(5982):1172-1176.
245. Su F, *et al.* (2012) Resistance to selective BRAF inhibition can be mediated by modest upstream pathway activation. *Cancer research* 72(4):969-978.
246. Zebary A, *et al.* (2013) KIT, NRAS, BRAF and PTEN mutations in a sample of Swedish patients with acral lentiginous melanoma. *Journal of dermatological science* 72(3):284-289.
247. Wiesner T, *et al.* (2012) A distinct subset of atypical Spitz tumors is characterized by BRAF mutation and loss of BAP1 expression. *The American journal of surgical pathology* 36(6):818-830.
248. Heikkinen T, *et al.* (2013) Eukaryotic translation initiation factor 4E (eIF4E) expression is associated with breast cancer tumor phenotype and predicts survival after anthracycline chemotherapy treatment. *Breast cancer research and treatment* 141(1):79-88.
249. Wendel HG, *et al.* (2004) Survival signalling by Akt and eIF4E in oncogenesis and cancer therapy. *Nature* 428(6980):332-337.
250. Wendel HG, *et al.* (2006) Determinants of sensitivity and resistance to rapamycin-chemotherapy drug combinations in vivo. *Cancer research* 66(15):7639-7646.
251. Basmadjian C, Thuaud F, Ribeiro N, & Desaubry L (2013) Flavaglines: potent anticancer drugs that target prohibitins and the helicase eIF4A. *Future medicinal chemistry* 5(18):2185-2197.
252. Hsieh AC, *et al.* (2012) The translational landscape of mTOR signalling steers cancer initiation and metastasis. *Nature* 485(7396):55-61.
253. Larsson O, *et al.* (2007) Eukaryotic translation initiation factor 4E induced progression of primary human mammary epithelial cells along the cancer pathway is associated with targeted translational deregulation of oncogenic drivers and inhibitors. *Cancer research* 67(14):6814-6824.
254. Forman SB, *et al.* (2008) Is superficial spreading melanoma still the most common form of malignant melanoma? *J Am Acad Dermatol* 58(6):1013-1020.
255. Sanchez A, *et al.* (2016) Primary genitourinary melanoma: Epidemiology and disease-specific survival in a large population-based cohort. *Urol Oncol* 34(4):166 e167-166 e114.
256. Chan KK, Chan RC, Ho RS, & Chan JY (2016) Clinical Patterns of Melanoma in Asians: 11-Year Experience in a Tertiary Referral Center. *Ann Plast Surg*.
257. Todd JR, Scurr LL, Becker TM, Kefford RF, & Rizos H (2014) The MAPK pathway functions as a redundant survival signal that reinforces the PI3K cascade in c-Kit mutant melanoma. *Oncogene* 33(2):236-245.
258. Lefevre G, *et al.* (2004) Roles of stem cell factor/c-Kit and effects of Glivec/STI571 in human uveal melanoma cell tumorigenesis. *J Biol Chem* 279(30):31769-31779.
259. Kuang D, *et al.* (2008) Stem cell factor/c-kit signaling mediated cardiac stem cell migration via activation of p38 MAPK. *Basic Res Cardiol* 103(3):265-273.
260. McDaniel AS, *et al.* (2008) Pak1 regulates multiple c-Kit mediated Ras-MAPK gain-in-function phenotypes in Nf1+/- mast cells. *Blood* 112(12):4646-4654.

261. Fan S, *et al.* (2009) Phosphorylated eukaryotic translation initiation factor 4 (eIF4E) is elevated in human cancer tissues. *Cancer Biol Ther* 8(15):1463-1469.
262. Frederick MJ, *et al.* (2011) Phosphoproteomic analysis of signaling pathways in head and neck squamous cell carcinoma patient samples. *Am J Pathol* 178(2):548-571.
263. Woodman SE, *et al.* (2009) Activity of dasatinib against L576P KIT mutant melanoma: molecular, cellular, and clinical correlates. *Mol Cancer Ther* 8(8):2079-2085.
264. Lindauer M & Hochhaus A (2014) Dasatinib. *Recent Results Cancer Res* 201:27-65.
265. Lock R, *et al.* (2016) Cotargeting MNK and MEK kinases induces the regression of NF1-mutant cancers. *J Clin Invest* 126(6):2181-2190.
266. Roux PP & Topisirovic I (2012) Regulation of mRNA translation by signaling pathways. *Cold Spring Harb Perspect Biol* 4(11).
267. Fukunaga R & Hunter T (1997) MNK1, a new MAP kinase-activated protein kinase, isolated by a novel expression screening method for identifying protein kinase substrates. *EMBO J* 16(8):1921-1933.
268. Waskiewicz AJ, Flynn A, Proud CG, & Cooper JA (1997) Mitogen-activated protein kinases activate the serine/threonine kinases Mnk1 and Mnk2. *EMBO J* 16(8):1909-1920.
269. Kitagawa M, *et al.* (1996) The consensus motif for phosphorylation by cyclin D1-Cdk4 is different from that for phosphorylation by cyclin A/E-Cdk2. *EMBO J* 15(24):7060-7069.
270. Porter PL, *et al.* (1997) Expression of cell-cycle regulators p27Kip1 and cyclin E, alone and in combination, correlate with survival in young breast cancer patients. *Nature medicine* 3(2):222-225.
271. Tang L, Li G, Tron VA, Trotter MJ, & Ho VC (1999) Expression of cell cycle regulators in human cutaneous malignant melanoma. *Melanoma Res* 9(2):148-154.
272. Bales E, *et al.* (2005) The low molecular weight cyclin E isoforms augment angiogenesis and metastasis of human melanoma cells in vivo. *Cancer research* 65(3):692-697.
273. Bell JB, *et al.* (2016) MNK Inhibition Disrupts Mesenchymal Glioma Stem Cells and Prolongs Survival in a Mouse Model of Glioblastoma. *Mol Cancer Res*.
274. Kosciuczuk EM, *et al.* (2016) Merestinib blocks MNK kinase activity in acute myeloid leukemia progenitors and exhibits antileukemic effects in vitro and in vivo. *Blood*.
275. Grzmil M, *et al.* (2016) Inhibition of MNK pathways enhances cancer cell response to chemotherapy with temozolomide and targeted radionuclide therapy. *Cell Signal* 28(9):1412-1421.
276. Kosciuczuk EM, Saleiro D, & Platanias LC (2016) Dual targeting of eIF4E by blocking MNK and mTOR pathways in leukemia. *Cytokine*.
277. Ascierto PA, *et al.* (2013) MEK162 for patients with advanced melanoma harbouring NRAS or Val600 BRAF mutations: a non-randomised, open-label phase 2 study. *Lancet Oncol* 14(3):249-256.
278. Zimmer L, *et al.* (2014) Phase I expansion and pharmacodynamic study of the oral MEK inhibitor RO4987655 (CH4987655) in selected patients with advanced cancer with RAS-RAF mutations. *Clin Cancer Res* 20(16):4251-4261.
279. Hirota S, *et al.* (1998) Gain-of-function mutations of c-kit in human gastrointestinal stromal tumors. *Science* 279(5350):577-580.

280. Isozaki K, *et al.* (2000) Germline-activating mutation in the kinase domain of KIT gene in familial gastrointestinal stromal tumors. *Am J Pathol* 157(5):1581-1585.
281. Douillard JY, *et al.* (2013) Panitumumab-FOLFOX4 treatment and RAS mutations in colorectal cancer. *N Engl J Med* 369(11):1023-1034.
282. Tie J, *et al.* (2011) Optimizing targeted therapeutic development: analysis of a colorectal cancer patient population with the BRAF(V600E) mutation. *Int J Cancer* 128(9):2075-2084.
283. Haller F, *et al.* (2008) Increased KIT signalling with up-regulation of cyclin D correlates to accelerated proliferation and shorter disease-free survival in gastrointestinal stromal tumours (GISTs) with KIT exon 11 deletions. *J Pathol* 216(2):225-235.
284. Grzmil M, *et al.* (2014) MNK1 pathway activity maintains protein synthesis in rapalog-treated gliomas. *J Clin Invest* 124(2):742-754.
285. Marzec M, *et al.* (2011) Simultaneous inhibition of mTOR-containing complex 1 (mTORC1) and MNK induces apoptosis of cutaneous T-cell lymphoma (CTCL) cells. *PloS one* 6(9):e24849.
286. Altman JK, *et al.* (2013) Inhibition of Mnk kinase activity by cercosporamide and suppressive effects on acute myeloid leukemia precursors. *Blood* 121(18):3675-3681.
287. Qin Y, Deng W, Ekmekcioglu S, & Grimm EA (2013) Identification of unique sensitizing targets for anti-inflammatory CDDO-Me in metastatic melanoma by a large-scale synthetic lethal RNAi screening. *Pigment Cell Melanoma Res* 26(1):97-112.
288. Madhunapantula SV, Sharma A, Gowda R, & Robertson GP (2013) Identification of glycogen synthase kinase 3alpha as a therapeutic target in melanoma. *Pigment Cell Melanoma Res* 26(6):886-899.